Chemical Composition of Soybean Root Epidermal Cell Walls

by
Xingxiao Fang

A thesis
presented to the University of Waterloo
in fulfillment of the
thesis requirement for the degree of
Master of Science
in
Biology

Waterloo, Ontario, Canada, 2006

© Xingxiao Fang 2006

I hereby declare that I am the sole author of this thesis. This is a true copy of the thesis, including any required final revisions, as accepted by my examiners.

I understand that my thesis may be made electronically available to the public.

Abstract

The root epidermis, being the outermost cell layer of the organ, is in contact with the soil environment. The position of the epidermis determines its important roles, such as taking up water and ions from the surrounding soil, and defending against harmful microorganisms. What is the chemical composition of the walls in this layer? The chemical nature of the soybean epidermal wall modifying substance was investigated in this study with the use of histochemical tests coupled with electron microscopy, and chemical depolymerizations in combination with chromatography. Soybean (*Glycine max*) was used as a test species in the present studay. Results of histochemical and electron microscopical studies indicated that the epidermal walls are modified with suberin. The suberized epidermal walls were permeable to apoplastic tracers, differing from those of cells with suberized Casparian bands, possibly due to the spatial distribution or chemical components of the suberin. Suberin may occur in a diffuse form linked with other wall components in the epidermis. What is the chemical nature of this modification, and does it play a role in pathogen resistance? The root epidermal wall compositions of two soybean cultivars were compared; one (cv. Conrad) is resistant to *Phytophthora sojae* and the other (cv. OX 760-6) is susceptible to this root-rot oomycete. Their epidermal walls were isolated enzymatically and subjected to two different degradation methods, i.e. BF_3-MeOH transesterification and nitrobenzene oxidation. The compositions of depolymerisates of the cell walls determined by GC-MS indicated four dominant suberin monomers varying in chain length from C16 to C24. In all epidermal cell walls, ω-hydroxycarboxylic acids were more abundant than diacids, carboxylic acids and alcohols. Two of the monomers detected (hydroxycarboxylic acid and α,ω-dicarboxylic acid) are known to be characteristic suberin markers. The quantitative chemical compositions significantly differed in the epidermal cell walls of the two soybean varieties. Walls of the resistant cultivar (Conrad) had a greater quantity of both the aliphatic and aromatic components of the polymer than the susceptible cultivar (OX760-6), providing evidence to support the hypothesis that preformed suberin plays a role in plant defense.

Acknowledgements

To my late father, who was a great educator himself and has brought up thousands of PhDs and Masters throughout his fruitful 38-year career, who has always given me abundant love, encouragement, support and humor. If there was one person in the world who would be happiest to see me complete my graduation study, I have no doubt that would have been my late father.

So this is for you, Dad, may you rest in peace and love now.

Many people have given me their generous support and advice academically and emotionally throughout the research and completion of my thesis. In the past year or so, these supports have been invaluable to me especially after I lost my father to cancer in the middle of my graduate study. I am very grateful to all. In particular,

I would like to thank my supervisor Dr. Carol Peterson for granting me the opportunity to study and work with her in her laboratory, and providing me with tireless guidance and encouragement. Without you, this research will not have been possible. Thank you!

I am also grateful to my committee members for taking time from their busy schedules to review and provide constructive feedback on my thesis. This has been a great learning and enlightening experience.

My sincere gratitude also goes to my colleague Fengshan Ma for his generous support in providing technical guidance during my lab research and patiently answering all my questions, big or small, smart or stupid… It has been fun working along side Fengshan.

I can’t thank our lab technician Daryl Enstone enough for her constant help, comforting advice and timely suggestions throughout my research and completion of

the thesis – you have kept me going and staying on the right track in good or bad times. Many thanks!

My special appreciation goes to Dr. Mark Bernards who was generous to provide me a friendly workplace to complete part of the research, and went through this thesis time after time.

I would like to thank all other members of Dr. Peterson's laboratory and technicians from the Biology department for the supportive working environment, wonderful friendship, creative learning and having fun together in the last couple years. I am very fortunate and thankful for being a member of this great lab.

Last but not least, I am very grateful to my loving and supportive family. I thank my husband Debo for his love and compromises. I love my mother for her strength and love in bringing everyone together as a close family in sickness or health, for richer or poorer. I very much appreciate the tireless support and advice my sister Zhengyu and brother-in-law Wangbin have given me over the years. I thank my adorable 19-month old nephew Austin for bringing so much love, joy, energy and life to the whole family.

My family is the reason and purpose of my being, so my accomplishment is for my family too.

Table of Contents

Title Page ....…………………………………………………………………………….i

Author's Declaration ..………………………………………………………………ii

Abstract …..…………………………………………………………………………iii

Acknowledgements ……..……………………………………………………...…iv

Table of Contents ……...…………………………………………………….……vi

List of Abbreviations ...……………………………………………………………...x

List of Tables ...……………………………………………………………….……xi

List of Figures ……………………………………………………………….……xii

1 Introduction 1

1.1 Root anatomy and function.. 1

1.2 Epidermis: structure and development 1

1.3 Plant cell walls 2

1.3.1 Locations of suberized walls in roots.. 3

1.3.2 Permeability of cell walls 10

1.3.3 Measuring pore sizes in walls 11

1.4 Chemical nature of suberized walls relative to pathogen resistance 15

1.4.1 Chemical components and structural model of suberin........................... 15

1.4.2 Identification of suberin 16

1.4.2.1 Histochemical tests 16

1.4.2.2 Chemical analyses... 16

1.4.3 Suberin components relative to pathogen resistance.............................. 25

1.5 Soybean root-*Phytophthora sojae* interactions.. 26

1.5.1 Soybean 26

1.5.2 Phytophthora sojae, a root rot pathogen 26

1.6 Research objectives 28

2 Materials and Methods 29

2.1 Plant material and growth conditions... 29

2.2 Histochemical detection of suberin... 29

2.2.1 Phenol tests 30

2.2.1.1 Autofluorescence 30

    - 2.2.1.2 Hoepfner-Vorsatz test 30
  - 2.2.2 Lipid testing with sudan red 7B 30
  - 2.2.3 Acid digestion 31
  - 2.2.4 Transmission electron microscopy (TEM) 31
- 2.3 Chemical analyses 34
  - 2.3.1 Plant material 34
  - 2.3.2 Isolation of epidermal cell walls 34
  - 2.3.3 Scanning electron microscopy 34
  - 2.3.4 Extraction of cell wall material and BF_3-MeOH transesterification of poly(aliphatics) 35
  - 2.3.5 Extraction of cell wall material and nitrobenzene oxidation of poly(phenolics) 35
  - 2.3.6 Chromatographic analysis 36
  - 2.3.7 Statistics 37
- 2.4 Epidermal viability test 37
  - 2.4.1 Evan's blue 37
  - 2.4.2 Disodium fluorescein (uranin) 37
- 2.5 Permeability studies 38
  - 2.5.1 Cellufluor tracer experiments 38
  - 2.5.2 Berberine–thiocyanate tracer experiments 38
- 2.6 Measurement of intermicrofibrillar space sizes 39
- 2.7 Pathogen-root interactions 41
  - 2.7.1 Plant material and growth conditions 41
  - 2.7.2 Preparation of zoospore inoculum 41
  - 2.7.3 Inoculation 42
  - 2.7.4 Staining techniques for viewing pathogen development 42
    - 2.7.4.1 Preserving and clearing root segments 42
    - 2.7.4.2 Chlorazol black E 42
    - 2.7.4.3 Trypan blue and aniline blue 43
    - 2.7.4.4 Cellufluor (for cellulose) 43
    - 2.7.4.5 Aniline blue (for callose) 43

2.7.5 Staining methods employed on infected roots 44
2.7.6 Acid digestion 44
2.8 Microscopy and photography 44
3 Results 46
3.1 Root morphology and anatomy 46
3.2 Suberin tests 46
3.2.1 Phenol tests 47
3.2.2 Lipid test 47
3.2.3 Acid digestion 48
3.2.4 Ultrastructure of epidermal cell walls 48
3.3 Chemical composition of epidermal cell walls 62
3.3.1 Scanning electron microscopy (SEM) 62
3.3.2 Monomers released by transesterification of epidermal cell walls 62
3.3.3 Nitrobenzene oxidation of epidermal cell walls 64
3.4 Viability of epidermal cells 77
3.4.1 Evan's blue 77
3.4.2 Disodium fluorescein (uranin) 77
3.5 Permeability of epidermal walls 77
3.6 Intermicrofibrillar pore sizes 92
3.7 Pathogen-root interactions 96
3.7.1 Development of *P. sojae* in etiolated seedlings 96
3.7.2 Staining techniques for evaluation of hyphal development 97
3.7.3 Acid digestion 103
4 Discussion 110
4.1 Chemical nature of soybean root epidermal walls as determined by histochemical tests 110
4.2 Chemical nature of soybean root epidermal walls as revealed by monomer analyses 113
4.2.1 Isolation and chemical compositions 113
4.2.2 The relationship of suberized epidermal walls to pathogen resistance .. 117
4.3 Physical properties of soybean root epidermal walls 118

4.3.1 Viability of the epidermal cells 118
4.3.2 Intermicrofibrillar pore sizes of epidermal cell walls 119
4.3.3 Permeability of epidermal walls 120
4.4 Interactions between soybean roots and microorganisms 122
4.4.1 Wall modification vs root nodulation 122
4.4.2 Soybean root-*Phytophthora sojae* interactions 123
4.4.2.1 Plant material and inoculation procedure 123
4.4.2.2 Growth condition of zoospores 124
4.4.2.3 Clearing and staining techniques 124
4.4.2.4 Disease development 125
4.4.2.5 Modifying substance relative to pathogen resistance 126
4.5 Conclusions 129
5 Bibliography 130
Appendix...144

List of Abbreviations

BF_3-MeOH: boron trifluoride-methanol

BP: band pass (exciter filter)

BS: berberine hemisulphate

BSTFA: N,N-bis-trimethylsilyltrifluoroacetamide

CBE: Chlorazol black E

CLSM: confocal laser scanning microscope

cv.: cultivar

DIC: differential interference contrast

FT: farb teiler (dichroitic mirror)

G: a simple glass filter (exciter filter)

GC-FID: gas chromatography-flame ionization detector

GC-MS: gas chromatography-mass spectrometry

LP: long pass (barrier filter)

H-V: Hoepfner-Vorsatz

NBO: microscale alkaline nitrobenzene oxidation

PEG: polyethylene glycol

PTS: trisodium 3-hydroxy-5,8,10-pyrene trisulfonate

QTL: quantitative trait locus

TBO: Toludine blue O

Tinopal CBS: disodium 4,4’-bis(2-sulfostyryl)biphenyl

TMS: Trimethylsilane

VAM: Vesicular-arbuscular mycorrhizae

List of Tables

Table 2.1 PEG concentrations and amounts that should cause plasmolysis in soybean epidermal cells. 40
Table 3.1 Summary of suberin tests in soybean root epidermal walls. 49
Table 3.2 Measurement of intermicrofibrillar pore sizes. 93
Table 3.3 Different staining techniques applied to inoculated soybean roots. 100

List of Figures

Figure 1.1 Schematic diagram of root cross-section and three types of suberin. 4

Figure 1.2 Albersheim model of cell wall structure.. 6

Figure 1.3 Tethered network model of cell wall structure... 8

Figure 1.4 Schematic sectional views of cells in a tissue undergoing plasmolysis and cytorrhysis. 13

Figure 1.5 A schematic model of a suberin lamella. 18

Figure 1.6 Schematic illustration of the experimental approach applied for the analysis of isolated epidermal walls of soybean roots. 20

Figure 1.7 BF_3-MeOH transesterification of poly(aliphatic) components................. 22

Figure 1.8 Schematic microscale alkaline nitrobenzene oxidation (NBO) technique. 24

Figure 2.1 Construction of section holders. 32

Figure 3.1 Unstained cross-sections of soybean root. 50

Figure 3.2 Development of autofluorescence. 52

Figure 3.3 Hoepfner-Vorsatz test for phenols in epidermal cell walls. 54

Figure 3.4 Sudan red 7B for lipid staining in epidermal cell walls. 56

Figure 3.5 Acid digestion of soybean root... 58

Figure 3.6 The ultrastructure of epidermal cell wall viewed with TEM. 60

Figure 3.7 Scanning electron micrographs of enzymatically isolated epidermal cell walls of soybean roots. 65

Figure 3.8 Aliphatic compound classes released after BF_3-MeOH transesterification. 67

Figure 3.9 Total aliphatic substances released after BF_3-MeOH transesterification. 69

Figure 3.10 Ester-linked aromatic compound classes (ferulic acid and *p*-coumaric acid) released after BF_3-MeOH transesterification. 70

Figure 3.11 Monomeric compositions and chain-length distribution of waxes. 72

Figure 3.12 Sum of wax monomers... 74

Figure 3.13 Total vanillin and syringin released after nitrobenzene oxidation.......... 75

Figure 3.14 Total aromatic substances released from isolated epidermal cell walls of cv. Conrad and cv. OX 760-6 roots. 76
Figure 3.15 Viability of epidermal cells. 78
Figure 3.16 Evan’s blue viability test of soybean epidermis.................................... 80
Figure 3.17 Uranin viability test of soybean epidermis... 82
Figure 3.18 Cellufluor tracer in soybean roots. 85
Figure 3.19 Berberine thiocyanate tracer in cv. Conrad root. 87
Figure 3.20 Berberine thiocyanate tracer in cv. OX 760-6 root. 89
Figure 3.21 Berberine thiocyanate tracer in soybean root cap. 91
Figure 3.22 Measuring pore sizes.. 94
Figure 3.23 Development of *P. sojae* in the soybean root. 98
Figure 3.24 Development of *P. sojae* hyphae in soybean root. 101
Figure 3.25 Response of soybean root to inoculation with *P. sojae*. 104
Figure 3.26 Penetration of *P. sojae* into soybean roots. 106
Figure 3.27 Acid digestion of inoculated soybean root. 108

1 Introduction

1.1 Root anatomy and function

The morphology of a plant root is designed to facilitate performance of its essential functions, i.e. anchoring the plant, supporting its shoot, storing food in the winter (in some species), and absorbing water and nutrient ions from the soil. The typical primary angiosperm root is composed of three tissue systems, i.e. dermal (epidermis), ground (cortex), and vascular (Fig. 1.1A, Esau, 1965). The vascular cylinder functions to conduct water and nutrient ions to the shoot, and photosynthates from the shoot. The cylinder is located in the central part of the root and is composed of the vascular tissues and some associated parenchyma. The cortex serves for food storage and consists of an endodermis, central cortex and, often, exodermis. The epidermis, being the outermost cell layer, is in contact with the soil environment. The position of the epidermis determines its importance as "the initial site of water and ion uptake and the first line of defense against harmful microorganisms" (Schreiber et al., 1999).

1.2 Epidermis: structure and development

Root epidermal cells are commonly tabular in shape and are tightly packed together. This layer originates from the protoderm of the root apical meristem, which is covered by a root cap. The epidermis of most angiosperms is composed of two cell types: those with root hairs (trichoblasts) and those without root hairs (atrichoblasts; Larkin et al., 2003). It has been pointed out by Hofer (1991) and Peterson and Farquhar (1996) that the root hairs increase the surface area of the root, interact with microbes, and possibly aid in nutrient acquisition and anchorage.

The walls of the epidermal cells vary markedly in thickness in different plants. The outer tangential wall is frequently thicker than the radial and inner tangential walls (Esau, 1965) and the walls of any underlying cells (Abeysekera and McCully, 1994). According to Abeysekera and McCully (1993), the epidermal surface of the maize root tip is composed of three wall layers: a helicoidal primary wall, and two outer, fibrillar pellicles. These three layers undergo structural changes with the development of cells, and thin to about half their maximum thickness during elongation.

1.3 Plant cell walls

The plant cell wall is a unique structure that is responsible for plant architecture, plays crucial roles in apoplastic diffusion of water and ions, and protects the internal protoplast. Generally speaking, walls possess a middle lamella, the outer most part of the wall, shared by adjacent cells. A primary wall is laid down internal to the middle lamella, and a secondary wall may form after enlargement of the primary wall ceases. The cell wall contains predominantly cellulose, matrix materials, and water. Cellulose, a major component of the primary and secondary wall layers, is a straight-chain polymer of glucose (β 1-4 glucan). Groups of 1000 to 10,000 cellulose molecules are covalently linked with hydrogen bonds to form microfibrils. Within the microfibrils, the crystalline areas are called micelles while the rest of the regions are paracrystalline. Matrix materials are composed of pectic substances, hemicelluloses, and structural proteins. These amorphous materials are distributed between the cellulose microfibrils (see Carpita and Gibeaut, 1993). Pectic substances (mostly polygalacturonic acids) with free carboxyl groups are responsible for most of the negative charges of the walls. Hemicelluloses are polymers of diverse groups of sugars such as xylose, glucose, and arabinose, and are abundant in primary walls. Cell walls also contain a variety of proteins, i.e. glycoprotein and extensin. Glycoprotein is a complex of sugars and proteins; and in the wall these proteins are characterized by abundant hydroxyproline and proline amino acids (Talmadge et al., 1973). One of the proteins, extensin, can link covalently with other proteins and wrap around other wall constituents (Lamport, 1986); it is often considered to be the major structural protein (Carpita and Gibeaut, 1993). In addition to cellulose and matrix materials, water fills approximately 50% of the space in typical primary walls. This water is generally in the channel system of intermicrofibrillar spaces (Frey-Wyssling, 1969).

How are these wall polymers assembled to form a strong network? Many hypothetical models have been proposed, such as the “Albersheim model”, “tethered network” model, "multicoat" model, and "stratified" model (see Cosgrove, 2001). The "Albersheim model" has been quite influential. Albersheim and co-workers proposed that xyloglucans hydrogen-bonded to cellulose microfibrils interlock cellulose microfibrils with other matrix materials, and all matrix materials are covalently linked to each other (Fig. 1.2, Keegstra et al., 1973; Albersheim, 1978; Brett and Waldron, 1990; Carpita and Gibeaut, 1993; Cosgrove, 2001). The "tethered network" model is currently the most popular one, in which a network of cellulose microfibrils tethered together with interlocking xyloglucans are embedded in an independent pectic matrix. In addition to the pectic substances, the structural proteins are covalently linked as well. Pectic substances and structural proteins are independent networks that physically entangle the cellulose-xyloglucan framework (Fig. 1.3, Fry, 1989; Hayashi, 1989; McCann et al., 1992; Carpita and Gibeaut, 1993; Cosgrove, 2001).

1.3.1 Locations of suberized walls in roots

Depending on the position and function of the cells, modifying substances such as lignin and suberin are also found in the walls. These wall modifications normally displace the water from the intermicrofibrillar channels and solidify the wall framework (see Peterson and Cholewa, 1998). Suberin, a complex polymer (see section 1.4.1) occurs in three configurations. First, in its least well-characterized form, it is interspersed among other wall components in the epidermis (Fig. 1.1B). This type of suberin has been studied in onion by Peterson and co-workers (1978). To date, the chemical components have been detected only by histochemical tests but not by chemical analysis. Second, suberin, as suberin lamella, occurs in the endodermis and exodermis of roots (Fig. 1.1C), in cork, and at wound surfaces. A suberin lamella is a hydrophobic wall layer covering the protoplast and is located between the primary wall and plasma membrane, and sometimes embedded in the tertiary walls. With electron microscopy, it is characterized by alternating electron-dense and -lucent bands, and is mainly composed of suberin and a small amount of lignin (Zeier et al., 1999a, b). Third, suberin, as a part of Casparian bands, occurs in the endodermis and exodermis of roots (Fig. 1.1C). Casparian bands form in the anticlinal walls and usually prior to other wall modifications in these cell layers (Perumalla et al., 1990; Peterson and Perumalla, 1990). The

Figure 1.1 Schematic diagram of root cross-section and three types of suberin.

A Cross-section of an exodermal root. **B** Casparian bands and suberin lamellae in exodermal and endodermal cells. **C** Diffuse suberin in epidermal cell walls.

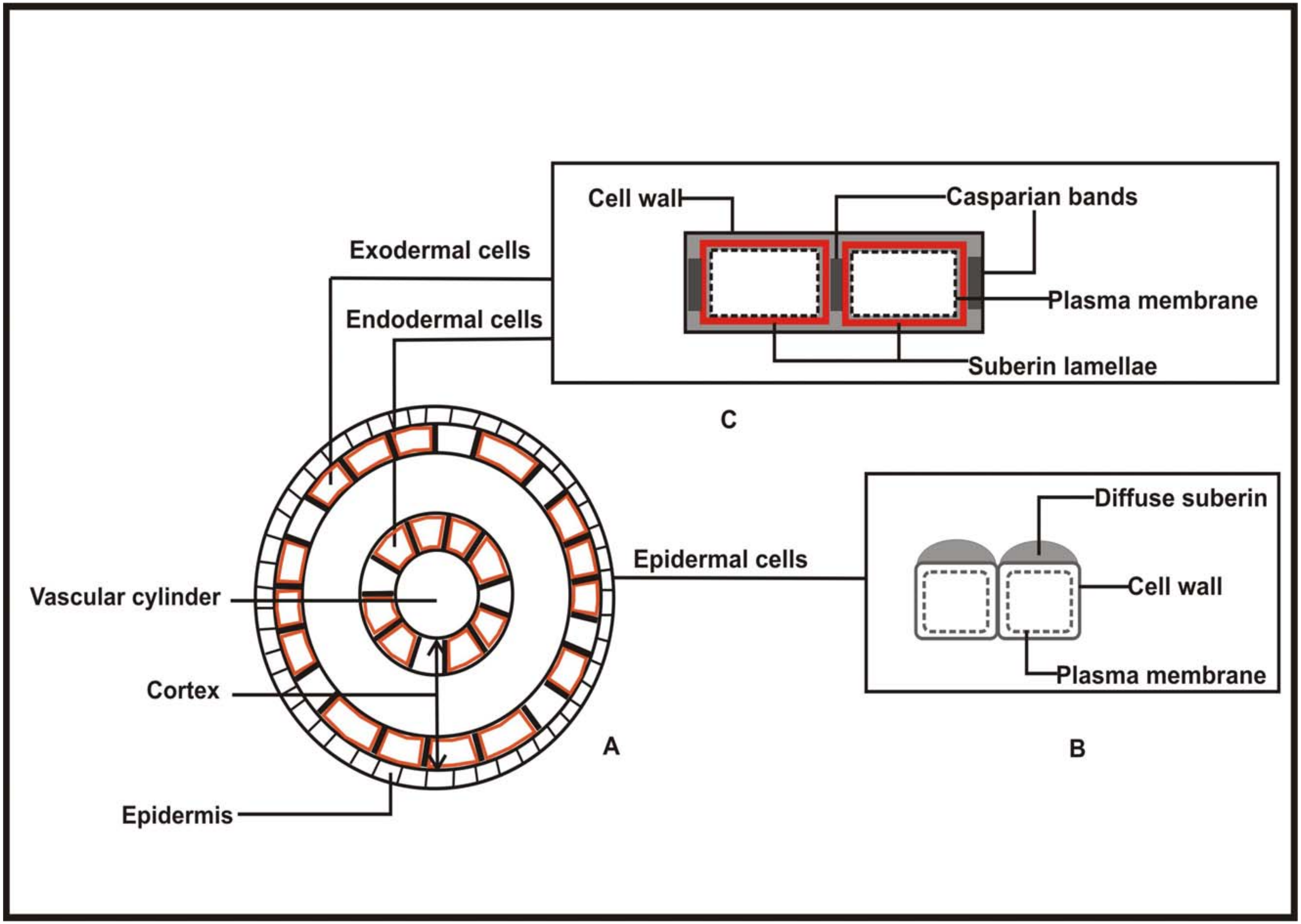
Exodermal cells
Endodermal cells
Cell wall
Casparian bands
Plasma membrane
Suberin lamellae
C
Vascular cylinder
Cortex
Epidermis
A
Epidermal cells
Diffuse suberin
Cell wall
Plasma membrane
B

Figure 1.2 Albersheim model of cell wall structure.

Xyloglucans interlock some cellulose microfibrils. Xyloglucans are also attached to pectic substances by hydrogen bonds while pectic substances are covalently attached to the structural proteins.

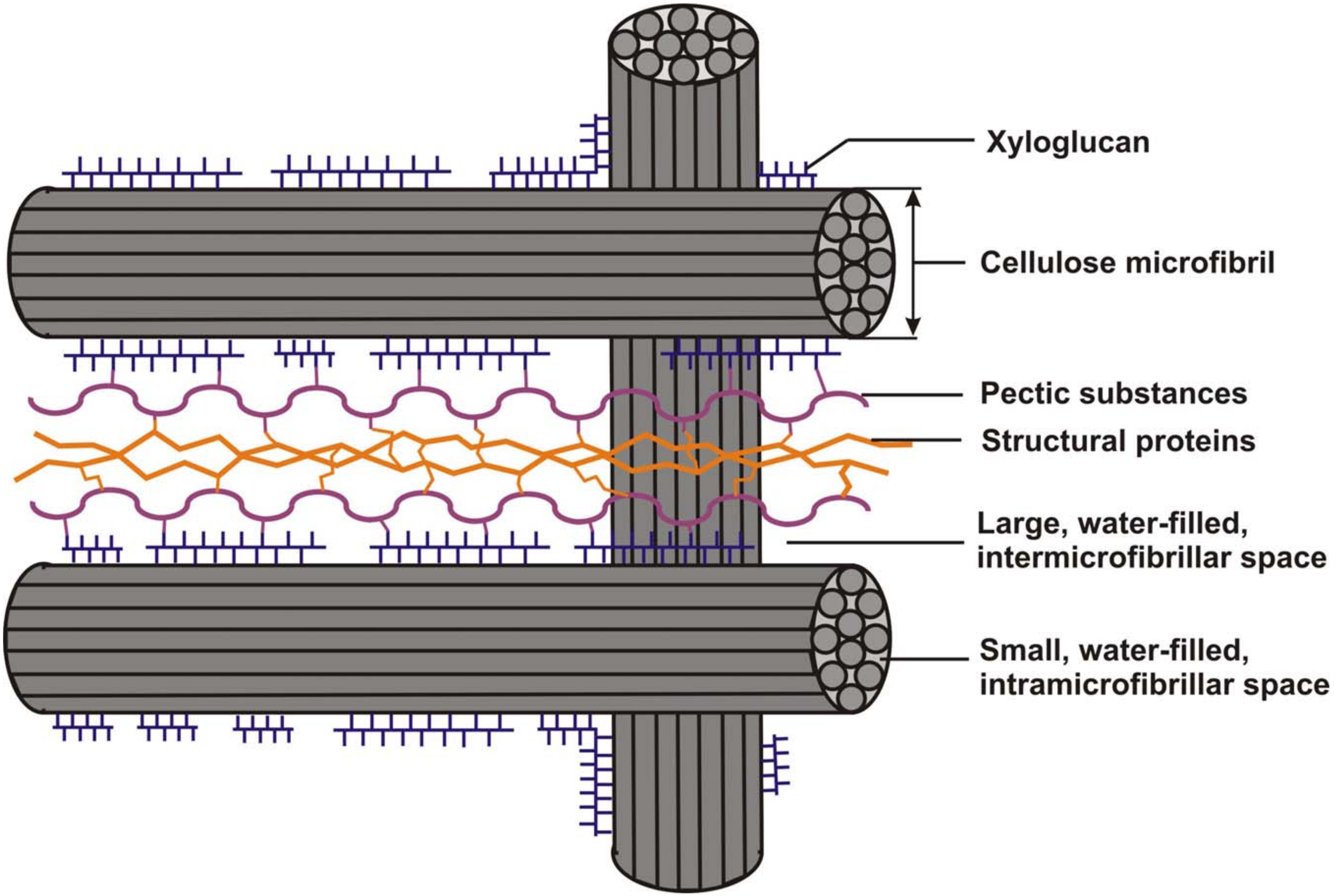
Xyloglucan
Cellulose microfibril
Pectic substances
Structural proteins
Large, water-filled, intermicrofibrillar space
Small, water-filled, intramicrofibrillar space

Figure 1.3 Tethered network model of cell wall structure.

Xyloglucans tether cellulose microfibrils together through hydrogen bonds. This network of cellulose microfibrils are embedded in an independent pectin matrix. In addition to the pectic matrix, the structural proteins are covalently linked as well. Pectic substances and structural proteins are independent networks that physically entangle the cellulose-xyloglucan framework.

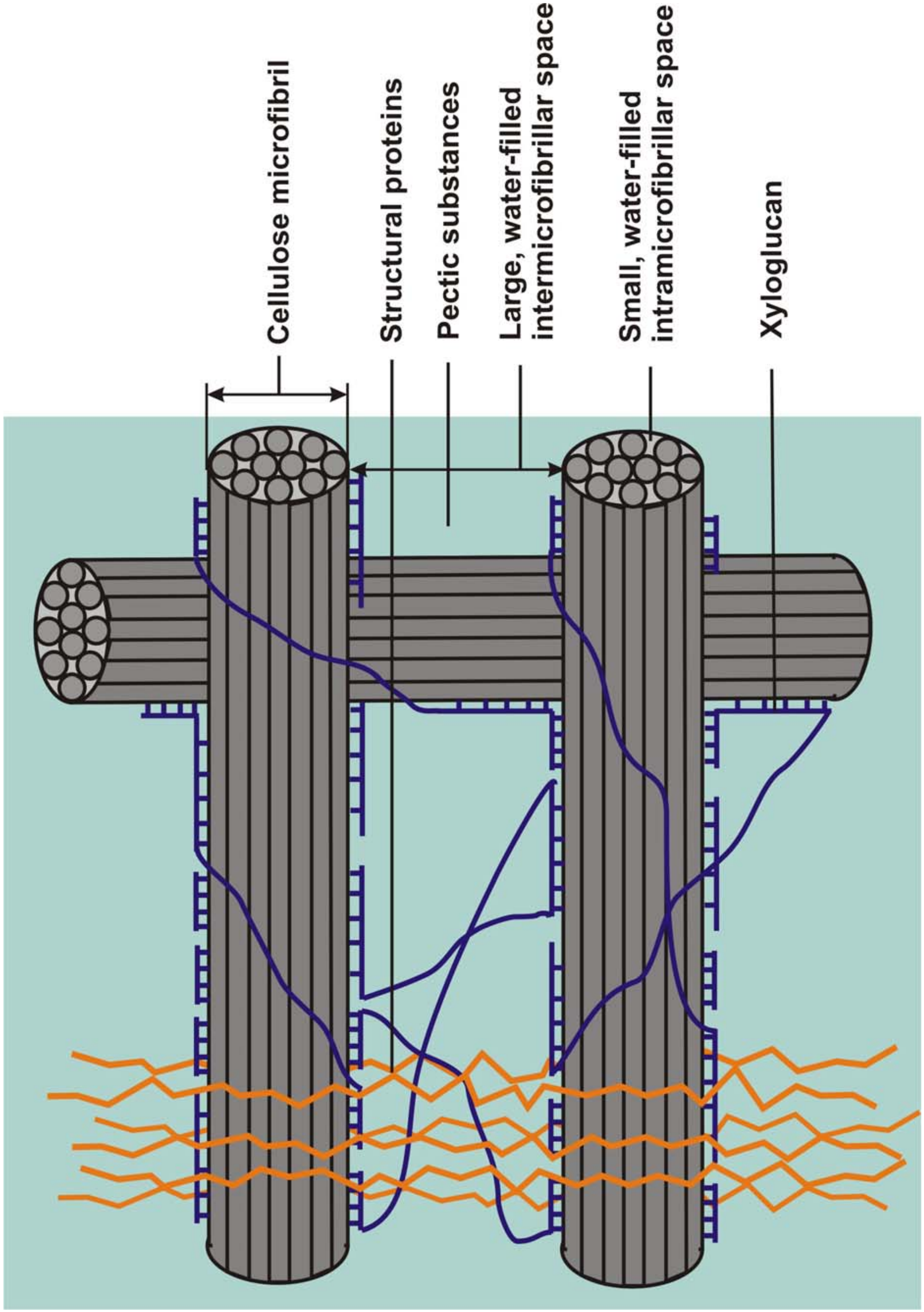
Cellulose microfibril
Structural proteins
Pectic substances
Large, water-filled intermicrofibrillar space
Small, water-filled intramicrofibrillar space
Xyloglucan

composition of this structure includes a prominent amount of lignin in addition to suberin (Schreiber et al., 1994; Schreiber, 1996; Zeier et al., 1999a and b).

1.3.2 Permeability of cell walls

The radial pathways of water and ions through the root can be described as apoplastic, symplastic, or transcellular (Peterson et al., 1999). Movement through the cell wall is a typical apoplastic transport, and this is frequently altered by the deposition of suberin. There have been many studies of suberized walls (especially those with Casparian bands) with respect to their permeability to fluorescent dyes, ions, and heavy metals. Robards and Robb (1972, 1974), Nagahashi and Thomson (1974), Peterson et al. (1986) and Lehmann et al. (2000) found that the suberized Casparian bands were impermeable to the heavy metals such as uranyl and lanthanum. The physical barrier property of the Casparian bands for ions was documented by Peterson (1987) and Cholewa and Peterson (2004) using sulphate and calcium ions, respectively. Apoplastic fluorescent tracers such as Tinopal CBS, PTS (Peterson et al., 1981), Calcofluor white M2R (cellufluor, Peterson and Perumalla, 1984), and berberine (Enstone, 1988; Enstone and Peterson, 1992a and b; Aloni et al., 1998) were used to show that the Casparian bands block the apoplastic movement of these dyes. Unlike the Casparian bands, the permeability of the suberin lamellae has been seldom investigated; only Evert et al. (1985) used tracer ions to determine the physiological barrier-property of this wall modification to the movement of ions in leaves.

One of the objectives of the present study was to compare the epidermal walls of soybean root with other suberized walls by determining their permeability. For this purpose, fluorescent apoplastic tracers were employed. One of the fluorescent procedures involving berberine was developed by Enstone and Peterson (1992a and b) to probe the permeability of the root apoplast. This technique is based on the mobility of the apoplastic dye berberine; in basic solution, this dye is unable to cross a membrane but it is mobile in unmodified plant cell walls. It can be precipitated by thiocyanate to form fluorescent crystals in unmodified walls. The chemical reaction is as followed:

berberine hemisulphate + potassium thiocyanate → berberine thiocyanate + potassium sulphate
(fluorescent crystals)

This technique provides a rapid way to detect the apoplastic pathway of the berberine and locate the barriers to its movement. Because berberine (with a molecular weight of 336) is much larger than water and ions, it can be assumed that the pore size of walls that allowed berberine movement would also be large enough for the movement of water and ions. Since the lumens of dead cells are part of apoplastic pathway, the viability of the epidermal cells was also determined. Therefore, the testing of wall permeability could be achieved with the above technique.

1.3.3 Measuring pore sizes in walls

Within cell walls, the intermicrofibrillar spaces are the pathway for water and ions. The movement of these molecules is controlled by the sizes of the pores and the charges of the wall. Therefore, measuring the pore size is relevant to the permeability of walls. There are only a few methods available to establish the diameter of the pores. Carpita et al. (1979) developed a solute exclusion technique to determine the limiting diameters of pores in the walls of root hair cells, cultured cells, and palisade parenchyma cells, and obtained values that ranged from 3.5-5.2 nm. Tepfer and Taylor (1981) measured the permeability of the plant cell walls by gel filtration chromatography. O'Driscoll et al. (1993) used both electron opaque (colloidal gold) and fluorescent (FITC-dextran) markers to measure the porosity of *Morinda citrifolia* cell walls; values ranged from 2.5 to 5.7 nm. In the present study, the solute exclusion of polyethylene glycol (PEG) method modified from Carpita et al. (1979) was used to estimate the pore diameters of the epidermal walls.

The solute exclusion technique involves observation of plasmolyzed and cytorrhyzed cells in PEG solutions with a range of different molecular weights (Fig. 1.4). When a cell is bathed in a solution with an osmotic potential lower than the water potential of the vacuole, water moves from within the cell to the external solution. If the molecules of the solute in the external solution are small enough to penetrate through the cell wall pores and thus contact the plasma membrane, plasmolysis (the pulling away of the plasma membrane from the cell wall) occurs (Fig. 1.4B). However, if the external solute molecules are too large to diffuse inward through the wall pores, a net movement of water out of the whole cell (including the wall) occurs, and the entire cell, including the wall, shrinks, which results in cytorrhysis. In the present study, the solute exclusion technique was employed on whole soybean root segments. The cells of the samples were first plasmolyzed to reduce their turgor pressure to zero. When these cells cytorrhized, the outer and inner tangential walls of the epidermis moved closer to each other and the vacuoles appeared to increase in size. The protoplasts of the cells, including the vacuoles, then collapsed (Fig. 1.4C). Therefore, the largest pore size within a wall can be determined by testing PEG of various molecular sizes and observing whether the cell undergoes plasmolysis or cytorrhysis. As stated by Carpita et al. (1979), “the maximum pore diameter should be equivalent to the diameter of the largest molecule capable of causing plasmolysis.”

Figure 1.4 Schematic sectional views of cells in a tissue undergoing plasmolysis and cytorrhysis.

Top row of cells indicate schematic surface view of epidermis. Bottom row of cells indicate diagrammatic view of cross sections of root epidermis. **A** Under normal conditions, the plasma membrane of the protoplast is tightly appressed to the wall. **B** When immersed in a solution of low osmotic potential, the vacuole loses water and the plasma membrane pulls away from the cell wall, resulting in plasmolysis. **C** When immersed in a solution of the same low osmotic potential, but in which the molecules of the solute are too large to enter the cell wall, water moves out of the vacuole, the outer and inner tangential walls of the epidermis move closer to each other, and the vacuoles appear to increase in size. The protoplasts of the cells, including the vacuoles, then collapse, resulting in cytorhysis.

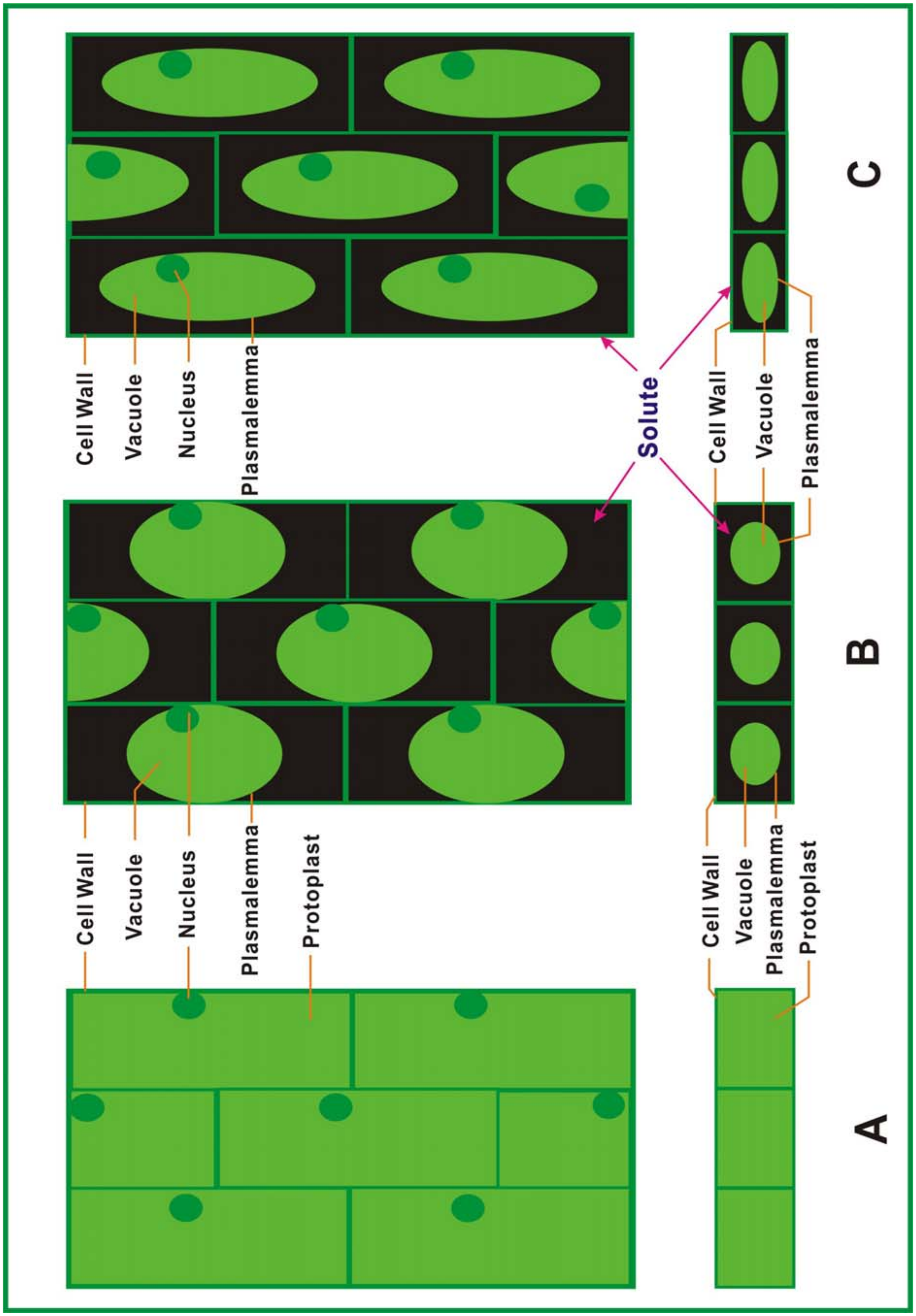
Cell Wall
Vacuole
Nucleus
Plasmalemma
Protoplast
Cell Wall
Vacuole
Plasmalemma
Protoplast
A
Cell Wall
Vacuole
Nucleus
Plasmalemma
Solute
Cell Wall
Vacuole
Plasmalemma
B
C

1.4 Chemical nature of suberized walls relative to pathogen resistance

1.4.1 Chemical components and structural model of suberin

Suberin, like lignin, is one of the complex biopolymers that can be found in specialized plant cell walls. However, suberin has received less attention than lignin that has been studied for over a century (Esau, 1965). The earlier workers intermixed the terms of cutin and suberin (see Peterson et al., 1978). However, in the late 1970s and early 1980s, Kolattukudy and co-workers pointed out the differences between these two polymers based on ultrastructural and chemical analyses of enzyme-digested plant tissues (Kolattukudy and Agrawal, 1974; Espelie et al., 1980; Kolattukudy 1980 and 1984). The chemical components of suberin can be divided into two major parts, i.e. lipids and phenols. The classic finding from chemical analyses of earlier workers was a high content of phenolic substances, a high proportion of ω-hydroxy acids, the corresponding α,ω-dicarboxylic acids and carboxylic acids, as well as alcohols containing more than 18 carbon atoms are characteristic of suberin and distinguish it from cutin (Kolattukudy and Agrawal, 1974; see Kolattukudy, 1980). In the 1990s, Bernards and co-workers introduced a new perspective regarding the phenolic matrix in suberized walls and pointed out that the suberin poly(aromatic) domain is unique and distinct from lignin (Bernards et al., 1995; Bernards and Lewis, 1998). They revealed that hydroxycinnamic acids (especially ferulic acid) along with monolignols are the major components of suberized walls (see Bernards, 2002).

There are two speculative suberin models to explain the electron-dense and electron-lucent bands seen in suberin lamellae. According to Kolattukudy (1980 and 1984), the phenolics and aliphatics are cross-linked, and occur in layers in between the cell wall and plasma membrane. Phenolics constitute the dark bands while aliphatics embedded in the waxes are responsible for the light bands observed in the electron micrographs. Bernards (2002) proposed another model for the structure of potato suberin, in which both suberin poly(aliphatic) domain and suberin poly(aromatic) domain are spatially distinct but covalently linked. Furthermore, the aromatic domain is proposed to be restricted to the primary cell wall while the aliphatic domain stacks with esterified phenolics to display light and dark bilayers between the cell wall and plasma membrane (Fig. 1.5).

1.4.2 Identification of suberin

1.4.2.1 Histochemical tests

Experimental approaches to identify suberin are based on its chemical components and their linkage to form a polymer. Peterson et al. (1978) and Wilson and Peterson (1983) have utilized various histochemical tests, such as the sudan dye family for lipids, Prussian blue and ferric chloride for phenols, and acid digestion for the suberin polymer, coupled with electron microscopy to show that 21 of the 27 plant species tested have suberized epidermal walls. Therefore, relevant histochemical techniques for investigation of lipids and phenols, and acid digestions to determine the polymer property were performed in the present study. In addition, detailed wall morphology was revealed with the use of a transmission electron microscope. These studies provided a basis for further chemical analyses.

1.4.2.2 Chemical analyses

Sophisticated depolymerization techniques coupled with gas chromatography and mass spectrometry (GC-MS) have made it possible to provide quantitative and qualitative monomer composition data from the complex polymers of modified walls. However, the application of these techniques to suberin has been limited to suberized potato tuber skin for a long time. In the 1990s, Schreiber and his co-workers reported the chemical composition of Casparian bands and suberin lamellae from isolated root endodermal, and a mixture of exodermal and epidermal walls. There is still no report on the chemical composition of modified epidermal walls alone. The present work is the first chemical analyses of these walls alone.

The experimental approach (Fig. 1.6) was based on the following considerations. Suberin is tightly attached to other components of the cell wall. Therefore, enzymatic digestion was employed to remove the wall carbohydrates and pectic substances. Next, organic solvents, i.e. chloroform and methanol, were used to extract the non-polymerized waxes and other soluble compounds from the enzyme-digested wall residue. Relevant degradation methods for aliphatic (e.g., boron trifluoride-methanol) and aromatic (e.g., microscale alkaline nitrobenzene oxidation) suberin domains were applied to depolymerize the polymer into its constitutive monomers. These were subjected to GC-MS analysis to identify the monomers based on a comparison of retention times with those of authentic standards (Kolattukudy, 1978).

Two depolymerization techniques were employed in the present study, i.e. boron trifluoride-methanol (BF_3-MeOH) transesterification (Fig. 1.7) and microscale alkaline nitrobenzene oxidation (NBO, Fig. 1.8). The ester bonds of the suberin aliphatic matrix and esterified aromatic polymer were cleaved with the BF_3-MeOH transesterification method and transformed into methoxy groups, while the hydroxyl functional groups were transformed into the corresponding trimethylsilyl (TMS) ethers with the use of BSTFA (N,N-bis-trimethylsilyltrifluoroacetamide). Both methyl- and TMS- derivatives can be detected with GC-MS (Kolattukudy, 1978; see Bernards, 2002, Fig. 1.7). NBO was initially introduced in 1939 for qualitatively and quantitatively determining lignin monomers (Chen, 1992) and has also been employed to depolymerize the aromatic portion of suberin, which yields mainly benzaldehydes (see Bernards, 2002, Fig. 1.8).

Figure 1.5 A schematic model of a suberin lamella.

This model displays the chemical nature and structure of a portion of a suberin lamella in suberized potato tuber skin. In the primary wall, the suberin (poly)phenolic domain is covalently attached to carbohydrate units (C). The suberin (poly)aliphatic domain is predominant between the primary wall and plasma membrane, with esterified “suberin phenolics”. The aliphatic zones would yield the electron-lucent bands (white areas) observed with TEM, while the phenolic-rich zones would yield the electron-dense bands (grey areas). Connections are to the following: C, carbohydrate; P, phenolic; S, suberin (Phenolic or aliphatic). Adapted from Bernards (2002).

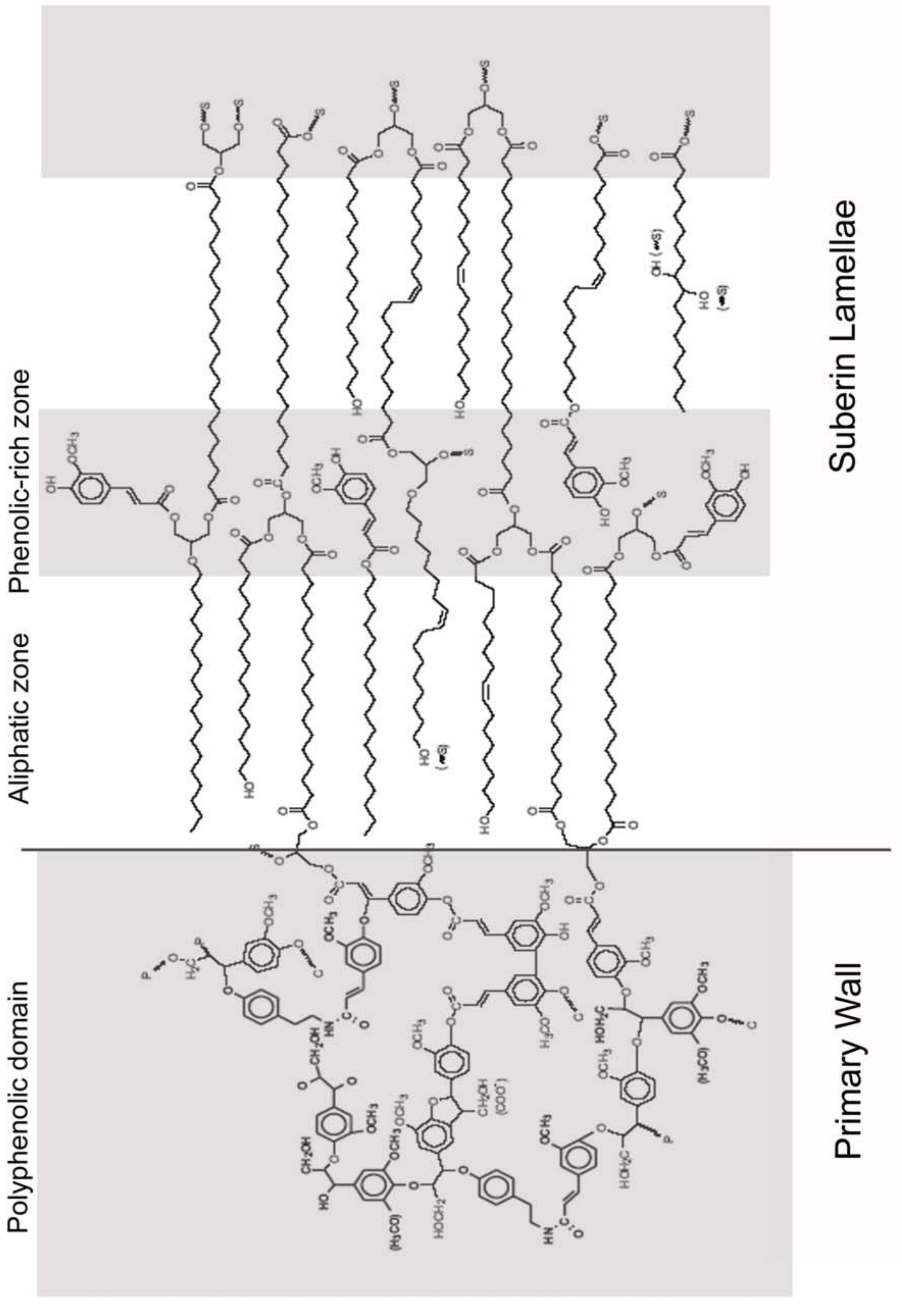
Polyphenolic domain
Aliphatic zone
Phenolic-rich zone
Primary Wall
Suberin Lamellae

Figure 1.6 Schematic illustration of the experimental approach applied for the analysis of isolated epidermal walls of soybean roots.

Root segments were first digested with cellulase and pectinase. Epidermal walls were isolated from the rest of the roots. Organic solvent extraction was applied to remove the non-polymerized waxes from the epidermal walls. BF_3-MeOH transesterification used to depolymerize the poly(aliphatic) component. Ester-linked phenolics were also cleaved into corresponding monomers. Nitrobenzene oxidation method was used to depolymerize the non-ester linked poly(aromatic) domain. All monomers were subjected to chromatographic analysis.

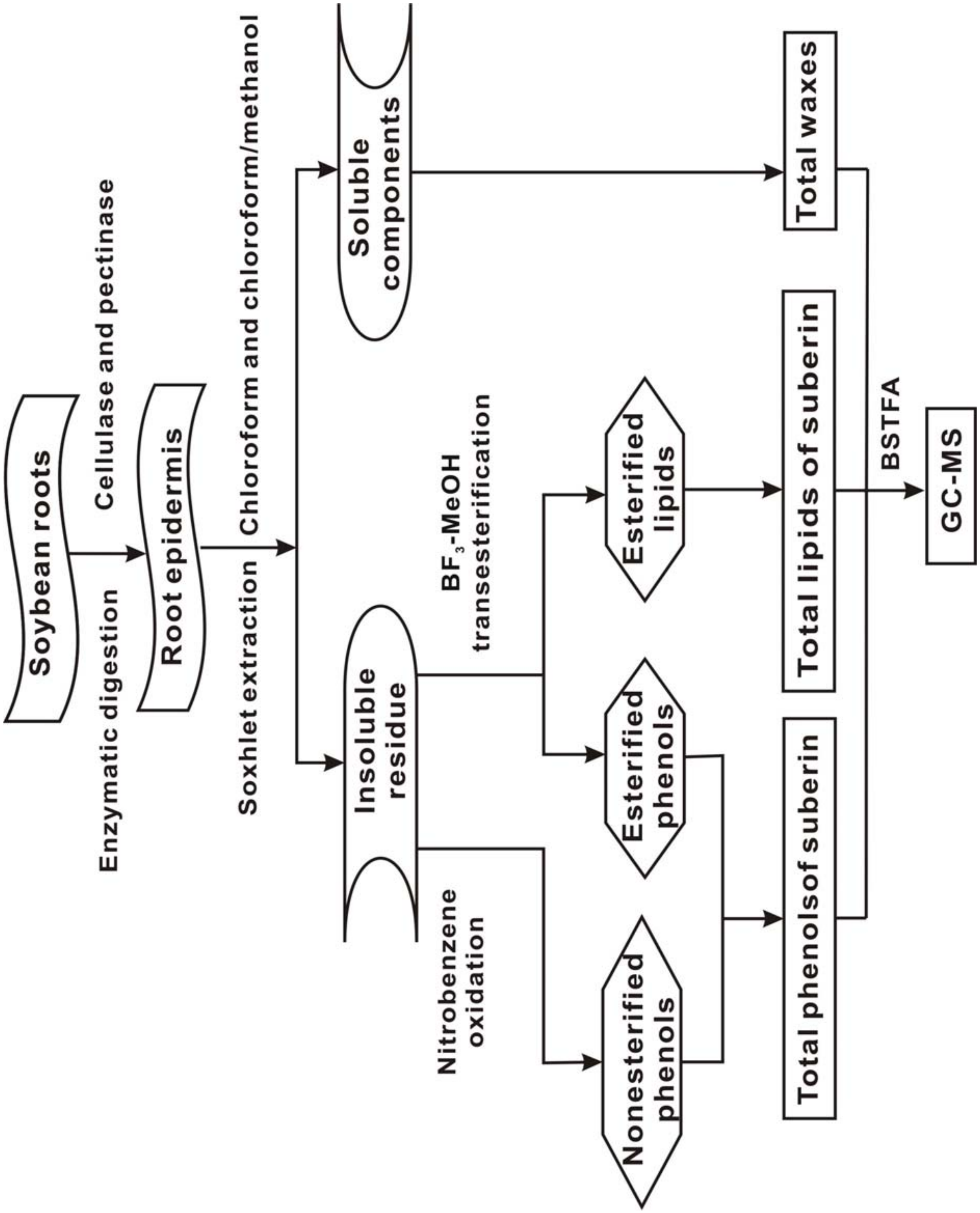
Soybean roots
Enzymatic digestion
Cellulase and pectinase
Root epidermis
Soxhlet extraction
Chloroform and chloroform/methanol
Insoluble residue
Soluble components
Nitrobenzene oxidation
BF_3-MeOH transesterification
Nonesterified phenols
Esterified phenols
Esterified lipids
Total phenolsof suberin
Total lipids of suberin
Total waxes
BSTFA
GC-MS

Figure 1.7 BF_3-MeOH transesterification of poly(aliphatic) components.

A Cleavage of esters (green arrows) with BF_3-MeOH yields methyl esters and free alcohol functional groups (**B**). Transformation of free hydroxyl functional groups into their corresponding trimethylsilane ethers (TMS, orange ovals) with the use of BSTFA yields derivatized aliphatics ready for GC analysis (**C**, personal communication, Mark Bernards, University of Western Ontario, Ontario).

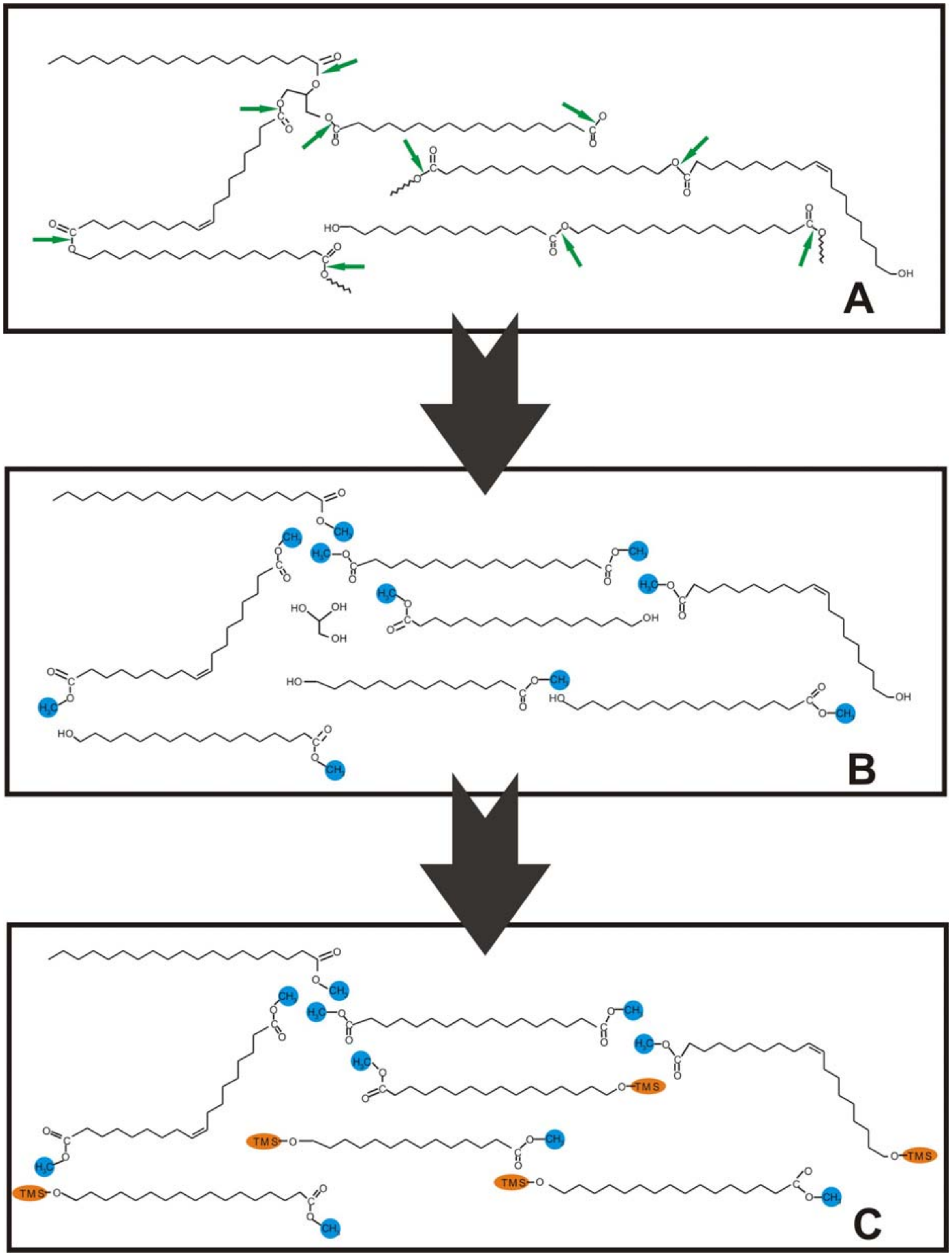
A
B
C
HO
OH
H_3C
CH_3
TMS

Figure 1.8 Schematic microscale alkaline nitrobenzene oxidation (NBO) technique.

R_1 and R_2 indicate the different substitution sites for both monolignols and hydroxycinnamic acids in the polymer (Bernards, 2002).

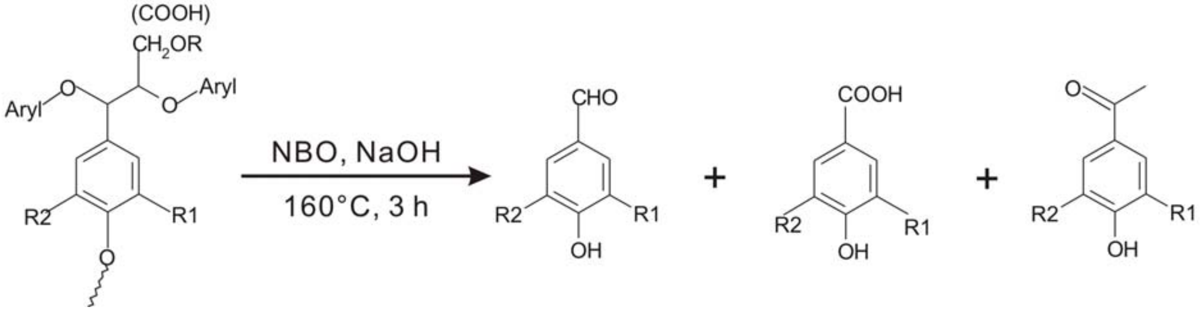

(COOH)
CH2OR
Aryl
O
O
Aryl
R2
R1
O
NBO, NaOH
160°C, 3 h
CHO
R2
R1
OH
+
COOH
R2
R1
OH
+
O
R2
R1
OH

1.4.3 Suberin components relative to pathogen resistance

As described in section 1.3.2, suberized tissues can act as apoplastic barriers to the movement of water and ions. In addition, suberin plays an important role in pathogen resistance (see Kolattukudy, 1980 and 1984). These physiological roles of suberin are made possible by its unique chemical composition, i.e. a complex polymer of lipids and phenols. The hydrophobic (lipophilic) matrix associated with waxes allows it to function as a barrier to solute movement, while the phenolic polymer releases toxic compounds such as cinnamic acids, upon degradation, to provide protection during pathogen invasion (see Kolattukudy, 1980 and 1984). Various investigators have confirmed that the rapid accumulation of phenols at infection sites has antimicrobial activity, and postulated that the rapid accumulation of the cinnamic esters slows the penetration of the pathogen, allowing time for the activation of secondary defense mechanisms (see Vance, 1980; Friend, 1981; Matern and Kneusel, 1988; Nicholson, 1992).

Deposition of suberin in response to infection by pathogens has been shown in some cases. Using a natural pathogen, *Verticillium albo-atrum* to induce coating of xylem vessel walls in two isolines of tomato (one resistant and one susceptible to the pathogen), Robb et al. (1991) found, after chemical analysis of depolymerization products, the vascular coatings of tomato petioles contain mainly suberin. The degree of suberization induced by fungal attack reflected the degree of resistance to this attack, with the amounts of aliphatic suberin components deposited on the walls of a resistant tomato line being many fold higher than those found in a susceptible cultivar. According to Lulai and Corsini (1998), inhibitors of suberin phenolic synthesis in potato tuber prevented development of resistance to infection of *Erwinia carotovora* (a causal organism of bacterial soft rot) and *Fusarium sambucinum* (a causal organism of fungal dry rot). These authors also indicated that the phenolic components may play an antibacterial role to prevent *E. carotovora* invasion, while the aliphatic polymer is needed for resistance to fungal infection by *F. sambucinum*. Kamula et al. (1995) reported that suberin lamellae in the exodermal cells block the invasion of *Fusarium culmorum* into roots of *Zea mays* and *Asparagus officinalis*. There are reports that a well-suberized wound is impenetrable to fungi, perhaps due to both physical (reducing pore sizes) and chemical (releasing toxic compounds) barriers (Kolattukudy and Espelie, 1989). Other reports indicate that older plant organs are resistant to pathogens because of a heavily suberized periderm, whereas very young organs without such protection are susceptible to pathogen attack (Lulai and Corsini, 1998). All this evidence supports the hypothesis that suberin and suberization play a major role in plant defense.

1.5 Soybean root-*Phytophthora sojae* interactions

1.5.1 Soybean

The test species chosen for the present study was soybean (*Glycine max* [L.] Merrill), a versatile and nutritious source of food, and the leading oilseed crop produced and consumed in the world (Wilcox, 2004). Soybean has an annual farm gate value of $645 million in Canada, and estimated 40% of all processed foods in North America contain soybean (personal communication, Dr. Mark Gijzen, Agriculture and Agri-Food Canada, London, Ontario). Furthermore, soybean belongs to a large family of legumes that contribute 94% of the nitrogen required for the world’s annual food production (Adjei et al., 2002). Nitrogen is an essential element for plant growth. However, the supply of nitrogen in the soil is limited, and most plants are unable to utilize the nitrogen gas in the atmosphere. Fortunately, legumes, such as soybean, have a dual capacity for symbiotic nitrogen fixation and nitrate uptake (Sinclair, 2004). Symbiotic nitrogen fixation provides a simple and inexpensive way to provide nitrogen to plants.

1.5.2 *Phytophthora sojae*, a root rot pathogen

Members of the oomycete genus *Phytophthora*, together with groups such as brown algae and diatoms, belong to the Kingdom Stramenopila that is a candidate kingdom, formerly categorized as Protista in the five kingdom system, and as Chromista in the seven kingdom system (Sogin and Silberman, 1998; Campbell et al., 1999; Duncan, 1999; Baldauf, et al., 2000). These fungus-like eukaryotes differ in many ways from true fungi as described by Judelson and Blanco (2005). For example, the major wall components of oomycetes are cellulose (β-1,4-linked glucose), callose (β-1,3-glucose), and β-1,6-linked glucose polymers.

Conversely, the major wall components of true fungi are usually chitin (β-1,4-linked N-acetylglucosamine) and/or chitosan (β-1,4-linked glucosamine), often with other β-1,3, and β-1,6 glucans.

Phytophthora species are major pathogens of innumerable crops; there are more than 50 species causing destructive diseases on thousands of plant species (Kamoun, 2000). For example, late blight of potato caused by *Phytophthora infestans* totally destroyed Ireland's potato crop in the mid-nineteenth century and resulted in widespread poverty, starvation, and emigration. *Phytophthora ramorum* causes "sudden oak death", and has emerged along the Pacific coast of the United States and in Europe (see Judelson and Blanco, 2005). Likewise, *P. cinnamomi* has caused severe epidemics in the jarrah tree forests in Western Australia (van West and Vleeshouwers, 2004).

Phytophthora sojae (formerly known as *Phytophthora megasperma* f. sp. *glycinea*) causes damping-off, and root and stem rot of soybean; and these are now worldwide diseases (Agrios, 1997; Wrather et al., 1997). Kaufmann and Gerdemann (1958) were the first to describe the causal agent of root rot even though it was first noted as early as 1948. *Phytophthora sojae* has a narrow host range and is a specialized pathogen on soybean and some lupin species (Grau et al., 2004). This soilborne homothallic oomycete produces motile zoospores that spread in water and are attracted to soybean root exudates (Gijzen, 2004). Once on the root surface, the zoospores encyst and begin to germinate. Hyphae penetrate into the root directly through the middle lamella of the epidermal cells without the formation of appressoria (Enkerli et al., 1997 and Kamoun, 2000). In susceptible cultivars, the hyphae advance to colonize the vascular tissues, and numerous oospores are produced. These can survive for long periods of time in soil and may be spread by animals or machinery (Gijzen, 2004). Water-saturated soil and temperatures of 25 to 30^{o}C are ideal conditions for oospore germination and sporangia production (Grau et al., 2004).

P. sojae root rot is a serious and endemic disease that is prevalent in Ontario. Currently, this disease is managed by developing cultivars that are resistant or tolerant to pathogen strains isolated from the field. It remains unknown whether there is any variation in the extent or nature of suberized cells among different cultivars prior to infection, and how this may affect disease resistance.

1.6 Research objectives

The first objective of the present research is to identify the substance modifying the root epidermal walls of soybean. The second objective is to determine whether or not quantitative or qualitative differences of the wall modifying substance are related to the resistance of the root to pathogen attack. The chemical nature of root epidermal walls will be determined with histochemical tests coupled with chemical analyses. The latter will include chemical depolymerizations in combination with chromatography. Those analyses will provide a qualitative and quantitative description of the wall modification of two soybean cultivars varying in their quantitative resistance to *P. sojae* root rot. Early stages of infection will be observed to determine whether or not suberin preexisting in the epidermal walls correlates with differences in pathogen resistance.

2 Materials and Methods

2.1 Plant material and growth conditions

Seeds of soybean (*Glycine max* [L.] Merr.) cultivars Conrad and OX 760-6 used in this study were obtained from field-grown plants at Agriculture and Agri-Food Canada in London, Ontario in 2003. The two cultivars have different levels of quantitative resistance (also called partial resistance, tolerance, or QTL resistance) to *Phytophthora sojae* (Kaufmann and Gerdemann, 1958). Cultivar (cv.) Conrad is resistant to *P.sojae* in the field, while cv. OX 760-6, a breeding line developed at the Greenhouse and Processing Crops Research Centre, Agriculture and Agri-Food Canada, Harrow, is susceptible to this pathogenic oomycete under field conditions (personal communication, Mark Gijzen, Agriculture and Agri-Food Canada, London, Ontario).

Seeds were soaked overnight in tap water and then planted in 195-mm-diameter plastic pots (195 mm depth) in vermiculite (#2A, Therm-O-Rock East, Inc. Canada) saturated with tap water. All seeds were positioned with the micropyle above the hilum to obtain straight roots, and then covered to a depth of one centimeter with vermiculite. They were sprouted in a glasshouse with alternating light and dark, approximately 16 h at 25^{o}C and 8 h at 20^{o}C, respectively, under 60% relative humidity. From day 2 to day 6 after planting, six seedlings were uprooted every day and the primary root lengths were measured. By day 6, the main roots were about 100 mm long and were used for the following experiments.

2.2 Histochemical detection of suberin

There is no single histochemical test for suberin. Suberin was considered to be present when the material stains positively for phenolics and lipids, and resists acid digestion (Peterson et al., 1978; Wilson and Peterson, 1983).

2.2.1 Phenol tests

2.2.1.1 Autofluorescence

Six days after planting, seedlings germinated as described above were uprooted from the pots and stored in containers with tap water. The vermiculite was washed from the roots. Free-hand sections were taken from three primary roots at distances of 5, 15, 25, 50, and 100 mm from the root tips, mounted in water, and then observed under white light with differential interference contrast (DIC) optics and viewed with blue light (BP 450-490 nm, FT 510 nm, LP 520 nm, see section 2.8). The presence of phenolic substances can be clearly recognized by the yellow autofluorescence observed under blue excitation (Peterson et al., 1978; Bernards and Lewis, 1998).

2.2.1.2 Hoepfner-Vorsatz test

Free-hand sections were placed in small section holders that were made of Canemco Beem Capsules (No. 00, Cat.No: EE108-2, Canton de Gore, Quebec, Canada). Each capsule has a body and a cap. The capsule body is composed of a cylinder with a cone bottom. The cone part and half of the cap were cut off. A piece of nylon mesh was placed between the lid and tube body to make a mesh-bottomed section holder (Fig. 2.1). This holder can be easily transferred from solution to solution without losing experimental sections. Root sections were transferred into an aqueous mixture of 2 mL 10% sodium nitrite and 2 mL 10% acetic acid for three min. They were mounted in 2 M sodium hydroxide and viewed with white light. A positive reaction produces a range of colors from red to yellow, depending on the phenolic groups present in the plant material (Reeve, 1951; Ling-Lee et al., 1977).

2.2.2 Lipid testing with sudan red 7B

The lipophilic stain sudan red 7B (C. I. 26050, Sigma Chemical Co., St. Louis, MO, USA) was prepared according to Brundrett et al. (1991). Fresh root sections of soybean in section holders were immersed in 0.1% sudan red 7B for two h at room temperature. Holders were removed from the staining solution, blotted dry, and rinsed briefly with three changes of distilled water. The sections were mounted in 75% glycerol and observed the next day with white light. Lipid deposits stain red.

2.2.3 Acid digestion

Cross-sections of soybean root were soaked on a slide with concentrated (95-98%) sulfuric acid for different periods of time. Sections to be acid-digested were viewed with white light and the condition of the cell walls remaining after the acid treatment was observed.

2.2.4 Transmission electron microscopy (TEM)

The TEM procedure was the same as described by Ma and Peterson (2000). Segments of root approximately 1 mm long were taken at distances of 5, 15, 25, 50, and 100 mm from the root tips, prefixed with a mixture of 3% glutaraldehyde and 3% paraformaldehyde in 0.2 M sodium phosphate buffer (pH 6.8), and stored at 4°C overnight. Fixed segments were rinsed in buffer and postfixed overnight in 0.5% osmium tetroxide (OsO_4) in the same buffer at 4°C. A vacuum was used to facilitate the penetration of OsO_4 into the sections. Dehydration was achieved with ethanol through a 10%-step graded series, and specimens were then embedded in Spurr resin with a graded series to absolute. Polymerization occurred at 70°C for 24 h. Semi-thin (100 nm) sections were cut with glass knives (made with a LKB KnifeMaker) on a Reichert Ultracut E ultramicrotome (Leica AG Reichert Division, Austria) and stained with 0.05% toluidine blue O (TBO, pH 11, C. I. 52040, Fisher Scientific Co., New Jersey, USA) in 0.05% sodium borate for light microscopy. Ultrathin sections (80 nm) for electron microscopy were collected on Formvar-coated, 75-mesh, hexagonal, copper grids, post-stained in 2% uranyl acetate and lead citrate in a CO_2-free chamber, and observed and photographed with a Philips CM 10 transmission electron microscope at 60 kV. Photos were captured on Kodak Electron Image Film SO-163.

Figure 2.1 Construction of section holders.

A Beem Capsules (No. 00, Cat.No EE108-2, Canton de Gore, Quebec, Canada) have a body and a cap. The capsule body is composed of a cylinder with a cone bottom. **B** The cone part and half of the cap were cut off. **C** A piece of nylon mesh was placed in between the lid and tube body to make a mesh-bottomed section holder.

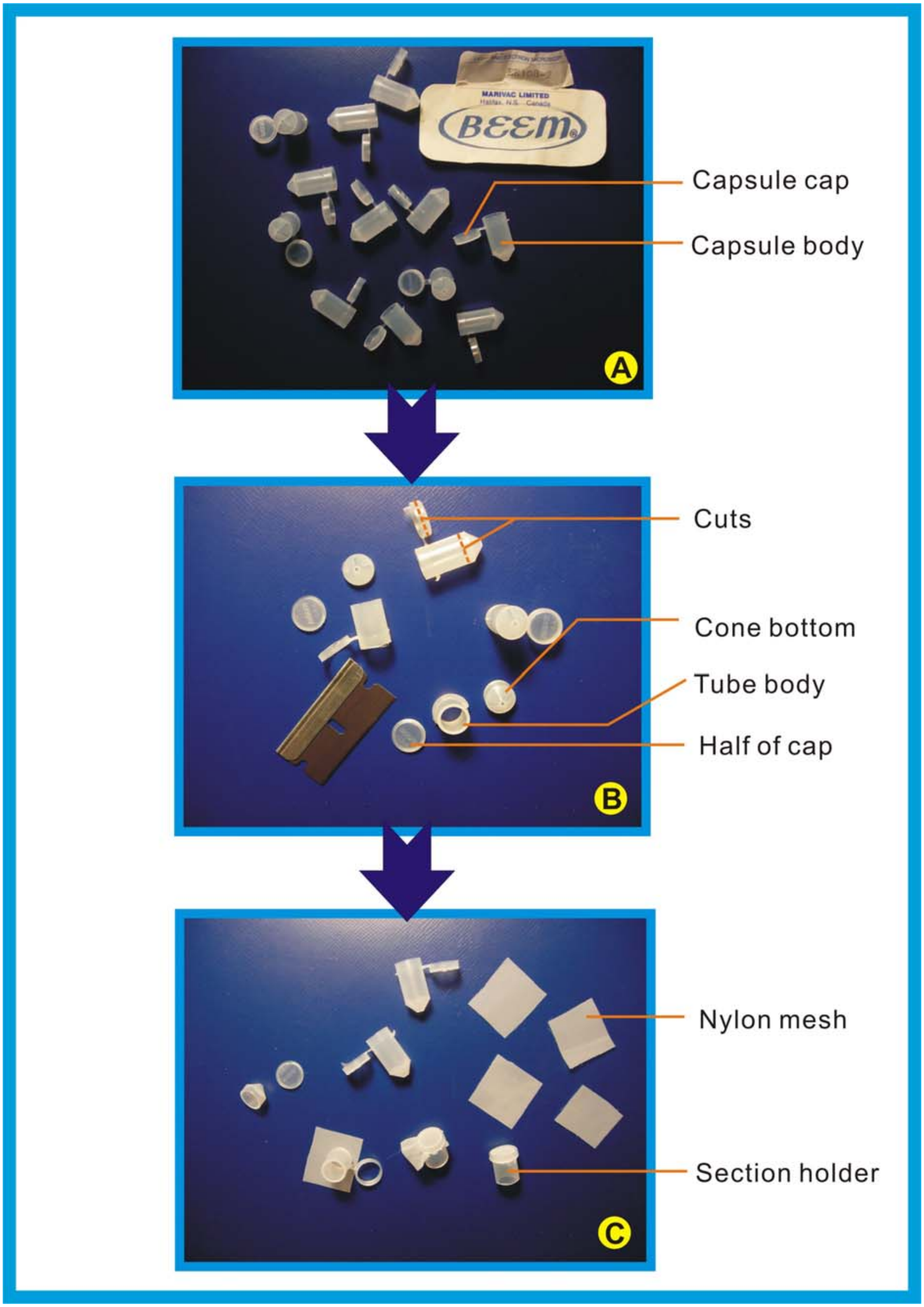
MARIVAC LIMITED
Halifax, N.S. Canada
BEEM
Capsule cap
Capsule body
A
Cuts
Cone bottom
Tube body
Half of cap
B
Nylon mesh
Section holder
C

2.3 Chemical analyses

2.3.1 Plant material

Soybean roots employed in this study were grown in the Department of Biology greenhouse at the University of Western Ontario, London, Ontario. Seeds of two soybean cultivars (Conrad and OX 760-6) were germinated in plastic pots (155 mm diameter) filled with vermiculite. The seedlings were watered with ¼ strength Knop's solution (Loomis and Schull, 1937) four d after germination. Ten days after planting, the main roots were over 200 mm long and were harvested for chemical analyses.

2.3.2 Isolation of epidermal cell walls

Intact roots were cut into 10-mm segments and separated into three categories: Region I (0-70 mm), Region II (90-160 mm), and Region III (160-200 mm). These segments were vacuum-infiltrated with 5% (w/v) pectinase (*Aspergillus niger*, 25 U mg^{-1}, Sigma Chemical Co., St. Louis, MO, USA) and 5% (w/v) cellulase (*Aspergillus niger*, 1.92 U mg^{-1}, Sigma Chemical Co., St. Louis, MO, USA) dissolved in 0.05 M sodium acetate buffer (pH 4) and incubated for 30 min at room temperature. The epidermal layer was carefully lifted and separated from the root with fine forceps under a dissecting microscope and returned to the enzymatic solution for an additional two weeks to remove as much of the wall carbohydrates as possible. The solution was changed every three to five d.

2.3.3 Scanning electron microscopy

Cell wall materials that had been digested with cellulase and pectinase were rinsed with deionized water several times and dehydrated through a graded series of acetone solutions (20% steps) to absolute. Critical point drying was performed with liquid CO_2 as the transitional fluid on a Denton Critical Point Drying Apparatus (DCP-1, Denton Vacuum Co., Cherry Hill, New Jersey, USA). The specimens were mounted on stubs, coated with a 10-20-nm-thick layer of gold in a Poaron E5000C PS3 Sputter Coater (Polaron Equipment

Co., Watford, England), and then visualized in a Hitachi S-570 scanning electron microscope. Photos were taken on 35 mm ILFORF PanF Plus film, ISO 50.

2.3.4 Extraction of cell wall material and BF_3-MeOH transesterification of poly(aliphatics)

Enzymatically isolated epidermal wall material obtained as described above was washed several times with deionized water and extracted with chloroform in a Soxhlet extractor overnight, followed by extraction with chloroform/methanol (2:1, v/v) for three h, twice, and then air-dried. The dry material was stored at –20°C for further use. The solvent with dissolved material from the chloroform/methanol extraction was evaporated on a rotary evaporator and subjected to chromatographic analysis (see section 2.6.6).

Chemical degradation of epidermal walls by means of transesterification was performed according to Kolattukudy and Agrawal (1974). The dry material was ground in liquid nitrogen and transferred to vials in approximately 10 mg portions. Samples were depolymerized with 200 µL 14% BF_3-MeOH at 70°C in a water bath for 24 h after adding 100 µL triacontane (1 mg/mL in hexane) as an internal standard. Samples were diluted with water (800 µL) and extracted twice with 1 mL anhydrous ethyl ether. The combined ether phases were evaporated under a stream of nitrogen, and the dried residue derivatized and analyzed by GC (see section 2.6.6). BF_3-MeOH transesterification releases monomers cross-linked by ester bonds and transforms acids into their corresponding methyl esters (Riederer and Schönherr, 1986).

2.3.5 Extraction of cell wall material and nitrobenzene oxidation of poly(phenolics)

Enzyme-digested epidermal walls prepared for nitrobenzene oxidation were first extracted with chloroform/methanol (2:1, v/v) overnight, followed by extraction with 80% methanol for 3 h, and then acetone (100%) for one h. The residue was air-dried and stored at –20°C until analyzed.

Microscale alkaline nitrobenzene oxidation (NBO) was performed according to Meyer et al. (1998). Briefly, dry samples were first saponified with 1.0 M NaOH at 37°C for 24 h, washed three times with water, once with 80% ethanol, once with acetone, and then air-dried. Samples (5 mg) were combined with 500 μL of 2 M NaOH and 25 μL of nitrobenzene and cooked at 160°C for three h. After cooling, 5 μL of a 20-mg/mL solution of 3-ethoxy-4-hydroxybenzaldehyde in pyridine was added into the samples as an internal standard. The mixture was extracted twice with 1 mL dichloromethane to remove the excess nitrobenzene. The oxidation mixture was acidified to pH 2 with concentrated HCl and further extracted twice with 900 μL of ether. The combined ether phase was dried with anhydrous sodium sulfate. Prior to GC analysis, samples were derivatized (see section 2.6.6).

2.3.6 Chromatographic analysis

The derivatives from BF_3-MeOH transesterification and NBO were dissolved in 100-μL pyridine and reacted with 100-μL BSTFA in a 70^{o}C water bath for 40 min. The combined methyl ester and TMS ether derivatives from BF_3-MeOH transesterification or TMS ether derivatives from NBO were quantitatively analyzed by GC on a Varian CP-3800 Gas Chromatograph combined with an ion trap mass spectrometer (GC-MS) and qualitatively analyzed by gas chromatography equipped with a flame ionization detector (GC-FID). The GC was equipped with a pair of CP-Sil 5 CB Low bleed MS columns (WCOT silica 30 m × 0.25 mm ID), one in line with the MS and the other in line with the FID oven at 300^{o}C. Samples (1 μL) were injected twice (once to each column) in splitless mode and simultaneously eluted with one of the following oven temperature program: (1) For BF_3-MeOH products, the initial oven temperature of 80^{o}C was held for 2 min, followed by a rapid increase (40.0^{o}C/min) to 200^{o}C, a 2 min hold at 200^{o}C and a slower increase (3.0^{o}C/min) to 300^{o}C. The final temperature was held for just over 9 min for a total run time of 50 min. (2) NBO products, the initial oven temperature of 140^{o}C was held for 1 min, followed by an increase (12.5^{o}C/min) to 270^{o}C. The final temperature was held for 5 min for a total run time of 16.4 min. High purity He was used as a carrier gas at 1 mL/min. Compounds were identified on the basis of their co-elution with authentic standards and their

EI-mass spectra (50-650 amu). Quantification was based on FID peak areas and independently derived calibration curves for each standard.

2.3.7 Statistics

Two parallel trials were performed for both cultivars. There were three replicates for each chemical analysis trial. Analysis of the raw data was performed with Student Edition of Statistix Version 2.0 (Analytical software, P.O., Box 12185, Tallahasse, Fl.). Data were first analyzed using a general analysis of variance (ANOVA); where treatment effects were significant, Fisher's least significant difference (LSD) was employed to compare the means.

2.4 Epidermal viability test

2.4.1 Evan's blue

To minimize the handling of roots, root systems of intact six-day-old seedlings removed from vermiculite were directly immersed in 0.5% Evan's blue (C. I. 23860, Fisher Scientific Co., New Jersey, USA) in distilled water for 15 min. They were rinsed briefly with distilled water. Seven segments were cut at 10-mm intervals along intact roots beginning 25 mm from the root tips. Segments were bisected, mounted in distilled water with the epidermal side up, and observed with white light. A blue staining of the nucleus and cytoplasm indicates a dead cell; lack of staining indicates viability (Gaff and Okong'O-Ogola, 1971). Segments were always handled at the ends with fine forceps; these zones were never included in the assessment of epidermal vitality. The numbers of living and dead epidermal cells in one microscope field at a magnification of 200-fold were counted (Barrowclough and Peterson, 1994).

2.4.2 Disodium fluorescein (uranin)

Epidermal cell viability was also determined with disodium fluorescein (uranin, C. I. 45350, J. T. Baker Chemical Co., Philipsburg, New Jersey, USA) that was applied at 0.01% in 0.067 M phosphate buffer (pH 5.2) for 15 min. After being rinsed twice with 0.067 M phosphate buffer, bisected roots were viewed with a confocal laser scanning microscope and a 10 × objective (CLSM, Carl Zeiss LSM 510, version 3.2 SP2, Carl Zeiss Canada, Mississauga, Ontario, Canada). Excitation lines of an argon ion laser of 488 nm were used with the META channel (ChS) in the single-track facility of the microscope. Epidermal cells with an accumulation of uranin in the nuclei and cytoplasms are living cells (Stadelmann and Kinzel, 1972).

2.5 Permeability studies

2.5.1 Cellufluor tracer experiments

Entire six-day-old roots were immersed into the apoplastic, fluorescent dye cellufluor (formerly called Calcofluor white M2R, Polysciences Inc., Warrington, PA.). Cellufluor was applied at 0.01% in 0.02 M phosphate buffer (pH 7.8). Prior to the treatment, an Acrodisc PF syringe filter with a non-cellulose membrane (0.2 µm pores) was used to filter the cellufluor solution to remove the precipitates of this dye. Roots were placed in a test tube (150 mm depth, 60 mL capacity) of cellufluor for 12 h. The tubes were covered with aluminum foil since cellufluor is sensitive to light. Roots were well rinsed with running tap water for more than two h. Cross-sections were cut from the three regions of the entire root, i.e. 0-20 mm from the root tip, 20-40 mm from the root tip, and 80-100 mm from the root tip, mounted in 70% glycerine, and observed immediately under violet (BP 395-440 nm, FT 460 nm, LP 470 nm) or ultraviolet light (G 365 nm, FT 395 nm, LP 420 nm, Fischer et al., 1985; Enstone, 1988).

2.5.2 Berberine–thiocyanate tracer experiments

Roots were cut into segments of 20 mm from three regions: 0-20 mm, 20-40 mm, and 80-100 mm from the apex. Both ends of the segments were first blotted dry and then sealed with molten sticky wax. After being placed in 0.05% (w/v) berberine hemisulphate (BS, Sigma Chemical Co., St. Louis, MO, USA) in 0.05 M phosphate buffer (pH 6.0) for 30 min, segments were removed from the berberine, rinsed briefly with buffer, lightly blotted, and placed in 0.05 M potassium thiocyanate (KSCN) for one h. Segments were sectioned, mounted in KSCN, and observed under violet light (BP 395-440 nm, FT 460 nm, LP 470 nm, Enstone, 1988).

2.6 Measurement of intermicrofibrillar space sizes

Seeds were planted as described above. Roots were cut into 10-mm segments starting from a distance of 10 mm above the root tips. Segments were first plasmolyzed with 0.5 M mannitol for 30 min, gently rinsed with 0.3 M NaCl that was dissolved in the phosphate buffer solution (pH 5.2, salt-buffer solution), and then stained with 0.01% uranin in salt-buffer solution (in order to keep cells plasmolyzed) for 10 min. The stained root segments were bisected, mounted in a drop of the salt-buffer solution, and viewed under violet light (BP 395-440 nm, FT 460 nm, LP 470 nm) with the use of the Zeiss Axiophot microscope at 400-fold magnification. PEGs with different molecular weights were dissolved in the salt-buffer solution (pH 5.2). Since the concentrations of 0.3 and 0.4 M NaCl plasmolyzed the epidermal cells of soybean root, the concentrations of PEG solutions were determined by the osmotic pressure of NaCl. According to Money (1989), the approximate osmotic pressure of 0.3-0.4 M NaCl is 1.5 MPa. This osmotic pressure corresponded to the different molarities of various PEG solutions (Table 2.1, Money, 1989). PEG solutions were added dropwise to one edge of the coverslip and drawn between the coverslip and the slide with the use of a piece of bibulous paper (a strongly absorbent paper) to the other edge of the coverslip. If no change occurred, the PEG treatment for a section was scored as "plasmolysis" and if the vacuoles appeared to increase in size, the PEG treatment for a section was scored as "cytorrhysis" (see section 1.3.4, Fig. 1.4).

Table 2.1 PEG concentrations and amounts that should cause plasmolysis in soybean epidermal cells.

(PEG concentrations was taken from Money, 1989.)

PEG Molecular Weight (g/mol)	Concentration (M)	Amount needed (g, in 10 mL of salt-buffer solution)
200	0.525	1.05
400	0.400	1.60
600	0.325	1.95
900	*	2.25**
1000	0.235	2.35

* value is not available.

** Estimated from PEG 600 and 1000.

2.7 Pathogen-root interactions

2.7.1 Plant material and growth conditions

Seeds of soybean cultivars Conrad and OX 760-6 were first surface-disinfected with 5% sodium hypochlorite (commercial Javex bleach) for 5 min and then rinsed several times with sterile deionized water. Sterilized seeds were germinated on sterile moistened filter paper in sterile Pyrex glass dishes (300 × 190 mm) at room temperature (20-22^{o}C) in the dark for three d.

2.7.2 Preparation of zoospore inoculum

A culture of *Phytophthora sojae* race 2 (strain P6497) isolated in Mississippi in the 1980's (Förster et al., 1994) was kindly supplied by Dr. Mark Bernards, Department of Biology, University of Western Ontario, London, Ontario, who had obtained it from Dr. Mark Gijzen, Agriculture & Agri-food Canada, London, Ontario. Cultures were maintained on 26% V-8 juice agar plates (8.4 g agar, 1.6 g calcium carbonate, 156 mL V-8 juice, and 440 mL distilled water) at 23 to 25°C in the dark. A zoospore suspension was produced from flooded culture plates at room temperature. To allow for the formation of zoospores, five- or six-day-old, double-plugged agar-inoculated V-8 plates were first flooded with sterile deionized water overnight to leach nutrients out into the water. The water was decanted and the plates were reflooded with fresh sterile, deionized water every half hour for at least five to six h. Flooded plates were observed under a microscope (10 × magnification). Once zoospores were seen swimming around, the culture plates were given three washes (30 min/wash). Zoospores were released into the water, and this water was poured into a sterile conical flask. This zoospore collection process was repeated four to five times per culture plate and was performed in an aseptic environment where all surfaces were sterilized with 75% alcohol.

Zoospore concentrations were determined with a hemacytometer (details can be found in http://arbl.cvmbs.colostate.edu/hbooks/pathphys/reprod/semeneval/hemacytometer.html). After adding one drop of 0.1% (w/v) aniline blue in lactophenol (1:1:1 85% lactic acid, phenol, and water, Eye et al., 1978) into 1 mL zoospore suspension, a 10-µL aliquot was loaded with a pipette into the hemacytometer. The zoospore concentration was calculated and adjusted to 1×10^4 zoospores mL^{-1} with sterile, deionized water.

2.7.3 Inoculation

Etiolated, three-day-old soybean seedlings were taken from the glass Pyrex dishes and immersed directly into a zoospore suspension (1×10^4 zoospores mL^{-1}) of *P. sojae* at room temperature for 30 min, 40 min, 50 min, 1, 2, 3, 4, 5, 6, 7, and 18 h. Time courses and comparisons of the infection progress were studied.

According to an initial time-course study, a two h inoculation was sufficient for accumulation and adhesion of zoospores to the surface of roots. Therefore, the etiolated soybean seedlings were inoculated with a zoospore suspension for two h and returned to the glass dishes. Inoculated seedlings were incubated at room temperature in the dark, and then observed microscopically every day for three d. Seedlings inoculated with sterile deionized water served as controls.

2.7.4 Staining techniques for viewing pathogen development

2.7.4.1 Preserving and clearing root segments

Infected roots were preserved in glacial acetic acid:95% ethanol (1:3) for 18 h, blotted dry, and then cleared in 85% lactic acid at 98°C for one h (Peterson and Fletcher, 1973). The delicate cleared roots were scooped out of the acid with loop, rinsed three times with deionized water (3 × 20 min), and then stored in 70% ethanol for further studies.

2.7.4.2 Chlorazol black E

Chlorazol black E (C. I. 30235, Sigma Chemical Co., St. Louis, MO, USA) was previously used by Brundrett et al. (1984 and 1996) to stain vesicular-arbuscular mycorrhizae (VAM). The staining solution consisted of equal volumes of 85% lactic acid, glycerol, and distilled water (lactoglycerol) with 0.03% (w/v) chlorazol black E, and was filtered through cheesecloth. Acid-cleared roots were transferred into the staining solution at 90°C for one h. Roots were destained in a 50% aqueous glycerol solution for 24 h, and observed under white light with DIC optics.

2.7.4.3 Trypan blue and aniline blue

Trypan blue (C. I. 23850, Sigma Chemical Co., St. Louis, MO, USA) was utilized at concentration of 0.03% (w/v) in lactoglycerol described in section 2.7.4.2. After being stained for one h, the cleared roots were destained in 50% glycerol (v/v) for one d and examined with DIC (Brundrett et al., 1984). The same method was used with 0.01% (w/v) aniline blue (C. I. 42755, Sigma Chemical Co., St. Louis, MO, USA).

2.7.4.4 Cellufluor (for cellulose)

Cellufluor was applied at 0.01% (w/v) in distilled water. Cleared roots were stained for 2 min, rinsed briefly in distilled water, and observed with ultraviolet light (G 365 nm, FT 395 nm, LP 420 nm; O'Brien and McCully, 1981; Hughes and McCully, 1975).

2.7.4.5 Aniline blue (for callose)

The aniline blue staining procedure was employed as described by Peterson and Fletcher (1973). Aniline blue was utilized at 0.2% in 0.1 M phosphate buffer (pH 7.5). Cleared roots were placed in the staining solution for 10 min, rinsed and examined in buffer under ultraviolet light (G 365 nm, FT 395 nm, LP 420 nm).

All staining techniques except cellufluor were also directly applied to the mycelia of the culture plate. A few hyphae were selected with a dissecting needle, transferred to a slide, and observed under white light with DIC optics.

2.7.5 Staining methods employed on infected roots

Cross root sections were excised from fresh, inoculated roots and stained for lipids with sudan red 7B as described in section 2.2.2.

Fresh, infected root segments were placed on a slide, stained with 0.05% TBO (pH 4.4) for 2 min, mounted in distilled water, and viewed under white light with DIC optics.

Chelidonium majus root extract solution was prepared following the description of Peterson et al. (1982). Two g of *Chelidonium majus* root powder was dissolved in 250 mL 95% ethyl alcohol, and the homogenate was filtered through a number 1 filter paper (Whatman, Canada). The remaining powder was redissolved with 175 mL of 95% alcohol and the second homogenate was filtered as well. The two filtrates were combined and stored in a brown glass bottle at 5°C. Lactic acid-cleared root segments were bisected longitudinally and stained with the *Chelidonium majus* root extract for 18 to 24 h. Stained samples were destained in 50% (v/v) ethanol for 18 h, rinsed in distilled water for 10 min, mounted in 70% (v/v) glycerin, and viewed with violet light (BP 395-440 nm, FT 460 nm, LP 470 nm).

2.7.6 Acid digestion

Cross-sections of inoculated soybean root were digested with concentrated sulfuric acid as described in section 2.2.3.

2.8 Microscopy and photography

Experimental specimens were observed with a Zeiss Axiophot microscope equipped with a HBO 100W Osram mercury lamp and epifluorescence optics. In accordance with the techniques used in each section, different filters were utilized. Each epifluorescence filter set was composed of an exciter filter, a chromatic beam splitter, and a barrier filter. Color photographs were captured on Kodak Ektachrome 35-mm film, ASA 200 and 400, or were taken with digital camera system (Q-Imaging, Retiga 2000R, Fast 1394, Cooled Mono, 12-bit, Quorum Technologies Inc., Guelph, ON).

3 Results

3.1 Root morphology and anatomy

The average length of soybean main roots that had grown for six d was 104 mm, so the plastic pots (with a depth of 195 mm) did not hinder their growth. Few or no lateral roots were present indicative of a strong apical dominance (Aloni et al., 2006). The average growth rate of soybean roots in vermiculite was 17.7 mm/day; therefore, the distances of 5 mm, 15 mm, 25 mm, 50 mm, and 100 mm from the root tips corresponded to the ages of 0.3, 0.8, 1.4, 2.8, and 5.6 d, respectively. Beyond 30 to 40 mm from the root tips, alternating long and short or no root hairs covered most of the epidermal surface. The texture of the soybean roots was fragile within 50 mm of the root tips, especially the apical 10 mm to 30 mm. Root caps extended 1.5 to 2 mm proximal to the tips. The root morphologies of two soybean cultivars were identical viewed with the naked eye except that the main roots of OX 760-6 (susceptible cv.) were generally longer (under 1 cm) than those of Conrad (resistant cv.).

Cross-sections of soybean roots demonstrated that the epidermal cells were much smaller than the neighbouring cortical cells (Fig. 3.1) regardless of distance from the root tips. The size of the epidermal cells remained constant while the size of the cortical cells increased gradually along the root. For example, the average cortical cell diameter was 7.1 μm at a distance of 5 mm from the root tip, while the diameter was 15.4 μm 100 mm from the root tip. Furthermore, the color of the epidermal cell walls changed gradually from white to yellowish brown while the walls of the cortical cells were always white (Fig. 3.1). It was difficult to pinpoint the precise location of initial epidermal browning. Generally in six-day-old soybean seedlings, browning of the epidermal cell walls could be recognized beyond 20 mm from the root apex (Fig. 3.1B and C).

3.2 Suberin tests

In order to test for suberin, three procedures were performed according to a widely accepted notion that suberin is a polymer containing phenols and lipids. Phenol testing included autofluorescence examination and the Hoepfner-Vorsatz test; lipids were tested with sudan red 7B; and acid digestion was performed to check the biopolymer property of the suberin. In addition, TEM was used to observe the ultrastructural properties of epidermal walls. There were none or few differences in cv. Conrad and cv. OX 760-6 with the identical histochemical techniques.

3.2.1 Phenol tests

Outer tangential epidermal walls were the first to show autofluorescence under blue excitation. At a distance of 5 mm from the root tip, yellow autofluorescence was visible in the epidermal cell wall (Table 3.1, Fig. 3.2A and F) and development of autofluorescence progressed inward through the cortical cell walls with increasing age (Fig. 3.2B-E and G-J). The cortical cell walls showed an uneven yellow autofluorescence (Fig. 3.2E and J). A rough comparison of autofluorescence intensity can be made by noting the photographic exposure times. For example, the exposure time for sections at a distance of 50 mm from the root tip was 75 s in cv. Conrad and 65 s in cv. OX 760-6. The shorter exposure time indicates that the susceptible cv. OX 760-6 has a stronger autofluorescence than resistant cv. Conrad. This difference is more obvious in fresh root sections taken less than 20 mm from the root tips (Fig. 3.2A, B, F and G).

Fresh root sections mounted in distilled water were used as controls for the Hoepfner-Vorsatz test. They displayed a yellowish brown outer tangential epidermal cell wall with white light (greater than 20 mm from the root tip, Fig. 3.3A). After application of the test solution, the outer tangential walls of the epidermal cells stained brown in the more mature regions (above 50 mm from the root tip, Table 3.1, Fig. 3.3B) in addition to stained tracheary elements. This phenomenon indicates a positive reaction for phenols.

3.2.2 Lipid test

The typical bright red after staining the epidermis with sudan red 7B was not obvious in the cross-sections of the white zone of soybean root (within 20 mm from the root tips). As the roots were becoming yellowish brown, a positive lipid staining was evident (Table 3.1, Fig. 3.4B) compared to a control, unstained section (Fig. 3.4A).

3.2.3 Acid digestion

Acid digestion of root cross-sections resulted in the preservation of walls of the epidermis, endodermis, and xylem vessel members from mature root zones (Table 3.1, Fig. 3.5A). Central cortical cells rapidly disappeared with sulfuric acid treatment. The digested epidermal walls appeared brown and had slight undulations in the radial walls (Fig. 3.5B).

3.2.4 Ultrastructure of epidermal cell walls

The TEM protocol developed by Ma and Peterson (2000) preserved the epidermal wall well. Epidermal cell walls displayed indistinct, alternating, electron-dense and less electron-dense bands after osmium tetroxide staining. These were especially located in the outer tangential walls of epidermis (Fig. 3.6A). Generally, the outer tangential epidermal cell walls were crescent-shaped in cross section and much thicker than the others (Fig. 3.6B).

Table 3.1 Summary of suberin tests in soybean root epidermal walls.

Distances from the root tips (mm)	Phenol tests		Lipid test	Resistance to acid digestion
	Autofluorescence	H-V test	Sudan red 7B	
5	+	-	-	+
15	+	-	-	+
25	+	-	-	+
50	+	+	+	+
100	+	+	+	+

+ positive reaction
- negative reaction

Figure 3.1 Unstained cross-sections of soybean root.

Fresh, freehand sections of cv. Conrad viewed with white light with differential interference contrast (DIC) optics. Scale bars = 15 µm. Arrows indicate the epidermis. **A** Five mm from the root tip. Epidermal cell walls are white. **B** Twenty-five mm from the root tip. Epidermal cell walls are yellowish brown. **C** One hundred mm from the root tip. Epidermal cell walls are dark brown.

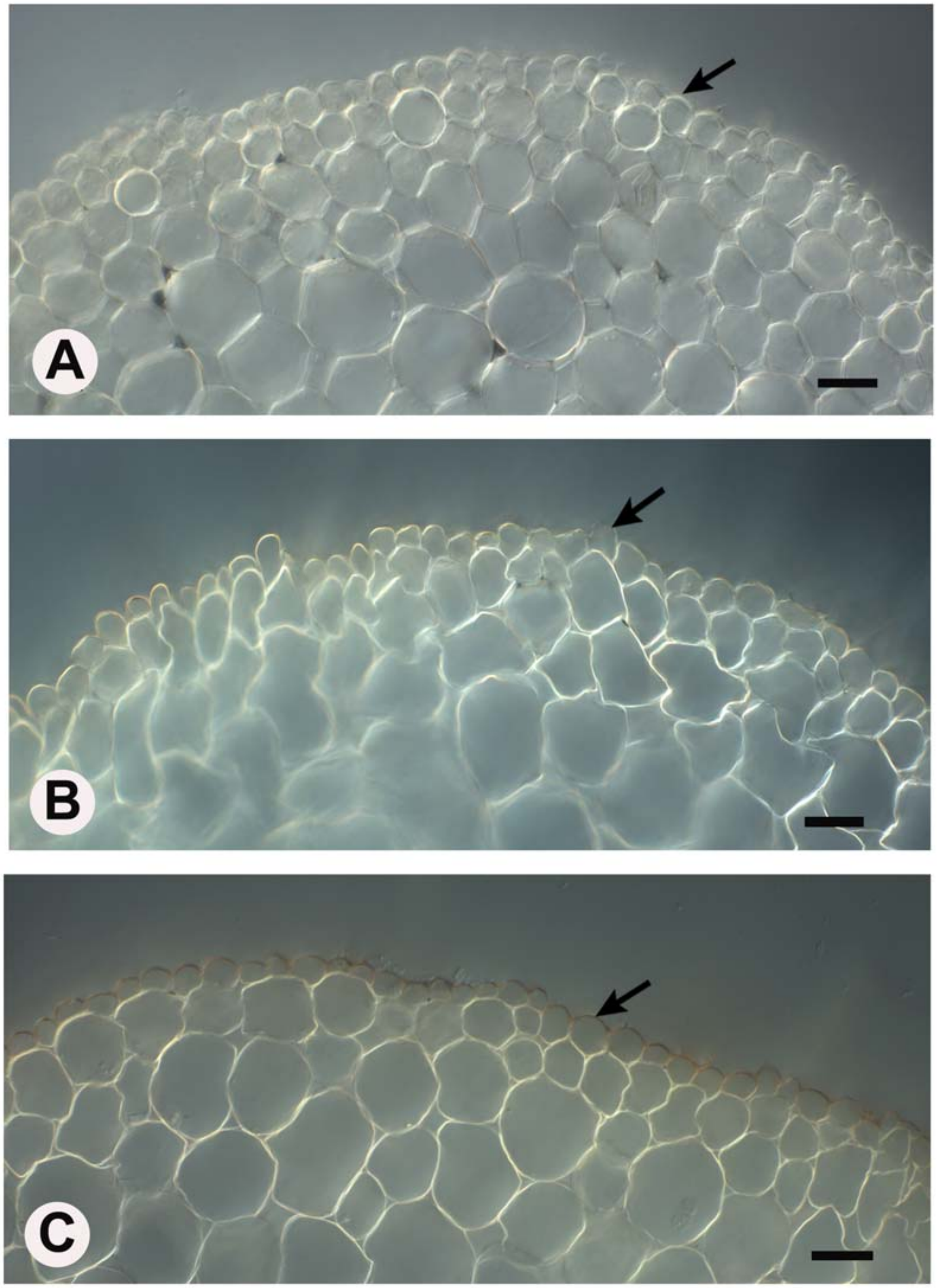
A
B
C

Figure 3.2 Development of autofluorescence.

Fresh, freehand, cross-sections of soybean roots mounted in water and viewed with blue light. Epidermal cell walls showed yellow autofluorescence as the root aged.

A-E Autofluorescence of cv. Conrad epidermis at 5 mm, 15 mm, 25 mm, 50 mm, and 100 mm from the root tip, respectively. **F-J** Autofluorescence of cv. OX 760-6 epidermis at 5 mm, 15 mm, 25 mm, 50 mm, and 100 mm from the root tip, respectively.

Scale bars = 50 μm.

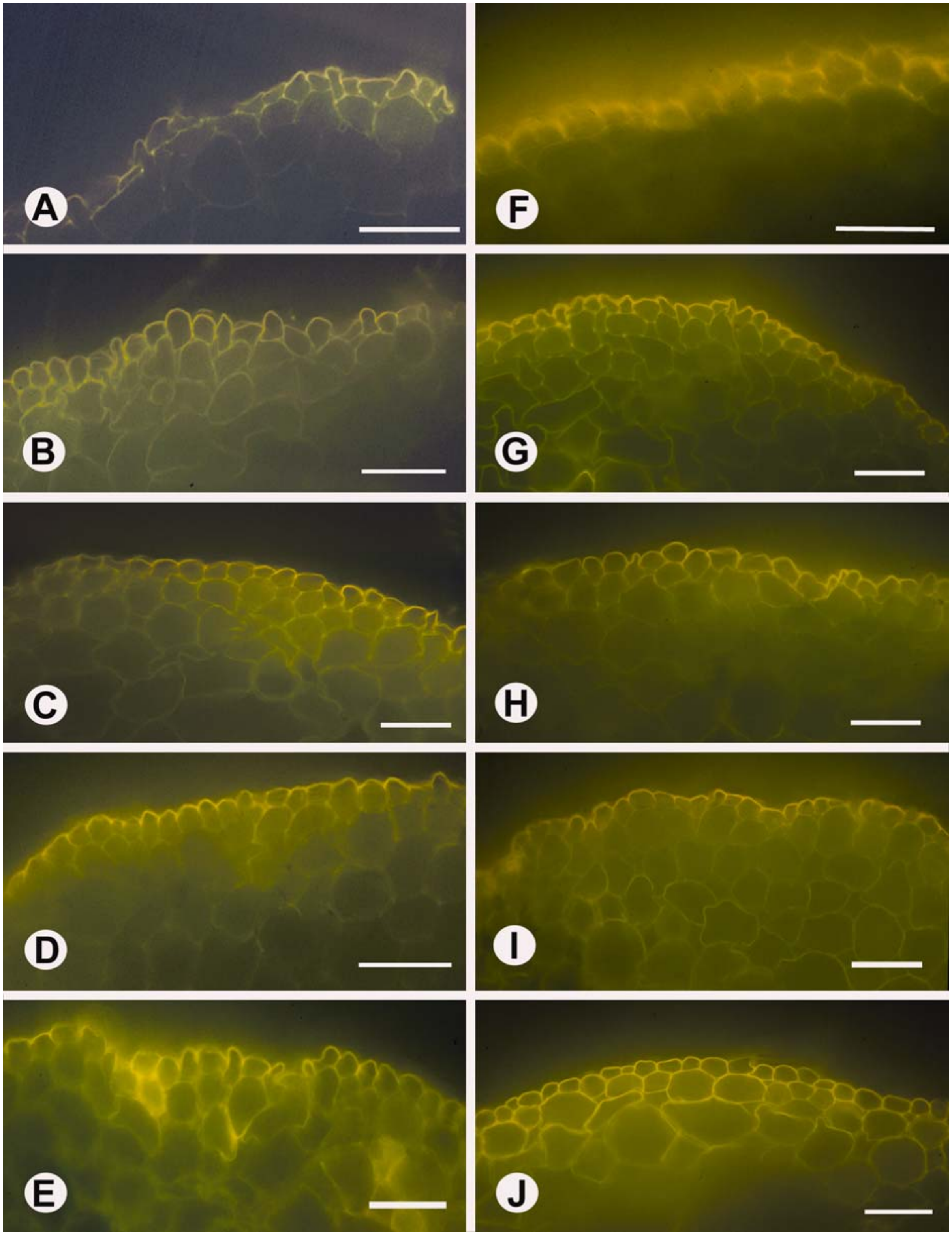
A
F
B
G
C
H
D
I
E
J

Figure 3.3 Hoepfner-Vorsatz test for phenols in epidermal cell walls.

Fresh, freehand, cross-sections of cv. OX 760-6 root taken at 100 mm from the root tip and viewed with white light. Scale bars = 15 µm. Arrows indicate the epidermis. **A** Section mounted in water (control). The outer tangential epidermal cell walls were yellowish brown. **B** Section treated with Hoepfner-Vorsatz reagent (treatment). The outer tangential epidermal cell walls stained brown.

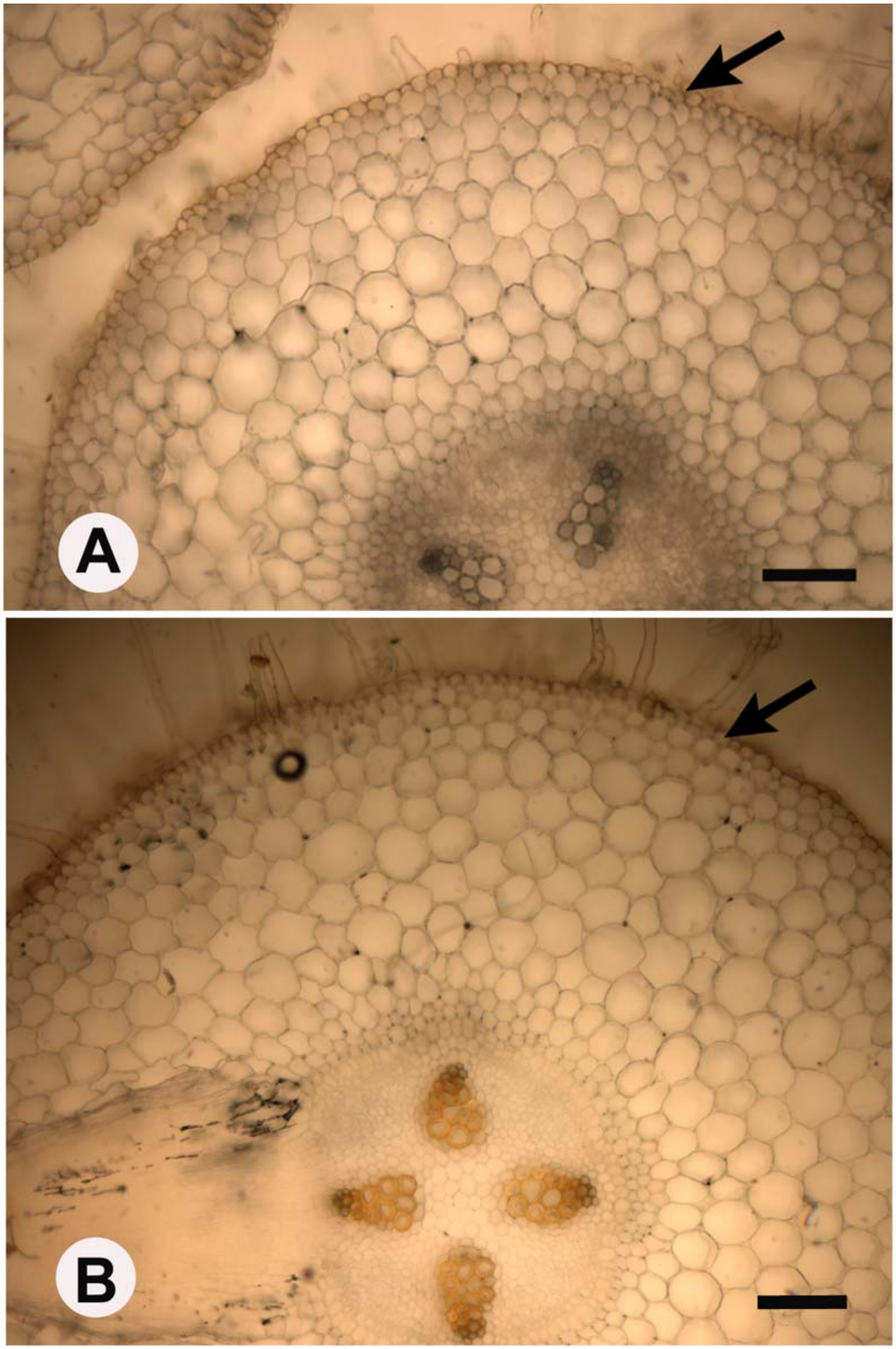
A
B

Figure 3.4 Sudan red 7B for lipid staining in epidermal cell walls.

Fresh, freehand, cross-sections of cv. OX 760-6 taken 100 mm from soybean root tips viewed under white light with DIC optics. Scale bars = 15 µm. Arrows indicate the epidermis. **A** Cross-section mounted in 75% glycerol (control). **B** Cross-section treated with sudan red 7B (treatment) showing bright red-stained epidermal walls.

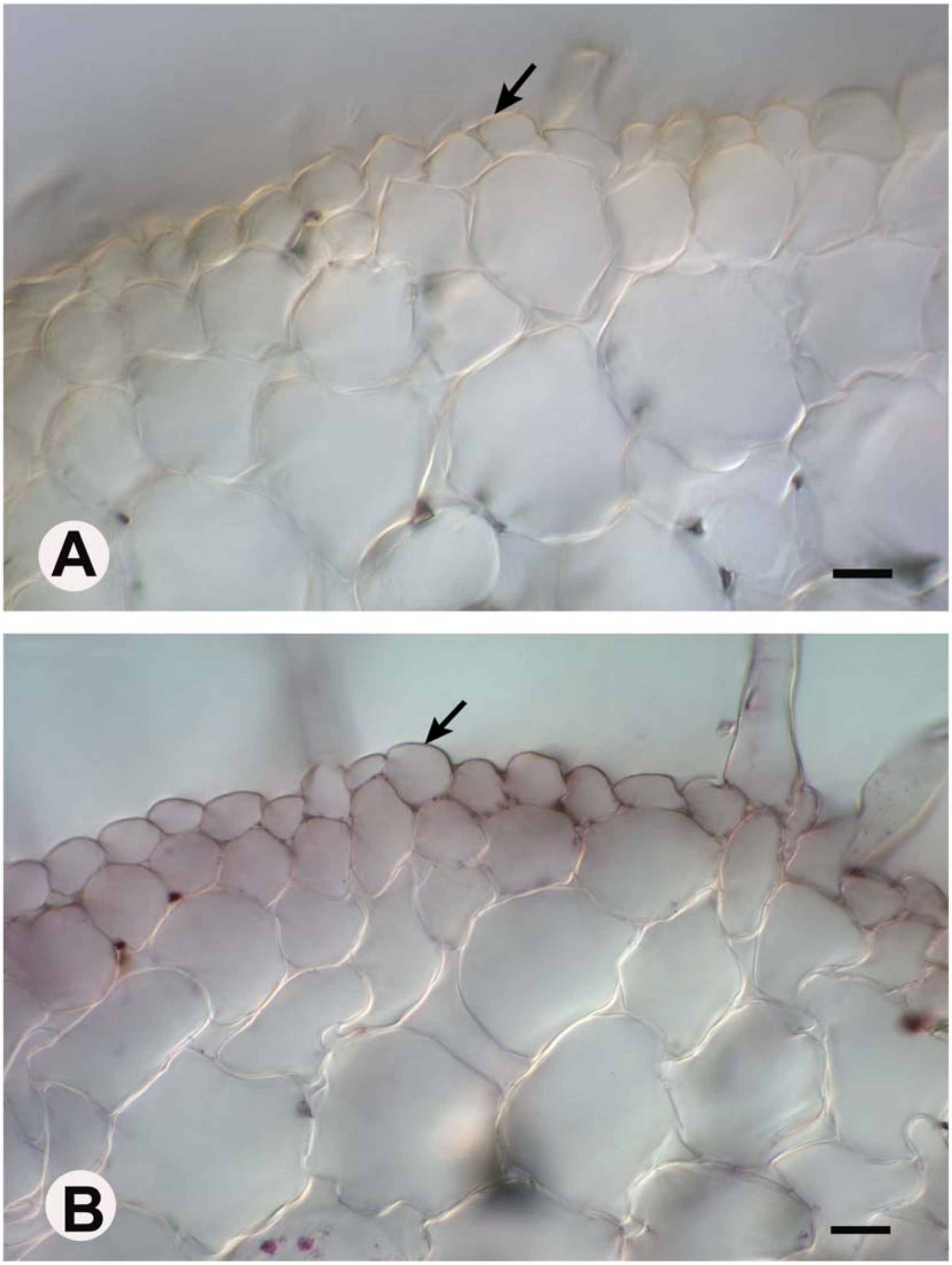
A
B

Figure 3.5 Acid digestion of soybean root.

Freehand, cross-sections of soybean root taken 100 mm from the root tips treated with concentrated sulphuric acid and viewed under white light with DIC optics. **A** Arrow indicates the epidermal walls. Arrowhead indicates a group of xylem vessels. Scale bar = 35 µm. **B** A fragment of acid-digested epidermal cell wall has toppled to longitudinal position. White arrowheads indicate undulating epidermal walls. Scale bar = 140 µm.

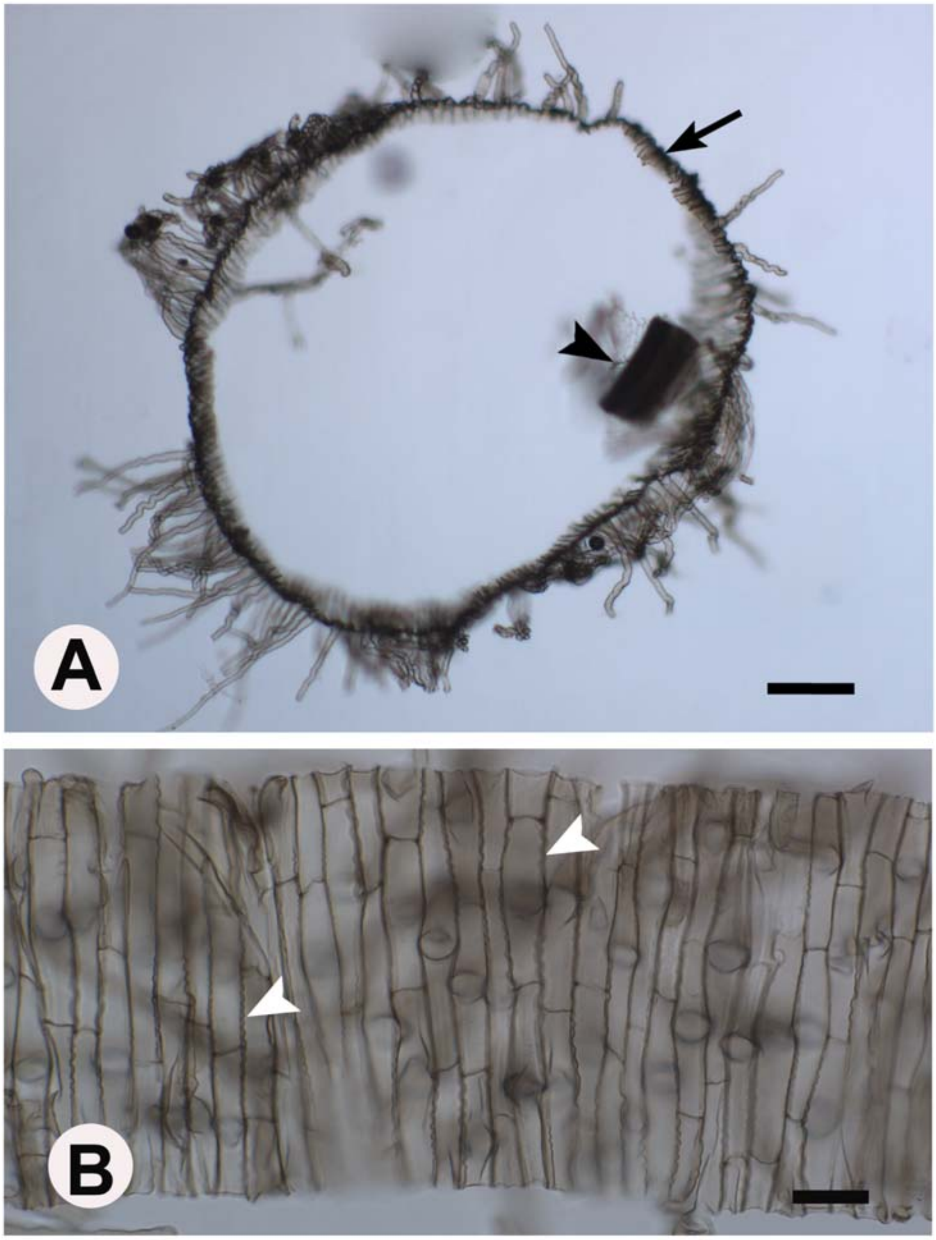
A
B

Figure 3.6 The ultrastructure of epidermal cell wall viewed with TEM.

Osmium-fixed, cross, ultra-thin section taken 50 mm from the soybean root tip. **A** The outer tangential epidermal wall displayed indistinct, alternating, electron-dense (red stars) and less electron-dense bands (blue stars). **B** A whole epidermal cell showing the thick, crescent-shaped outer tangential wall. Scale bars = 1 µm.

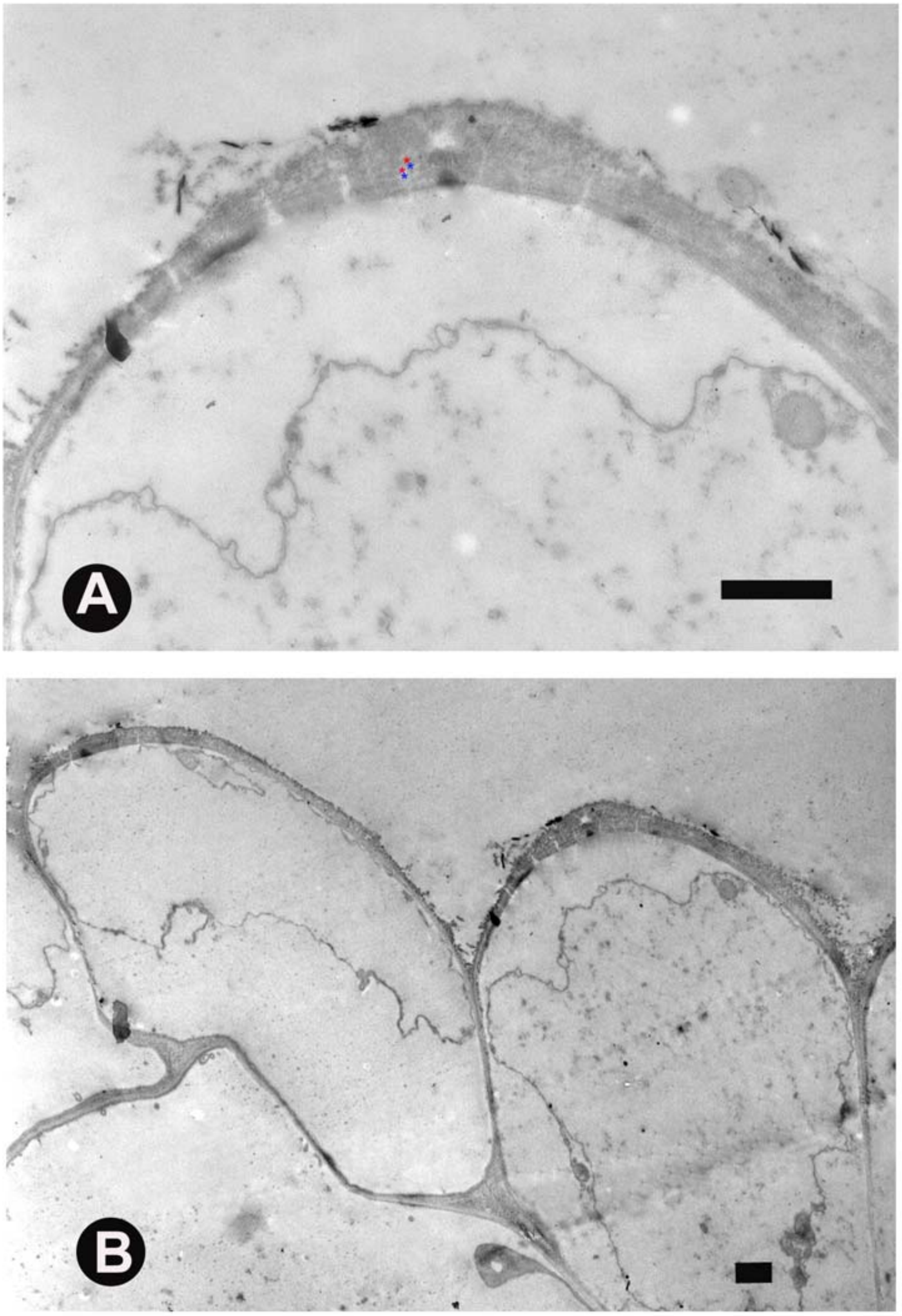
A
B

3.3 Chemical composition of epidermal cell walls

3.3.1 Scanning electron microscopy (SEM)

When enzymatically isolated epidermal cell walls were viewed with SEM, it was evident that various amounts of cell wall material were left at different distances from the root apex. At distances up to 20 mm from root tips, the outer tangential and radial walls of the epidermis were clearly visible (Fig. 3.7A and B). In older regions, the walls of the epidermis and the outer tangential and radial edges of the first cortical cells endured the wall-degrading enzymes; these were preserved and remained attached to each other (Fig. 3.7C and D). The cortical cells were much wider but shorter than the epidermal cells (Fig. 3.7A and C). Walls of all root hairs from epidermal cells remained intact (Fig. 3.7B).

3.3.2 Monomers released by transesterification of epidermal cell walls

The polymers extracted from enzymatically digested epidermal walls were subjected to BF_3-MeOH transesterification. Monomers released were analyzed with GC-MS (see Fig. 1.6). There were no differences in the types of aliphatic monomers released from the epidermal cell walls of the two soybean cultivars, except that a trace amount of 1-alkanols was detected in Region III (160-200 mm from root tips) of cv. Conrad (Fig. 3.8C, Appendices 1 and 2). Transesterification of the insoluble material of epidermal cell walls yielded aliphatic depolymerisates and phenolic compounds (see Fig. 1.6). Aliphatic depolymerisates contained four classes of monomers, i.e. α,ω-dicarboxylic acids, ω-hydroxycarboxylic acids, 1-alkanols, and carboxylic acids (Fig. 3.8, Appendices 1 and 2). Additionally, ester-linked phenolic compounds, ferulic acid and *p*-coumaric acid, were detected in the depolymerisates of insoluble epidermal wall material. The carbon chain-lengths of all aliphatic monomers ranged from C16 to C24 with even-chain homologues. Most aliphatic components were saturated. Unsaturated constituents were found with carbon chain-lengths of 16 and 18 (Fig. 3.8, Appendices 1 and 2).

Amongst the aliphatic monomers identified in the depolymerisates obtained from the insoluble materials of both soybean (Conrad and OX 760-6) root epidermal walls, ω-hydroxycarboxylic acids were the most abundant compound class (77.2 % in cv. Conrad, Appendix 1, and 77.3% in cv. OX 760-6, Appendix 2). The percentages of carboxylic acids, dicarboxylic acids and 1-alkanols were smaller, making up 20.1%, 2.6%, and 0.1% of total detected aliphatic monomers, respectively, in cv. Conrad (Appendix 1), and 18.8%, 4.0%, and 0%, respectively, in cv. OX 760-6 (Appendix 2). The amounts of homologues within the different monomeric classes varied. Carbon 18 unsaturated ω-hydroxycarboxylic acid (C18:1) was the most abundant monomer in cv. Conrad (30.0 ng mm^{-2}, 18.2%, Appendix 1) followed by carbon 24 saturated ω-hydroxycarboxylic acid (C24:0) and carbon 22 saturated ω-hydroxycarboxylic acid (C22:0). C24:0 ω-hydroxycarboxylic acid was the dominant monomer in cv. OX 760-6 (14.4 ng mm^{-2}, 20.8%, Appendix 2) followed by C18:1 ω-hydroxycarboxylic acid and C20:0 ω-hydroxycarboxylic acid.

Depolymerisates from epidermal cell walls taken from different locations of roots differed significantly ($P < 0.05$) in their relative composition (Figs. 3.9). The epidermal cell walls from older root segments contained more aliphatic substances than the younger segments. Region I, II, and III contained 31.8 (SE = 0.2), 69.0 (SE = 3.4), and 64.1 ng mm^{-2} (SE = 0.2) aliphatic substances in cv. Conrad and 14.8 (SE = 0.01), 32.8 (SE = 0.3), and 22.0 ng mm^{-2} (SE = 2.1) aliphatic components in OX 760-6 (Figs. 3.9, Appendices 1 and 2). The amounts of aliphatic components of epidermal cell walls from the two cultivars were also significantly different ($P < 0.05$). Epidermal cell walls in the resistant cv. Conrad contained over twice the quantity of aliphatic substances than did susceptible cv. OX 760-6 (i.e. 164.9 ng mm^{-2} in cv. Conrad compared to 69.5 ng mm^{-2} in cv. OX 760-6, Fig. 3.9, Appendix 1 and 2).

The total amount of ester-linked phenolic components, ferulic acid and *p*-coumaric acid released by BF_3-MeOH transesterification was consistent along the root length in both resistant cv. Conrad and susceptible cv. OX 760-6 (Fig. 3.10, Appendix 3). These aromatic compounds contributed less to the total mass of insoluble epidermal cell wall components than did the esterified aliphatic compounds (Appendix 3). There were only 7.8 ng mm^{-2} esterified phenolics in cv. Conrad and 5.0 ng mm^{-2} in cv. OX 760-6. The amount of both ester-linked aromatic components differed significantly ($P < 0.05$) between both cultivars (Fig. 3.10, Appendix 3).

In addition to monomers found from the insoluble root residues, alkanes, alcohols and carboxylic acids (Fig. 3.11, Appendices 4 and 5) were the three compound classes identified chromatographically from soluble root material prior to transesterification (see Fig. 1.6). These components represent suberin-associated waxes and had chain lengths ranging from C16 to C32 (Fig. 3.11). There were 45.2 ng mm^{-2} and 24.4 ng mm^{-2} alkanes in cv. Conrad and cv. OX 760-6, respectively, which accounted for 88.2% of the waxes in cv. Conrad and 86.7% of the waxes in cv. OX 760-6 (Appendices 4 and 5). Moreover, the long chain (C28 to C32) alkanes stood out from all wax components and were predominant compounds (Fig. 3.11, Appendices 4 and 5). Waxes in cv. Conrad were 51.3 ng mm^{-2}, nearly twice as high as in cv. OX 760-6 (28.1 ng mm^{-2}, Appendices 4 and 5). The amount of wax material increased significantly ($P < 0.05$) along the length of cv. Conrad roots; however, it remained relatively consistent along the length of cv. OX 760-6 roots (Fig. 3.12).

3.3.3 Nitrobenzene oxidation of epidermal cell walls

The polymers extracted from enzymatically digested epidermal walls were subjected to nitrobenzene oxidation; monomers released were analyzed with GC-MS (see Fig. 1.6). There were two non ester-linked aromatic substances released by microscale alkaline nitrobenzene oxidation: vanillin and syringin (Fig. 3.13). Only small amounts of nitrobenzene oxidation products (i.e. 4.7 ng mm^{-2} in cv. Conrad and 5.0 ng mm^{-2} in cv. OX 760-6) were present in the total monomers released from epidermal cell walls (Appendix 3). Even though a slightly lower amount of non-esterified aromatic components was present in the resistant cv., cv. Conrad still had a higher total amount of aromatic compounds (12.5 ng mm^{-2}) than did the susceptible cv. OX 760-6 (8.8 ng mm^{-2}) since esterified aromatic compounds were much higher in cv. Conrad (Appendix 3). Comparing both cvs, the total amounts of aromatic substances in Region I (0-70 mm from root tips) were not significantly different ($P < 0.05$); however, significant differences ($P < 0.05$) were apparent in Region II (90-160 mm from root tips) and III (160-200 mm from root tips, Fig. 3.14).

Figure 3.7 Scanning electron micrographs of enzymatically isolated epidermal cell walls of soybean roots.

A Segment taken 10-20 mm from root tip, inner side of layer facing up. Scale bar = 60 µm. Arrows indicate outer tangential walls of epidermis. Arrowheads indicate anticlinal walls of epidermis. **B** Segment taken 10-20 mm from root tip, outer side of layer facing up. Scale bar = 100 µm. Arrow indicates outer tangential wall of epidermis. Arrowheads indicate root hairs. **C** Segment taken 40-50 mm from root tip, inner side of layer facing up. Scale bar = 60 µm. Arrows indicate outer tangential walls of the cortical cells adjacent to epidermis. Arrowheads indicate anticlinal walls of the cortical cells adjacent to epidermis. **D** Segment taken 40-50 mm from root tip, outer side of layer facing up. Scale bar = 136 µm. Arrow indicates outer tangential wall of epidermis.

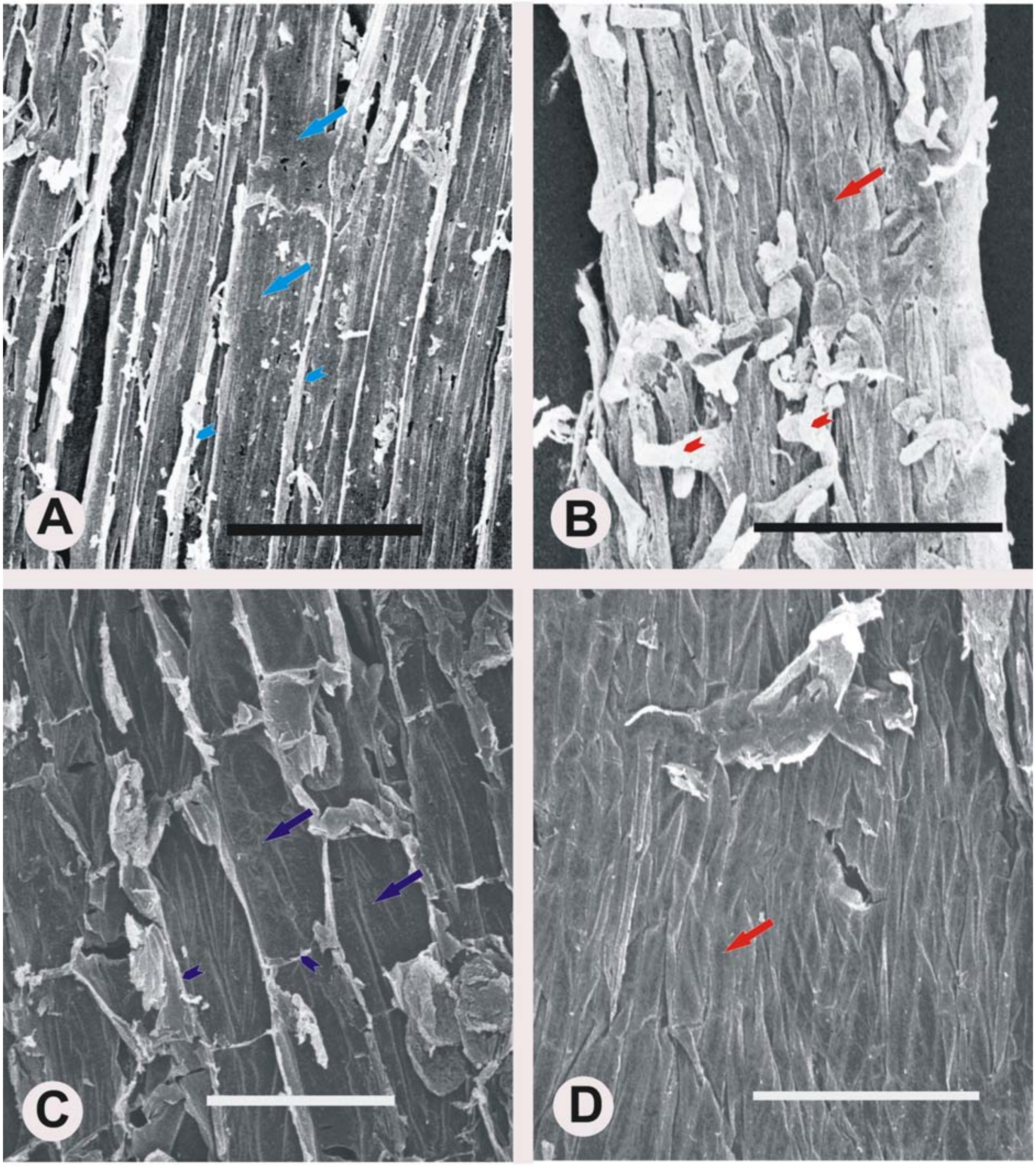
A
B
C
D

Figure 3.8 Aliphatic compound classes released after BF_3-MeOH transesterification.

Soybean epidermal cell walls were isolated from primary roots of 10-day-old seedlings by digestion with cellulase and pectinase, and extracted with chloroform and methanol. Insoluble material of epidermal walls was degraded into the corresponding aliphatic compound classes by BF_3-MeOH transesterification and analyzed by chromatography. Amounts of substances expressed as weight (ng) per root surface area (mm^2). Bars indicate standard errors of the means. **A-C** Different segments from resistant cv. Conrad epidermis. **D-F** Different segments from susceptible cv. OX 760-6 epidermis.

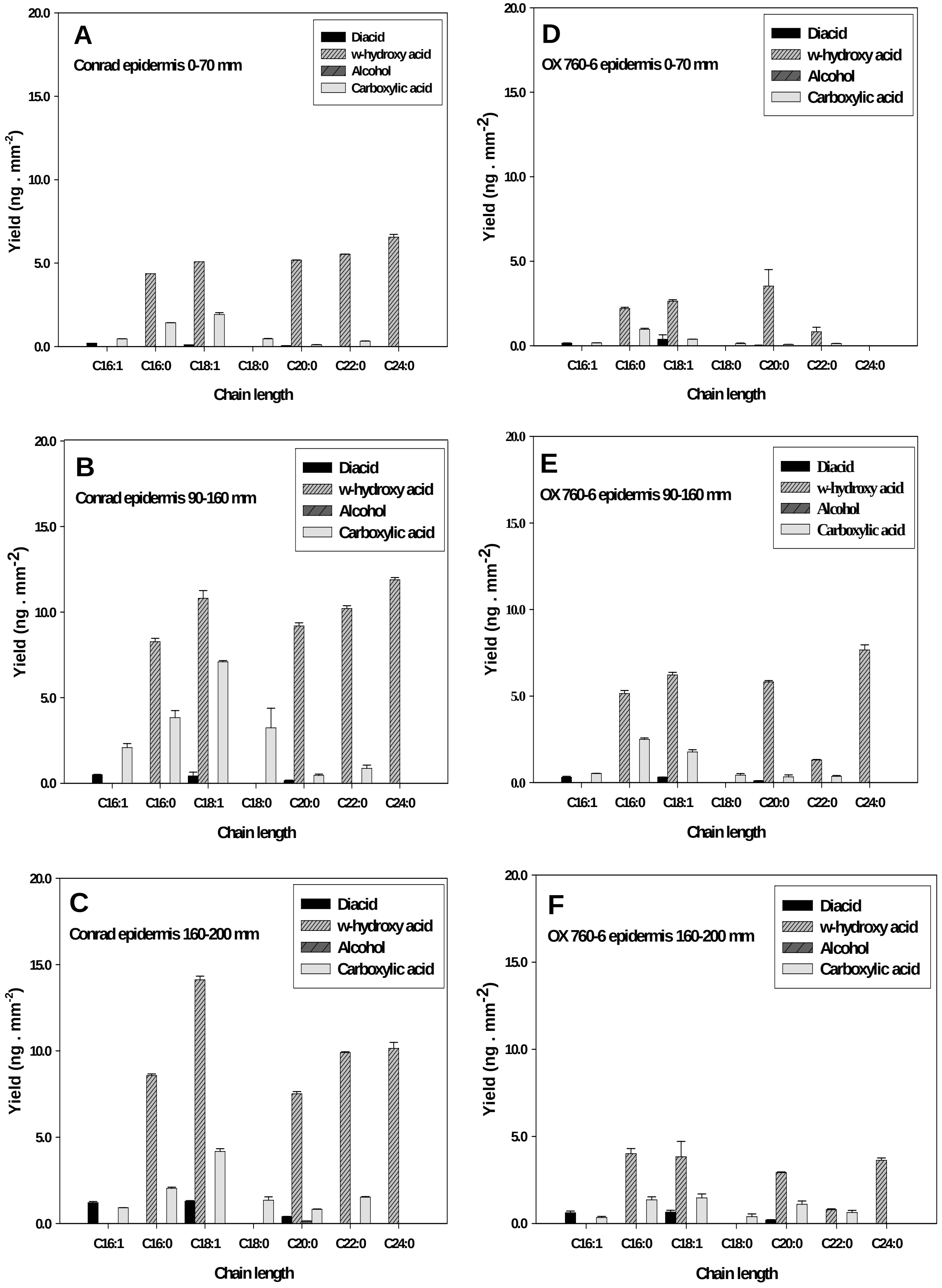
A
Conrad epidermis 0-70 mm
B
Conrad epidermis 90-160 mm
C
Conrad epidermis 160-200 mm
D
OX 760-6 epidermis 0-70 mm
E
OX 760-6 epidermis 90-160 mm
F
OX 760-6 epidermis 160-200 mm
Diacid
w-hydroxy acid
Alcohol
Carboxylic acid
Yield (ng . mm-2)
Chain length
C16:1
C16:0
C18:1
C18:0
C20:0
C22:0
C24:0
0.0
5.0
10.0
15.0
20.0

Figure 3.9 Total aliphatic substances released after BF_3-MeOH transesterification.

Soybean epidermal cell walls were isolated from primary roots of 10-day-old seedlings by digestion with cellulase and pectinase, and extracted with chloroform and methanol. Insoluble material of epidermal walls was depolymerized by BF_3-MeOH transesterification and analyzed with GC-MS. Amounts of substances are expressed as weight (ng) per root surface area (mm^2). Bars indicate standard errors of the means. Values with different letters are significantly different ($P < 0.05$).

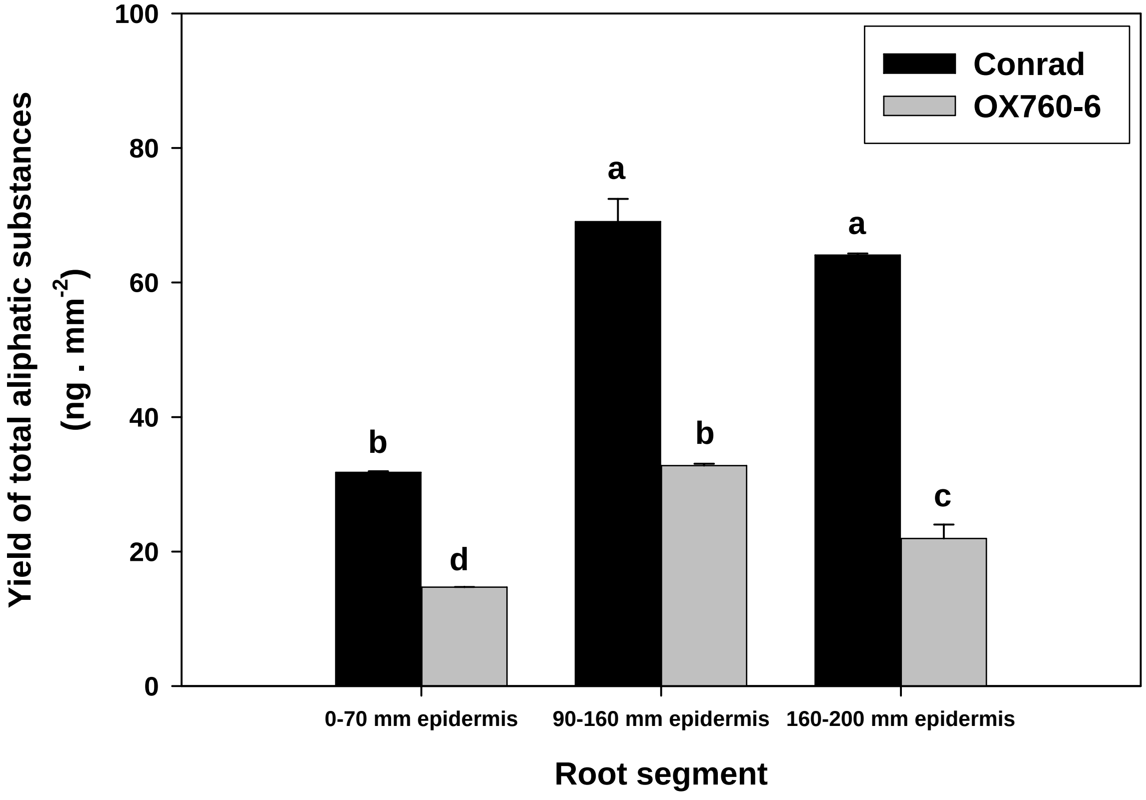

Figure 3.10 Ester-linked aromatic compound classes (ferulic acid and *p*-coumaric acid) released after BF_3-MeOH transesterification.

Soybean epidermal cell walls were isolated from primary roots of 10-day-old seedlings by digestion with cellulase and pectinase, and extracted with chloroform and methanol. Insoluble material of epidermal walls was depolymerized by BF_3-MeOH transesterification and analyzed with GC-MS. Amounts of substances are expressed as weight (ng) per root surface area (mm^2). Bars indicate standard errors of the means. Values with different letters indicate significant differences ($P < 0.05$). **A** Ferulic acid. **B** *p*-Coumaric acid.

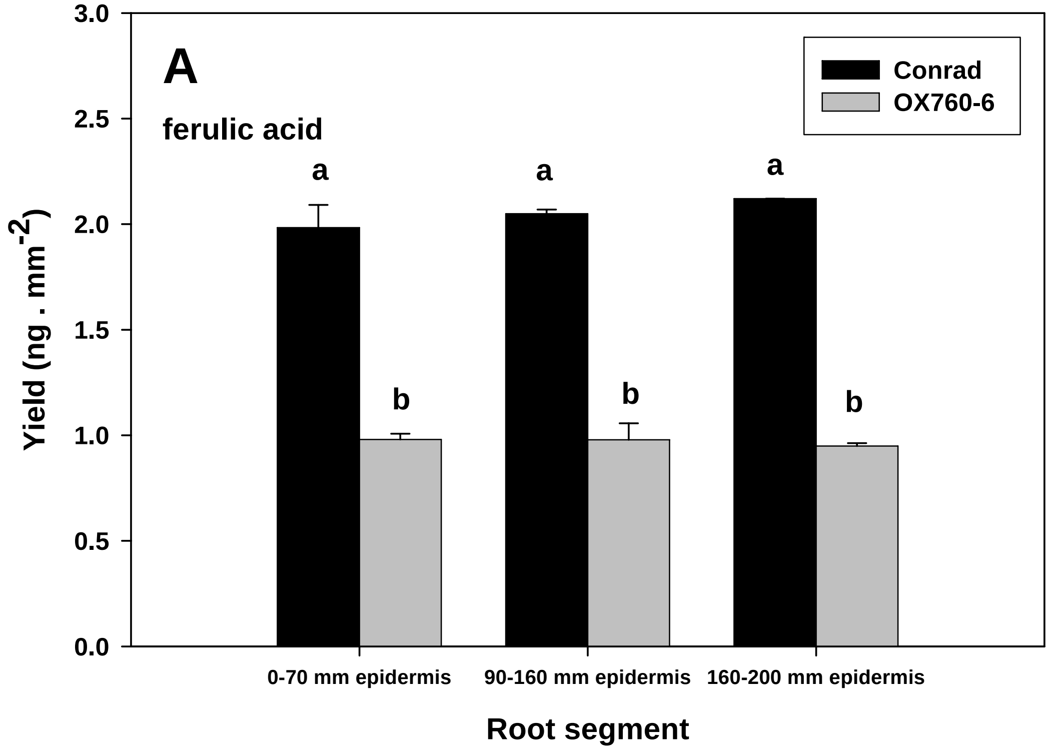
A
ferulic acid
Conrad
OX760-6
a
a
a
b
b
b
3.0
2.5
2.0
1.5
1.0
0.5
0.0
Yield (ng . mm^{-2})
0-70 mm epidermis
90-160 mm epidermis
160-200 mm epidermis
Root segment

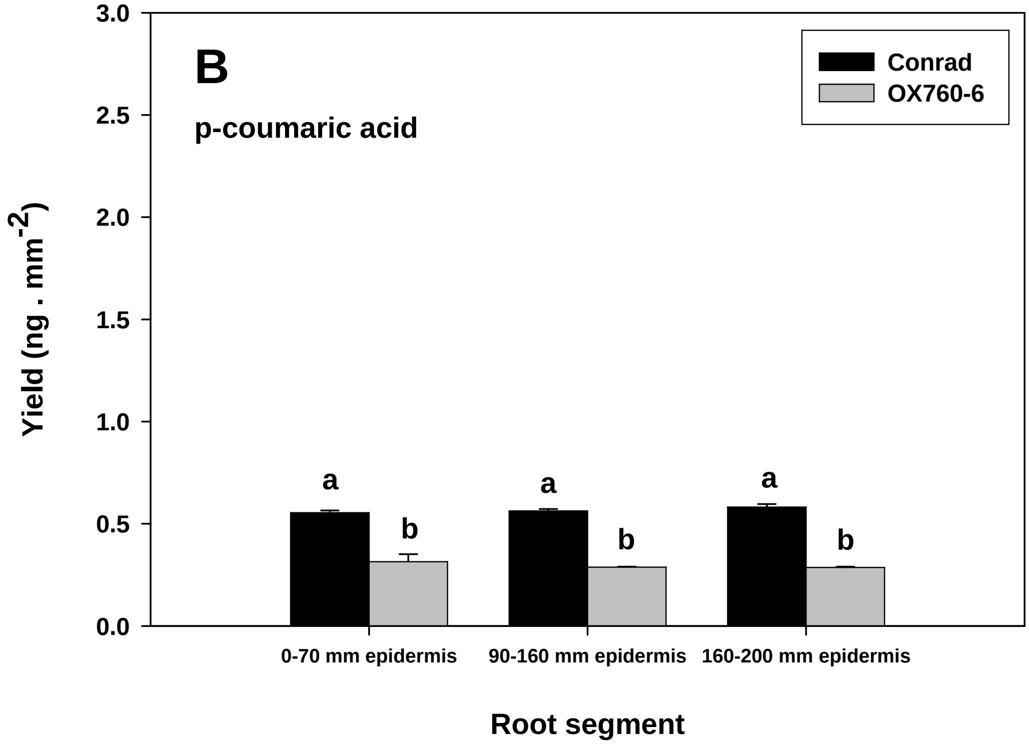
B
p-coumaric acid
Conrad
OX760-6
a
a
a
b
b
b
3.0
2.5
2.0
1.5
1.0
0.5
0.0
Yield (ng . mm^{-2})
0-70 mm epidermis
90-160 mm epidermis
160-200 mm epidermis
Root segment

Figure 3.11 Monomeric compositions and chain-length distribution of waxes.

Soybean epidermal cell walls were isolated from primary roots of 10-day-old seedlings by digestion with cellulase and pectinase, and extracted with chloroform and methanol. Soluble material of epidermal walls was analysed with GC-MS. Amounts of substances are expressed as weight (ng) per root surface area (mm^2). Bars indicate standard errors of the means. **A-C** Different segments of resistant cv. Conrad roots. **D-F** Different segments of susceptible cv. OX 760-6 roots.

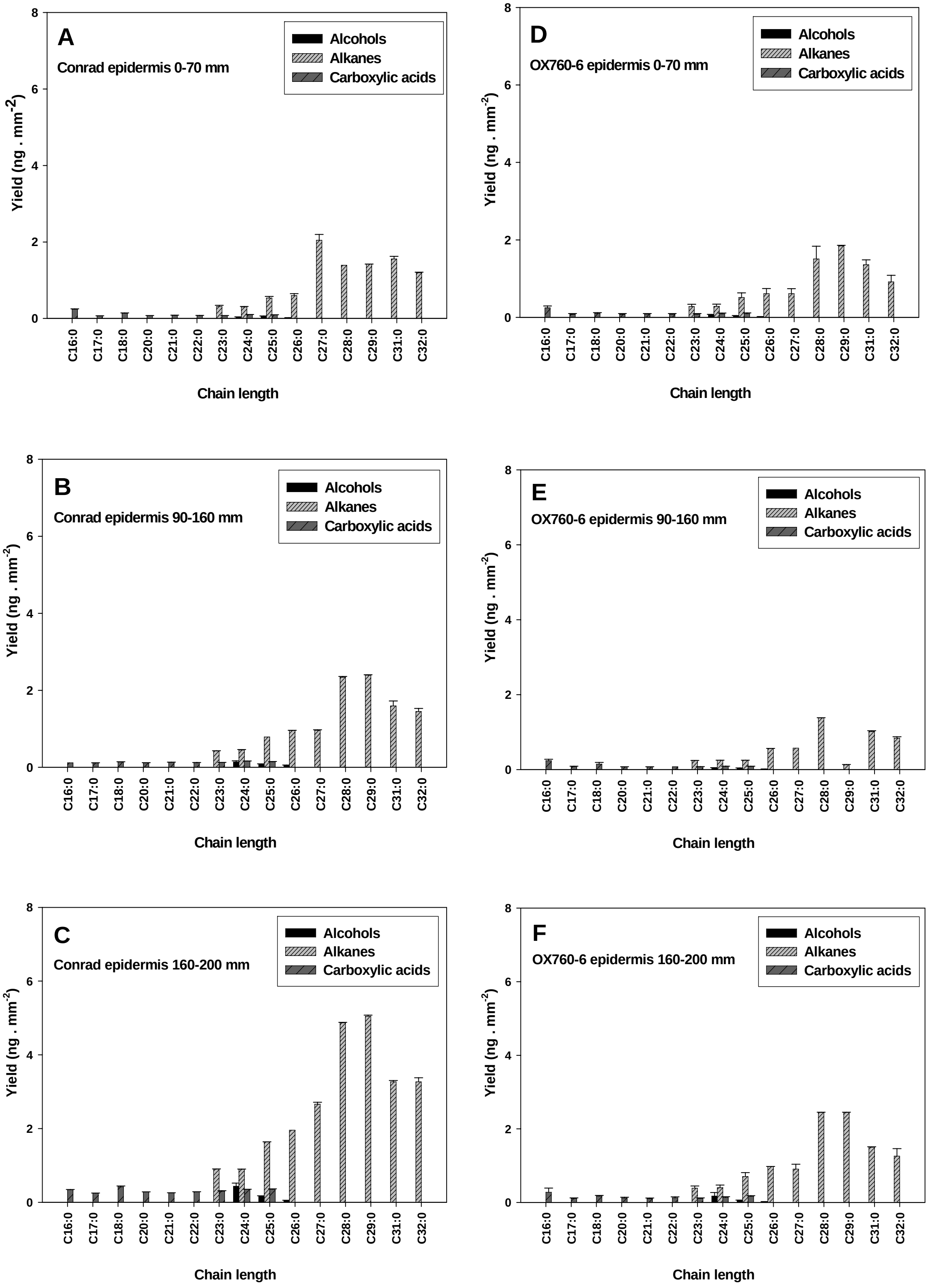
A
Conrad epidermis 0-70 mm
B
Conrad epidermis 90-160 mm
C
Conrad epidermis 160-200 mm
D
OX760-6 epidermis 0-70 mm
E
OX760-6 epidermis 90-160 mm
F
OX760-6 epidermis 160-200 mm
Alcohols
Alkanes
Carboxylic acids
Yield (ng . mm-2)
0
2
4
6
8
Chain length
C16:0
C17:0
C18:0
C20:0
C21:0
C22:0
C23:0
C24:0
C25:0
C26:0
C27:0
C28:0
C29:0
C31:0
C32:0

Figure 3.12 Sum of wax monomers.

Soybean epidermal cell walls were isolated from primary roots of 10-day-old seedlings by digestion with cellulase and pectinase, and extracted with chloroform and methanol. Soluble material of epidermal walls was analyzed with GC-MS. Amounts of substances are expressed as weight (ng) per root surface area (mm^2). Bars indicate standard errors of the means. Values with different letters are significantly different ($P < 0.05$).

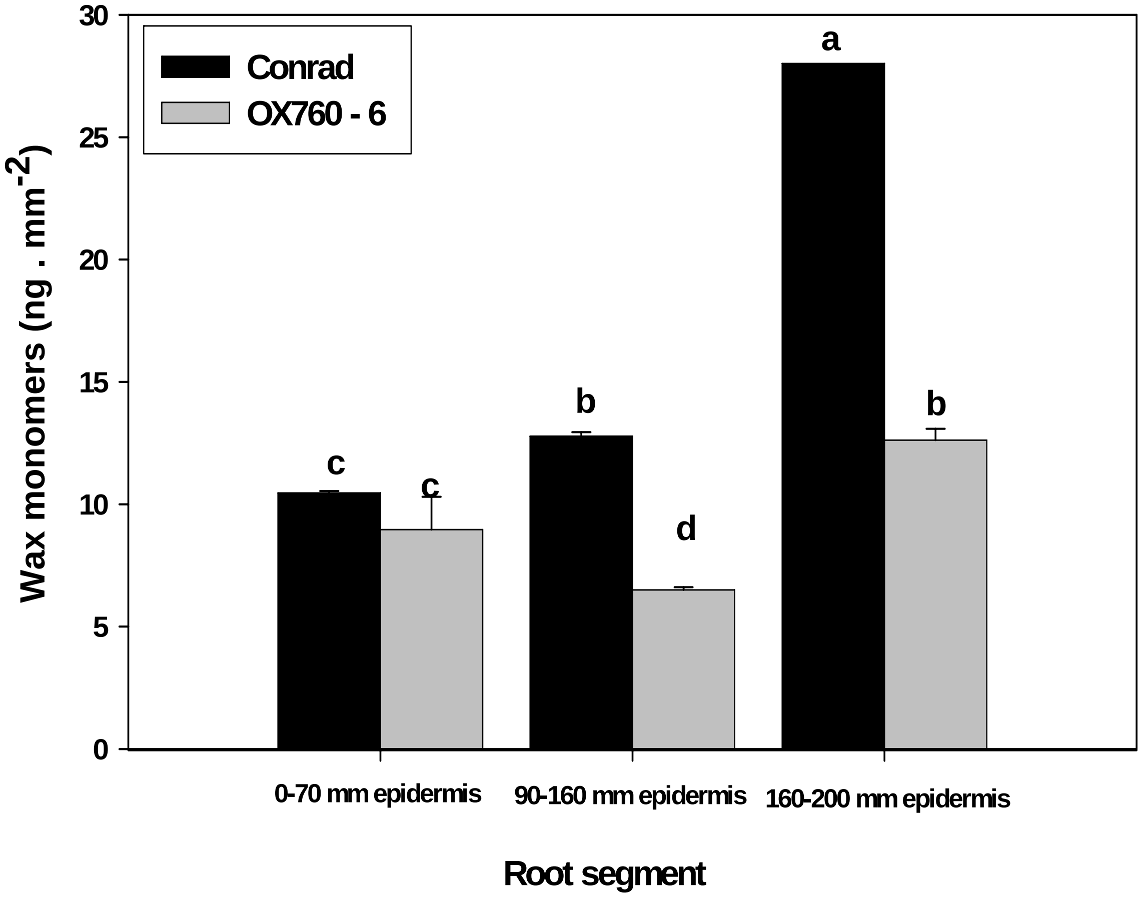

Figure 3.13 Total vanillin and syringin released after nitrobenzene oxidation.

Soybean epidermal cell walls were isolated from primary roots of 10-day-old seedlings by digestion with cellulase and pectinase, and extracted with organic solution. Insoluble material of epidermal walls was degraded into the corresponding aromatic compounds by microscale alkaline nitrobenzene oxidation and analyzed with GC-MS. Amounts of substances are expressed as weight (ng) per root surface area (mm^2). Bars indicate standard errors of the means. Values with different letters are significantly different ($P < 0.05$).

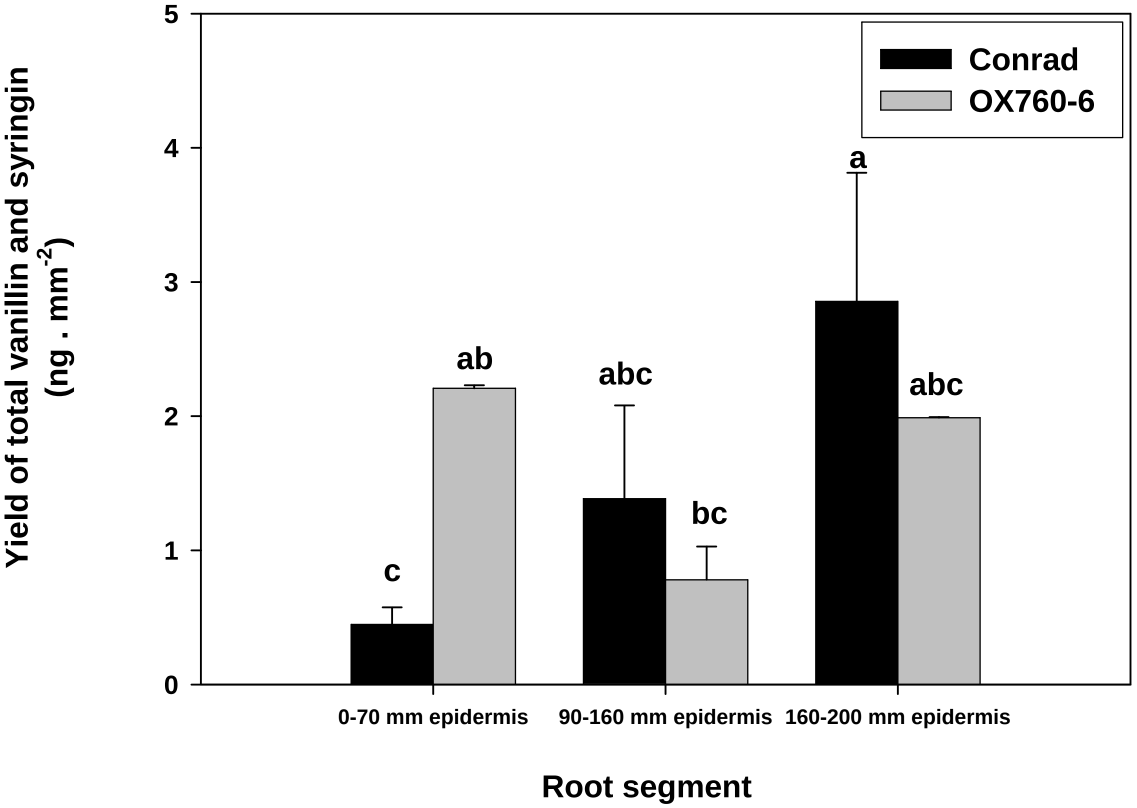

Figure 3.14 Total aromatic substances released from isolated epidermal cell walls of cv. Conrad and cv. OX 760-6 roots.

Soybean epidermal cell walls were isolated from primary roots of 10-day-old seedlings by digestion with cellulase and pectinase, and extracted with organic solution. Insoluble material of epidermal walls was degraded into the corresponding aromatic compounds by microscale alkaline nitrobenzene oxidation and transesterification and analyzed with GC-MS. Amounts of substances are expressed as weight (ng) per root surface area (mm^2). Bars indicate standard errors of the means. Values with different letters are significantly different ($P < 0.05$).

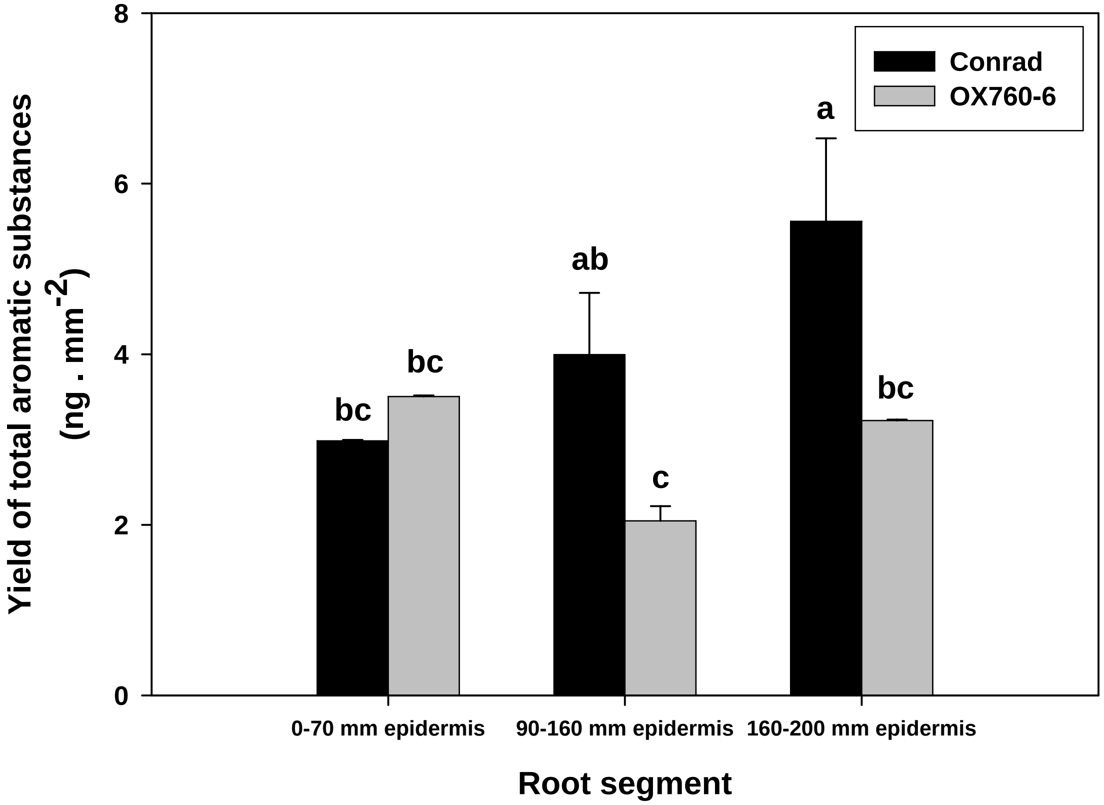

3.4 Viability of epidermal cells

Two chemicals were utilized to test the viability of epidermal cells. Evan’s blue is a non-permeable dye and is excluded from the protoplast by the selectively permeable plasmalemma of living cells. Uranin is a permeable fluorochrome and accumulates in the cytoplasms and nuclei of living cells.

3.4.1 Evan’s blue

Viability testing of epidermal cells with Evan’s blue indicated that the majority was alive in all tested areas of both cv. Conrad and cv. OX 760-6 (Figs. 3.15A and 3.16). The viability of the epidermis was relatively constant along the root length (Fig. 3.15A). However, the zones of epidermal cells with root hairs (30 mm, 50 mm, 70 mm from root tips) tended to have a higher percentage of dead cells than others (Figs. 3.15A and 3.16B).

3.4.2 Disodium fluorescein (uranin)

The epidermal cells stained with uranin indicated that more than 60% of the cells were alive, as they had yellow fluorescein in their nuclei and cytoplasms (Figs. 3.15B and 3.17). The percentage of dead cells was higher with the uranin viability test than with Evan’s blue test (Fig. 3.15). However, the uranin test also showed that the majority of epidermal cells of soybean root remained alive as the roots aged (Figs. 3.15B and 3.17).

3.5 Permeability of epidermal walls

Two apoplastic tracers were employed to examine the permeability of epidermal walls. The first, cellufluor, tended to precipitate from solution. Nevertheless, with the use of a buffer as solvent and with the Acrodisc PF syringe filtration step (with a non-cellulose membrane), the precipitates were diminished. However, excessive fluorescence of all cell contents after staining with cellufluor precluded the examination of wall permeability. In contrast, the

Figure 3.15 Viability of epidermal cells.

Viability of epidermis of cv. Conrad and cv. OX 760-6 roots grown for six d in vermiculite. **A** Evan’s blue viability test. **B** Uranin viability test.

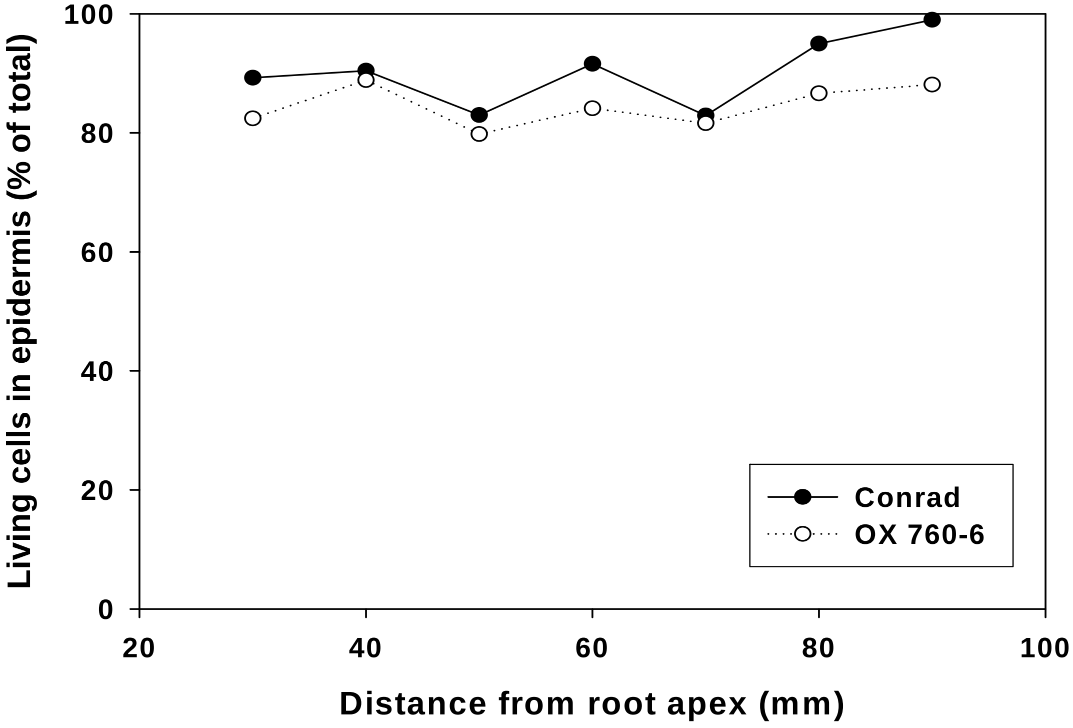
Living cells in epidermis (% of total)
100
80
60
40
20
0
20
40
60
80
100
Distance from root apex (mm)
Conrad
OX 760-6

A

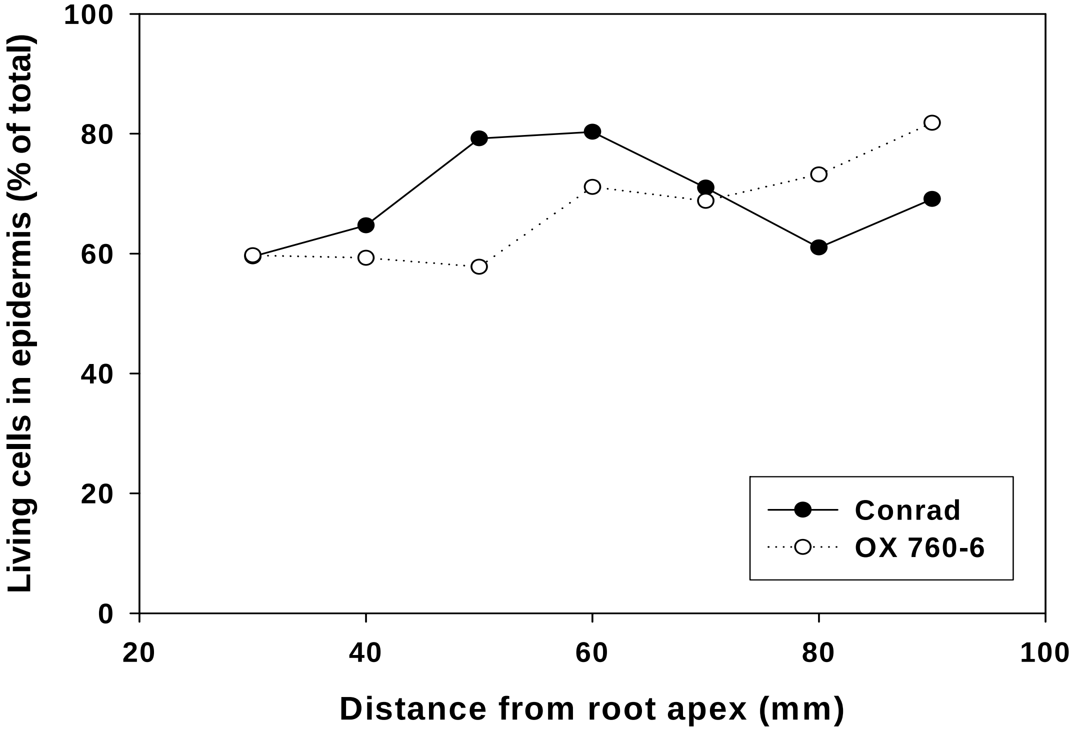
Living cells in epidermis (% of total)
100
80
60
40
20
0
20
40
60
80
100
Distance from root apex (mm)
Conrad
OX 760-6

B

Figure 3.16 Evan's blue viability test of soybean epidermis.

Fresh root segments from cv. OX 760-6 stained with Evan's blue and viewed with white light. Arrows indicate examples of living cells that excluded Evan's blue. Arrowheads indicate examples of dead cells in which the nuclei and cytoplasms were stained blue. Scale bars = 200 µm. **A** Segment taken from non-hair zone. **B** Segment taken from root-hair zone.

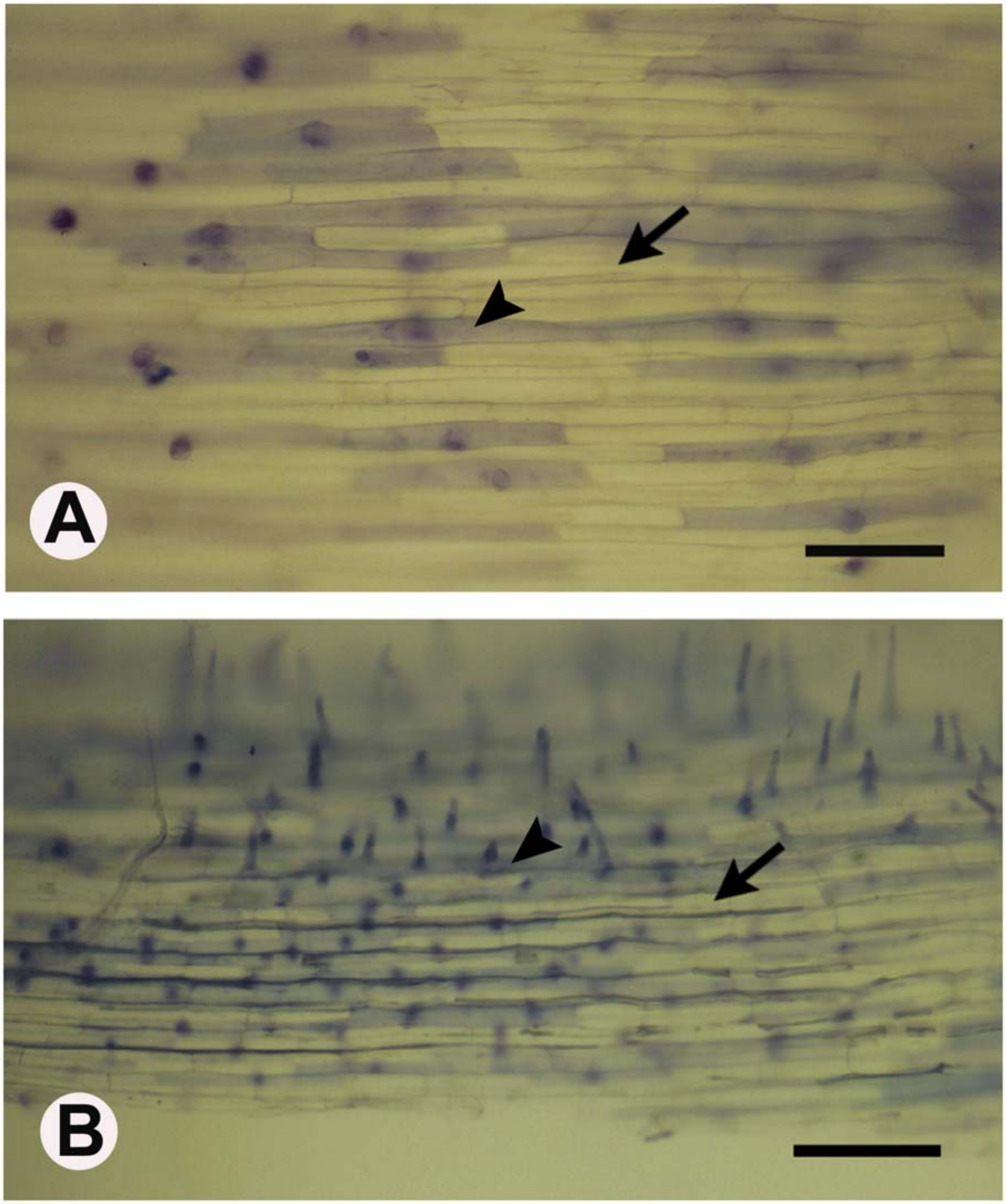
A
B

Figure 3.17 Uranin viability test of soybean epidermis.

Fresh root segments from cv. Conrad stained with uranin and viewed with CLSM. Arrows indicate examples of living cells that had accumulated uranin in their nuclei and cytoplasms. Arrowheads indicate examples of dead cells that excluded uranin. Scale bars = 100 µm. **A** Segment taken 30 mm from the root tip. **B** Segment taken 60 mm from the root tip. **C** Segment taken 100 mm from the root tip.

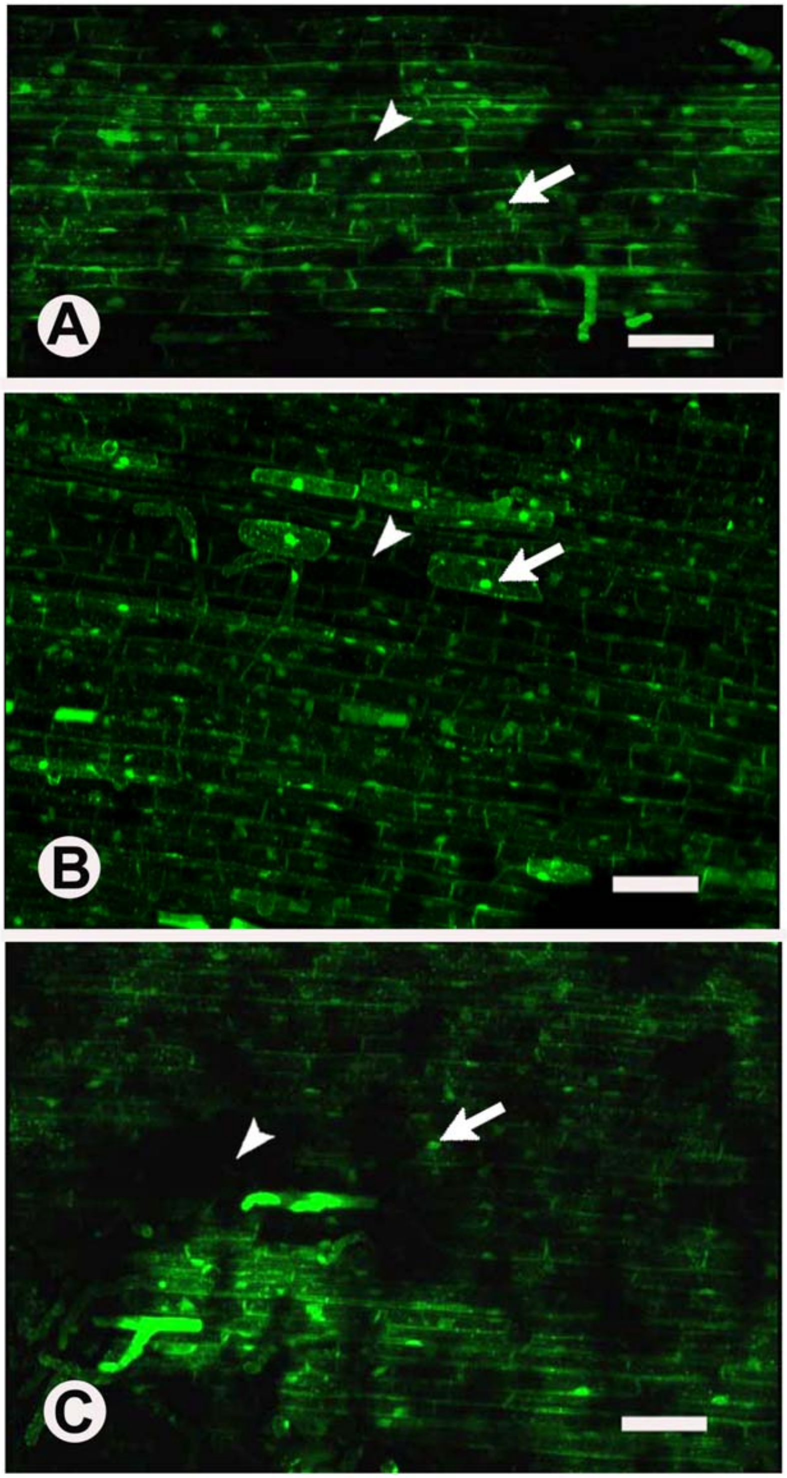
A
B
C

berberine-thiocyanate tracer experiment was easy to perform and the results obtained were clear.

Epidermal cell walls, except those at the extreme root apex (meristem region, Figs. 3.18A, 3.19A, and 3.20A), were permeable to both tracers. From this point of view, both cellufluor and berberine-thiocyanate tracer techniques demonstrated identical results. Cellufluor tended to progressively penetrate into the epidermal wall. At region 0-40 mm from the root tips, cellufluor only stained the outer epidermal walls (Fig. 3.18B and D), then this tracer penetrated through the epidermal wall and stained the outer tangential walls of the first cortical layer as the roots aged (the region of 80-100 mm from the root tip, Fig. 3.18F and H). The cellufluor did not stain beyond the first cortical layer.

Berberine and thiocyanate penetrated further into the root than did cellufluor. (Compare Figs. 3.18, 3.19, and 3.20.) Diffusion of both berberine and thiocyanate progressed inward through the central cortex but halted at the radial walls of the endodermis. Control sections stained with berberine alone showed bright yellow fluorescence throughout the whole sections (Figs. 3.19A3, B3, C3, and D3 and 3.20A3, B3, C3, and D3). However, berberine-thiocyanate precipitations were evident as bright yellow crystals that were typically more concentrated in the inner part of the cortex than in the outer part of the older root sections (the region of 80-100 mm from the root tips, Figs. 3.19D1 and 3.20D1). The berberine-thiocyanate tracer test also demonstrated that the root cap was completely permeable; it contained heavy crystal deposits (Fig. 3.21). There were almost no crystals formed in the root proper apex (Figs. 3.19A1 and 3.20A1). Wax sealed both the cut ends, successfully blocking the penetration of tracers into the steles. In all sections, there were no crystals found in the central steles (Figs. 3.19 and 3.20).

Figure 3.18 Cellufluor tracer in soybean roots.

Fresh, freehand sections from soybean cv. OX 760-6 roots that had been given an external treatment with cellufluor and from untreated (control) roots. Scale bars = 100 µm. Orange arrows indicate the epidermis. Pink arrowheads indicate the cortical cells adjacent to the epidermis. **A** Median longitudinal section through the root apex; cellufluor was excluded from meristem (orange asterisk). **B** Cross-section taken 10 mm from the root tip viewed with UV light. Epidermis stained with cellufluor. **C** Cross-section taken 10 mm from the tip of an untreated root used as a control for B. **D** Same section as B viewed with violet light. Epidermis stained with cellufluor. **E** Same section as C set as a control for D viewed with violet light. **F** Cross-section taken 100 mm from the root tip viewed with violet light. Cellufluor penetrated into epidermis and stained the outer tangential walls of the first cortical layer. **G** Cross-section taken 100 mm from the root tip set as a control for F. **H** Same section as F viewed with UV light. Cellufluor penetrated into epidermis and stained the outer tangential walls of the first cortical layer. **I** Same section as G set as a control for F viewed with UV light.

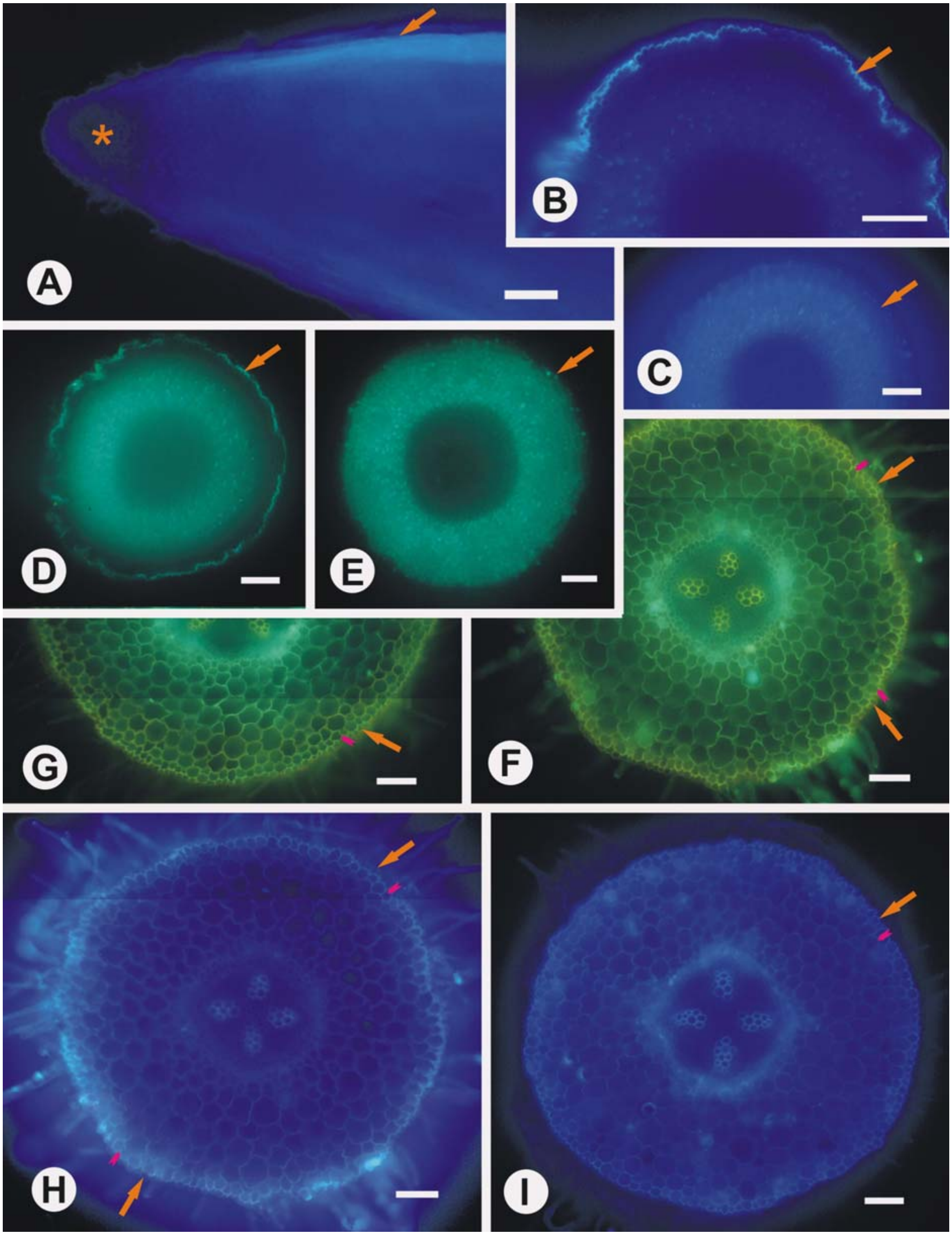
A
B
C
D
E
F
G
H
I

Figure 3.19 Berberine thiocyanate tracer in cv. Conrad root.

Fresh, freehand sections from soybean roots that had been given an external treatment with berberine and thiocyanate (treatment) and berberine alone (staining control) and from untreated (control) roots. Scale bars = 200 µm**. A1, B1, C1, and D1** Cross-sections were treated with BS/KSCN tracers. **A2, B2, C2, and D2** Cross-sections were mounted in water as a control. **A3, B3, C3, and D3 C**ross-sections were stained with berberine as a staining control. **A** Root apex. **A1** No crystals formed. **B** Sections taken 5 mm from the root tip. **B1** Crystals formed in all cortex. **C** Sections taken 25 mm from the root tip. **C1** Crystals are more concentrated in the inner cortical cells but are not found at the endodermis. **D** 100 mm from the root tip. **D1** Crystals are more concentrated in the inner cortical cells but none are found in the endodermis or stele.

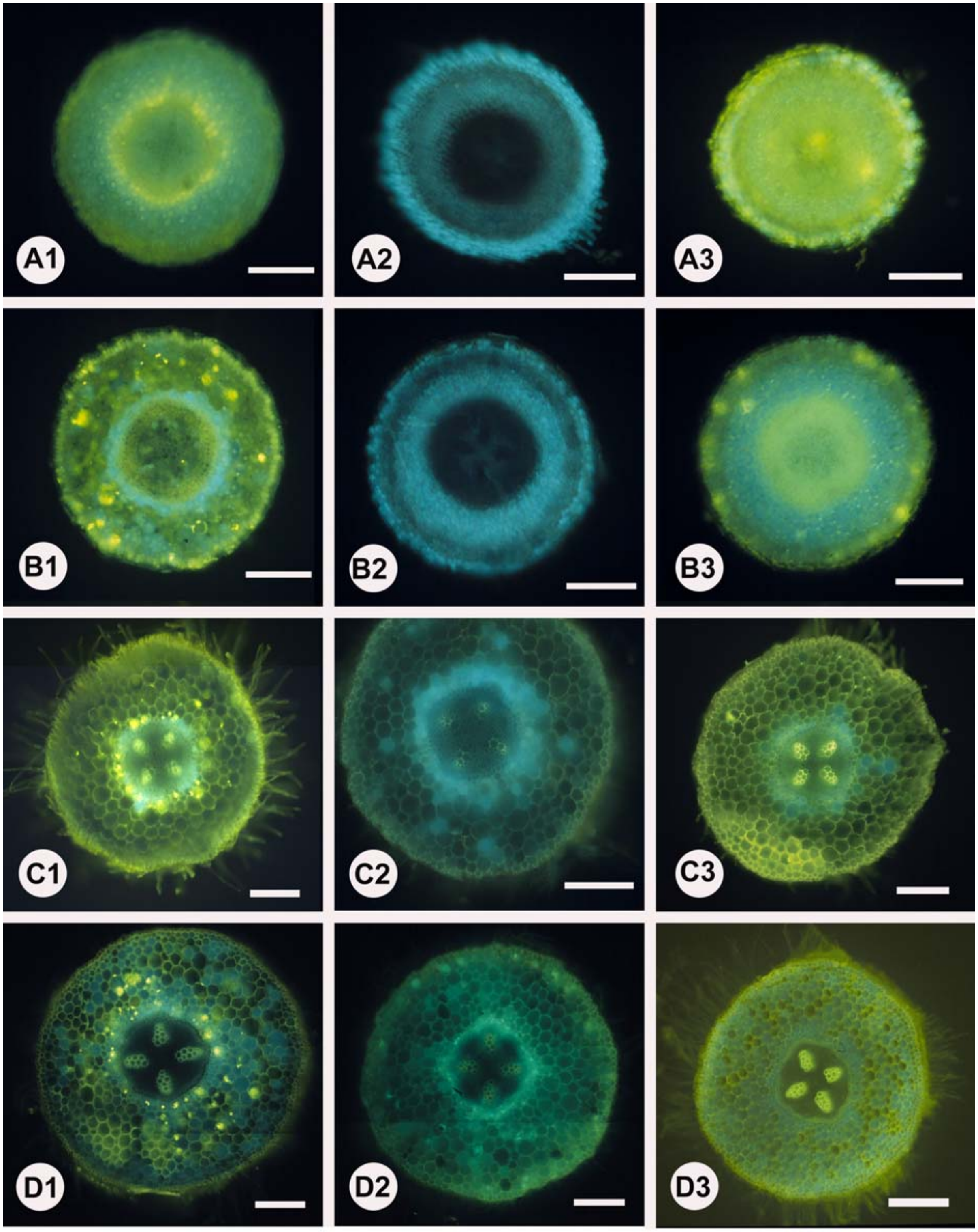
A1
A2
A3
B1
B2
B3
C1
C2
C3
D1
D2
D3

Figure 3.20 Berberine thiocyanate tracer in cv. OX 760-6 root.

Fresh, freehand sections from soybean roots that had been given an external treatment with berberine and thiocyanate (treatment) and berberine alone (staining control) and from untreated (control) roots. Scale bars = 200 µm**. A1, B1, C1, and D1** Cross-sections were treated with BS/KSCN tracers. **A2, B2, C2, and D2** Cross-sections were mounted in water as a control. **A3, B3, C3, and D3 C**ross-sections were stained with berberine as a staining control. **A** Root apex. **A1** Almost no crystals formed. **B** Sections taken 5 mm from the root tip. **B1** Crystals are more concentrated in the outer cortical cells. **C** Sections taken 25 mm from the root tip. **C1** Crystals are formed in all cortical cells. **D** 100 mm from the root tip. **D1** Crystals are more concentrated in the inner cortical cells but none are found in the endodermis or stele.

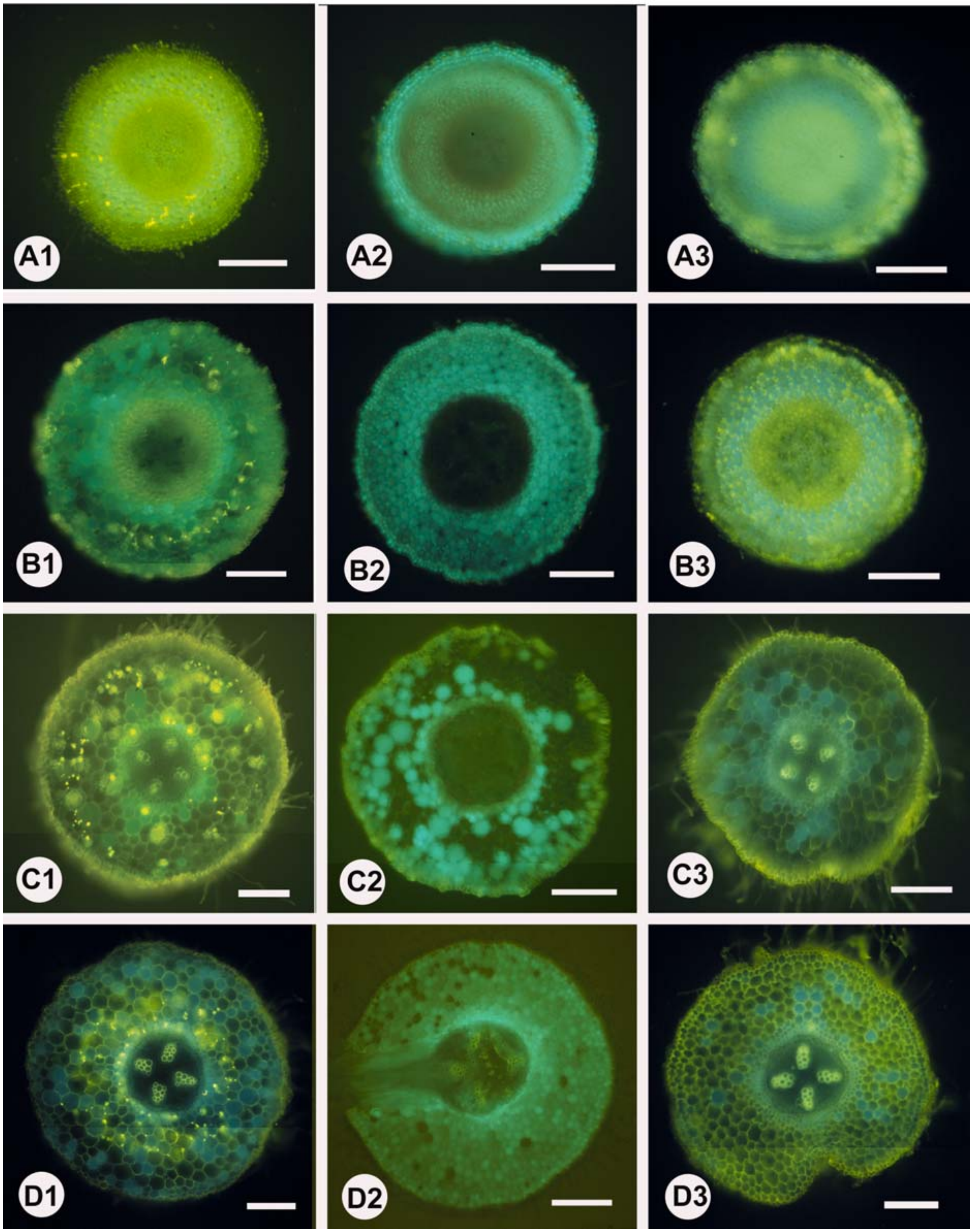
A1
A2
A3
B1
B2
B3
C1
C2
C3
D1
D2
D3

Figure 3.21 Berberine thiocyanate tracer in soybean root cap.

Fresh, freehand, cross-section of soybean cv. OX 760-6 root was taken through root cap region and treated with BS/KSCN. Numerous crystals were found in the root cap region. Scale bar = 200 μm. Blue stars indicate some of the crystals.

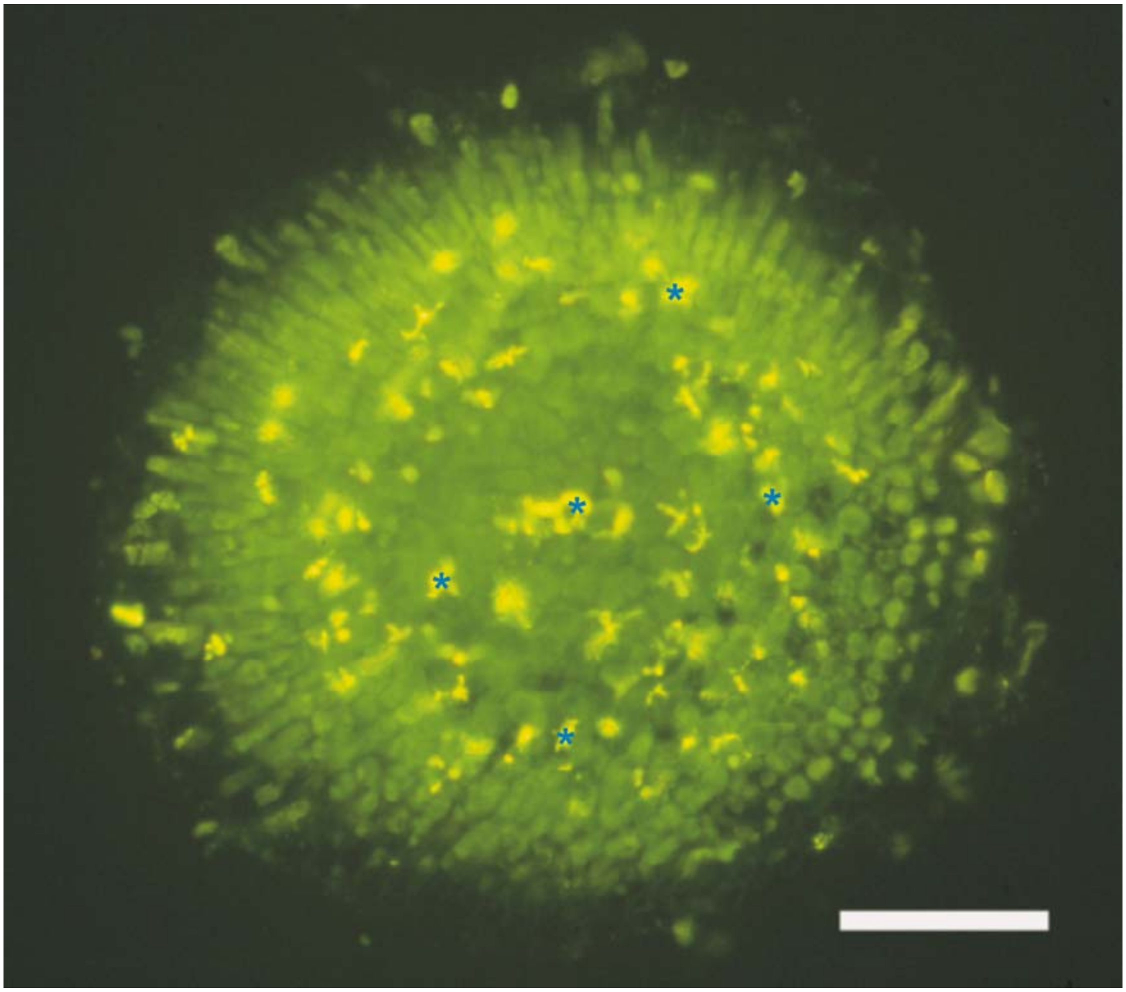

3.6 Intermicrofibrillar pore sizes

Pore sizes in the epidermal cell walls ranged from 2.2 nm to 3.5 nm at distances of 40 mm to 90 mm from the root tips, respectively (Table 3.2). Epidermal cells exhibited two different reactions in response to external addition of PEG. For example, at a distance of 50-60 mm from root tips, PEG-200 had no effect upon the appearance of the plasmolyzed cells. Cells stained with uranin displayed yellow greenish fluorescence in the central vacuole and cytoplasm encased with the plasma membrane that had pulled away from cell walls (Fig. 3.22A). Using PEG with a molecular weight above 400 induced cytorrhysis in the cells; these had collapsed vacules (Fig. 3.22B). There was no difference in pore sizes of resistant cv. Conrad and susceptible cv. OX 760-6. However, a progressive increase of pore size was observed along the root length ranging from 2.2 to 3.5 nm (Table 3.2).

Table 3.2 Measurement of intermicrofibrillar pore sizes.

Various molecular weights and sizes of polyethylene glycol (PEG, Carpita et al., 1979) solutes with their ability to cause plasmolysis (P) or cytorrhysis (C) of soybean epidermal cells.

Solute	Molecular weight (Da)	Molecular diameter (nm)	Distance from root tip (mm)							
			10-20	20-30	30-40	40-50	50-60	60-70	70-80	80-90
PEG-200	200	<2.2	C	P&C	P&C	P	P	P	P	P
PEG-400	400	2.2	C	C	P&C	P&C	P&C	P&C	P	P
PEG-600	600	2.9	C	C	P&C	P&C	P&C	P&C	P&C	P
PEG-900	900	~3.5	C	C	C	C	C	P&C	P&C	P&C
PEG-1000	1000	3.5	C	C	C	C	C	C	P&C	P&C
Maximum pore size (nm)				<2.2	<2.2	2.2	2.2	2.2	2.9	~3.5

Figure 3.22 Measuring pore sizes.

Longitudinal sections taken 50-60 mm from the root tip of soybean cv. Conrad, stained with uranin, plasmolyzed with mannitol, and viewed with violet light. Scale bars = 50 µm. **A** Arrowhead indicates plasmolyzed cell**.** **B** Section was treated with PEG-900 (Molecular diameter is around 3.5 nm). Cytorrhysis occurred. Arrowhead indicates cytorrhyzed cell.

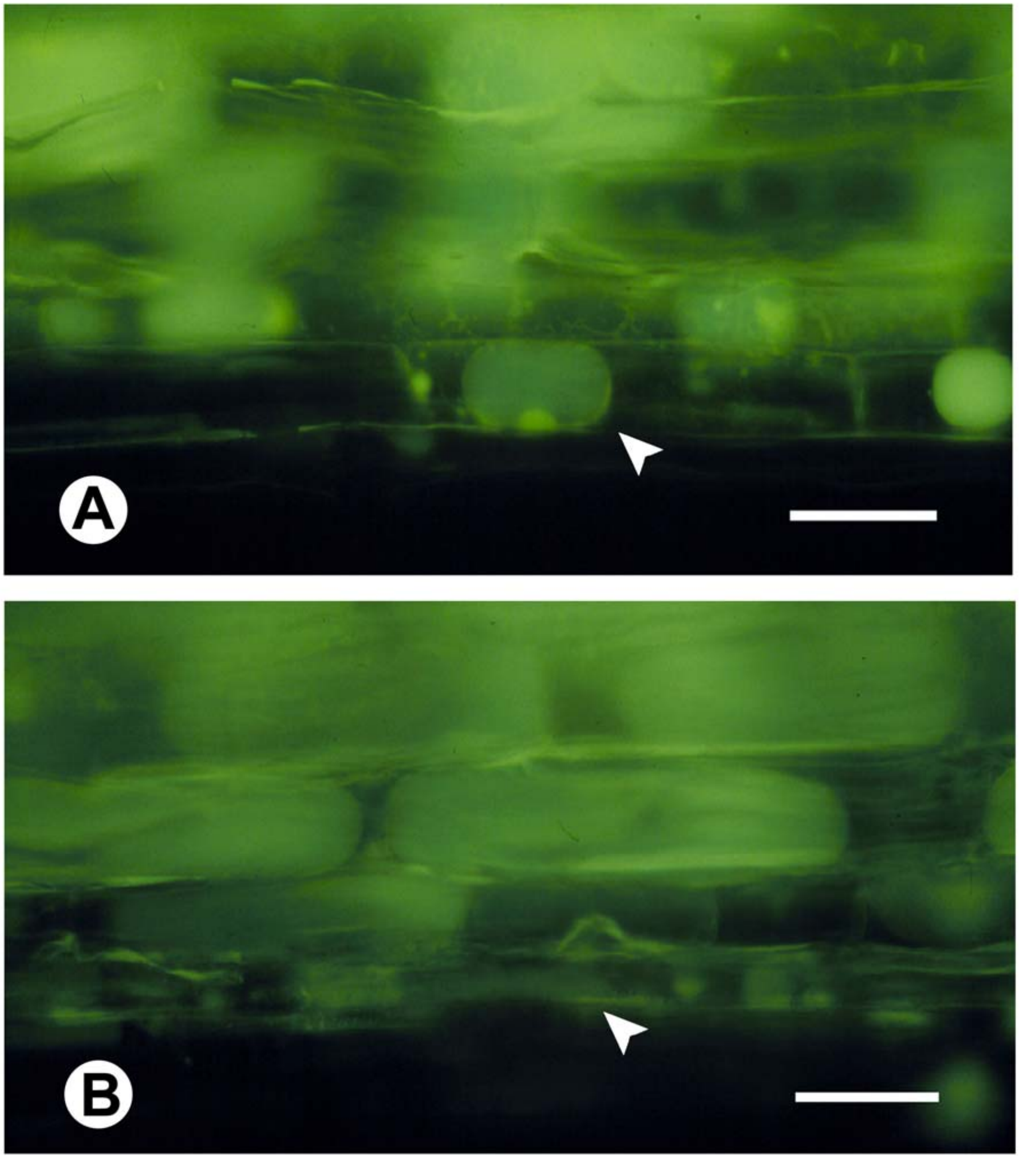
A
B

3.7 Pathogen-root interactions

3.7.1 Development of *P. sojae* in etiolated seedlings

Zoospores of *P. sojae* were equally attracted to 3-day-old roots of resistant (cv. Conrad) and susceptible (cv. OX 760-6) soybean cultivars, and distributed themselves uniformly over the entire root surfaces (Fig. 3.23A and B) except for the root cap that extended along the root for a distance of 1.5 mm from root tip. Only a single germ tube emerged from each zoospore cyst and invaded directly between epidermal walls. Very few germ tubes swelled after adhering to the root surface. Furthermore, these swollen tips were separated from germ tubes with visible septa (Fig. 3.23C). Effective adhesions could be recognized as highly refractive, elliptical halos on the epidermis around the point of penetration. Penetrations of germ tubes were always between the anticlinal walls of epidermal cells (Fig. 3.23D). This early disease development was similar on roots of cv. Conrad and cv. OX 760-6 (Fig. 3.23A and B).

Accumulation and adhesion of zoospores to the root surface happened within 50 min of inoculation. However, the penetration of hyphae occurred much slower compared with the adhesion of zoospores. The first penetration of hyphae in cv. Conrad took more than seven h, before penetration pegs could be seen in the interior of epidermal cells (Fig. 3.23D), while the first penetration of hyphae in cv. OX 760-6 happened within four to six h of inoculation. Hyphae in cv. OX 760-6 at seven-h incubation time (7 h) had already extended into the epidermal cells (Fig. 3.23F).

Initially intercellular extension of hyphae in the cortex of resistant cv. Conrad was mostly parallel to the longitudinal root axis (Fig. 3.23E). In contrast, in susceptible cv. OX 760-6, hyphae developed both parallel and perpendicular to the root axis (Fig. 3.23G). The lengths of hyphae differed significantly in both cultivars. Hyphae in cv. OX 760-6 (Fig. 3.23G) were much longer and more extensive than in cv. Conrad (Fig. 3.23E) 18 h after inoculation. The extension of hyphae in cv. Conrad was limited to the epidermal cells and the first cortical cell layer (Fig. 3.23E) whereas hyphae in cv. OX 760-6 extended as far as a few outermost cortical layers (Fig. 3.23G).

Twenty-four h after incubation, the color of the root surface had changed from pale to dark brown in the resistant cv. Conrad; whereas, in susceptible cv. OX 760-6, there was only a light browning of the tissue (Fig. 3.23H). From the cross-sections, patchy browning also occurred in the cortical cells adjacent to epidermis (Fig. 3.25A). Lateral roots emerged from the infected primary roots of cv. Conrad but not cv. OX 760-6. All roots from both cultivars were rotten and stopped growing after four d of incubation.

3.7.2 Staining techniques for evaluation of hyphal development

Several different techniques for viewing the development of hyphae were tried (Table 3.3). Prior to staining the hyphae in the cleared root, these techniques were first applied to fresh mycelium from the culture plate. The most successful method for staining hyphae of *P. sojae* was aniline blue in basic solution, viewed with ultraviolet light.

Chlorazol black E solution applied to the cleared roots formed numerous blue-black precipitates, preventing observation of hyphal development. Only elliptical halos were stained with trypan blue; however, neither elliptical halos nor hyphae were stained with aniline blue in lactoglycerol. The fresh mycelia from the culture plate were stained blue with the use of three stains, i.e. Chlorazol black E, trypan blue, and aniline blue in lactoglycerol. Cellufluor stained the epidermal cell walls a bright blue, and the walls of zoospores and germ tubes white under ultraviolet light.

Although the aniline blue in basic solution (pH 7.5) staining technique was the best method to demonstrate the development of *P. sojae*, the intercellular hyphae could not be seen with this dye. However, two hemispherical dense pads around the hyphal penetration sites were visible with aniline blue soon after infection (Fig. 3.24A). The haustoria growing from the intercellular hyphae into cell protoplasts were encased with callose. This glucose polymer was stained with aniline blue as well (Fig. 3.24B). This phenomenon happened 18 h after inoculation.

Figure 3.23 Development of *P. sojae* in the soybean root.

Cleared, whole mount of inoculated soybean root viewed with white light and DIC optics. Scale bars of A, B, and E are 35 µm. Scale bars of C, D, G and F are 15 µm. **A** Zoospores are distributed uniformly on the root surface of cv. Conrad after two h inoculation. Asterisks indicate some of the zoospores. **B** Zoospores are distributed uniformly on the root surface of cv. OX 760-6 after two h inoculation. Asterisks indicate germ tubes. **C** Only a single germ tube (arrows) germinated from each zoospore cyst (asterisks). Very few germ tubes swelled after adhering to the root surface. Black arrowhead denotes a swollen tip that was separated from the germ tube by a septum (white arrowhead). **D** The penetrations of germ tubes were through the anticlinal walls of epidermal cells in resistant cv. Conrad with seven h inoculation. Hyphae were not seen at this stage except for very tiny penetration pegs (arrows). Arrowheads denote hightly refractive, elliptical halos on the epidermis around the points of penetration. **E** Infected segments of resistant cv. Conrad after 18 h inoculation stained with TBO. Arrow indicates a hypha parallel to the longitudinal root axis between the epidermal cells. **F** Arrow indicates the penetration of hypha in susceptible cv. OX 760-6 after seven h inoculation as compared to D. **G** Extensive growth of hyphae (arrows) distributed in the root of susceptible cv. OX 760-6 stained with TBO after 18 h inoculation as compared to E. **H** Infected soybean roots turned brown. Resistant cv. Conrad displayed heavier patchy browning (arrowheads) than susceptible cv. OX 760-6.

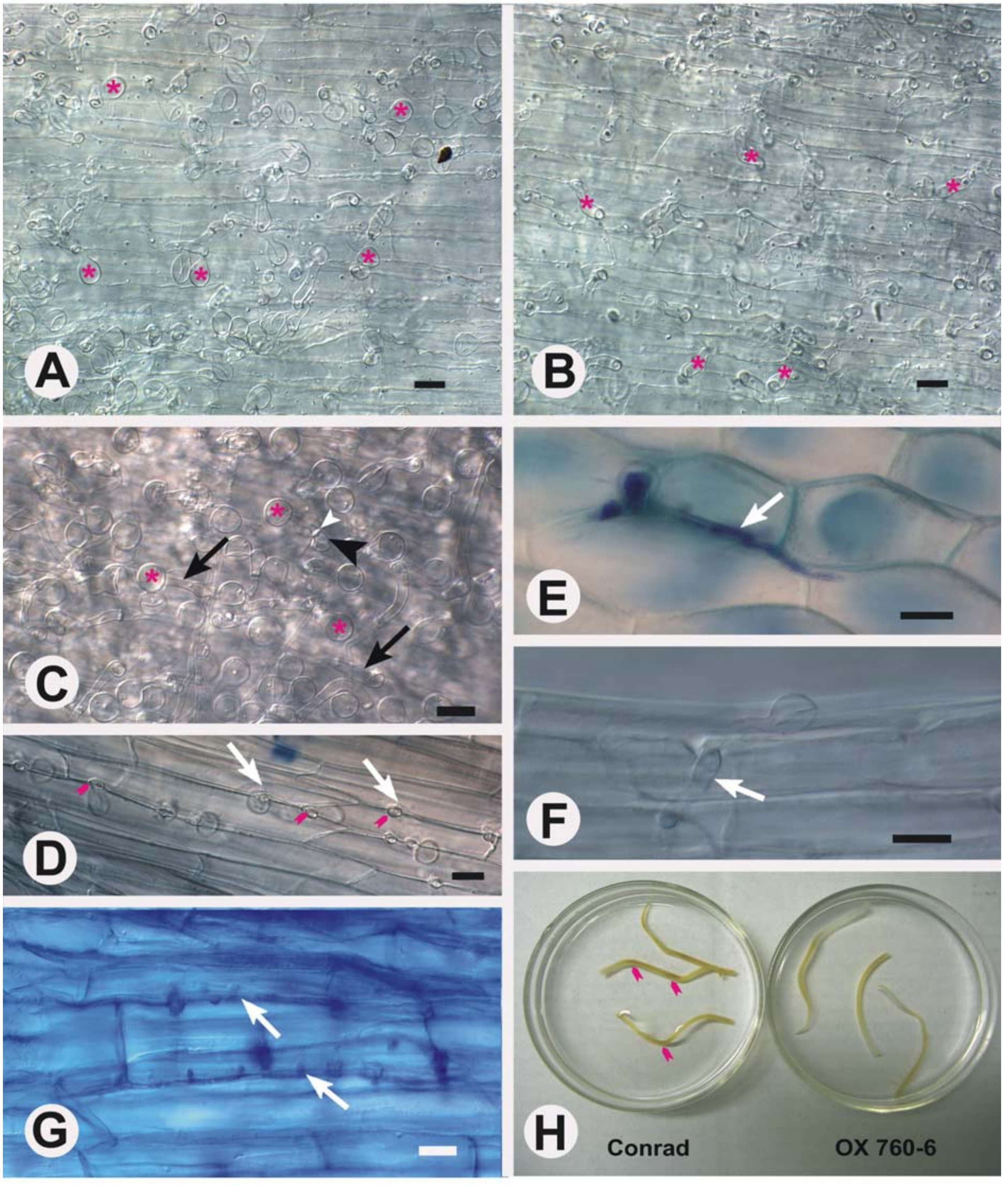
A
B
C
D
E
F
G
H
Conrad
OX 760-6

Table 3.3 Different staining techniques applied to inoculated soybean roots.

Dyes	Light	Fresh mycelium	Zoospore	Hypha (in cleared root)	Haustorium (associated with callose)
Chlorazol black E	**W**	**+**		**-**	**-**
Trypan blue	**W**	**+**		**-**	**-**
Aniline blue (in lactoglycerol)	**W**	**+**		**-**	**-**
Cellufluor	**UV**		**+**		
Aniline blue (in basic solution)	**UV**	**+**		**+**	**+**

W white light
UV ultraviolet light
+ positive staining
- negative staining

Figure 3.24 Development of *P. sojae* hyphae in soybean root.

Cleared, whole mount segments of inoculated soybean root stained with aniline blue in basic solution and viewed with UV light. Scale bars = 15 µm. **A** Root of resistant cv. Conrad was inoculated with zoospore suspension for two h, and then incubated for 24 h. Arrowheads denote two hemispherical dense pads around the hyphal penetration sites. **B** Root of susceptible cv. OX 760-6 was inoculated with zoospore suspension for 18 h. Arrowheads indicate haustoria growing from the intercellular hyphae.

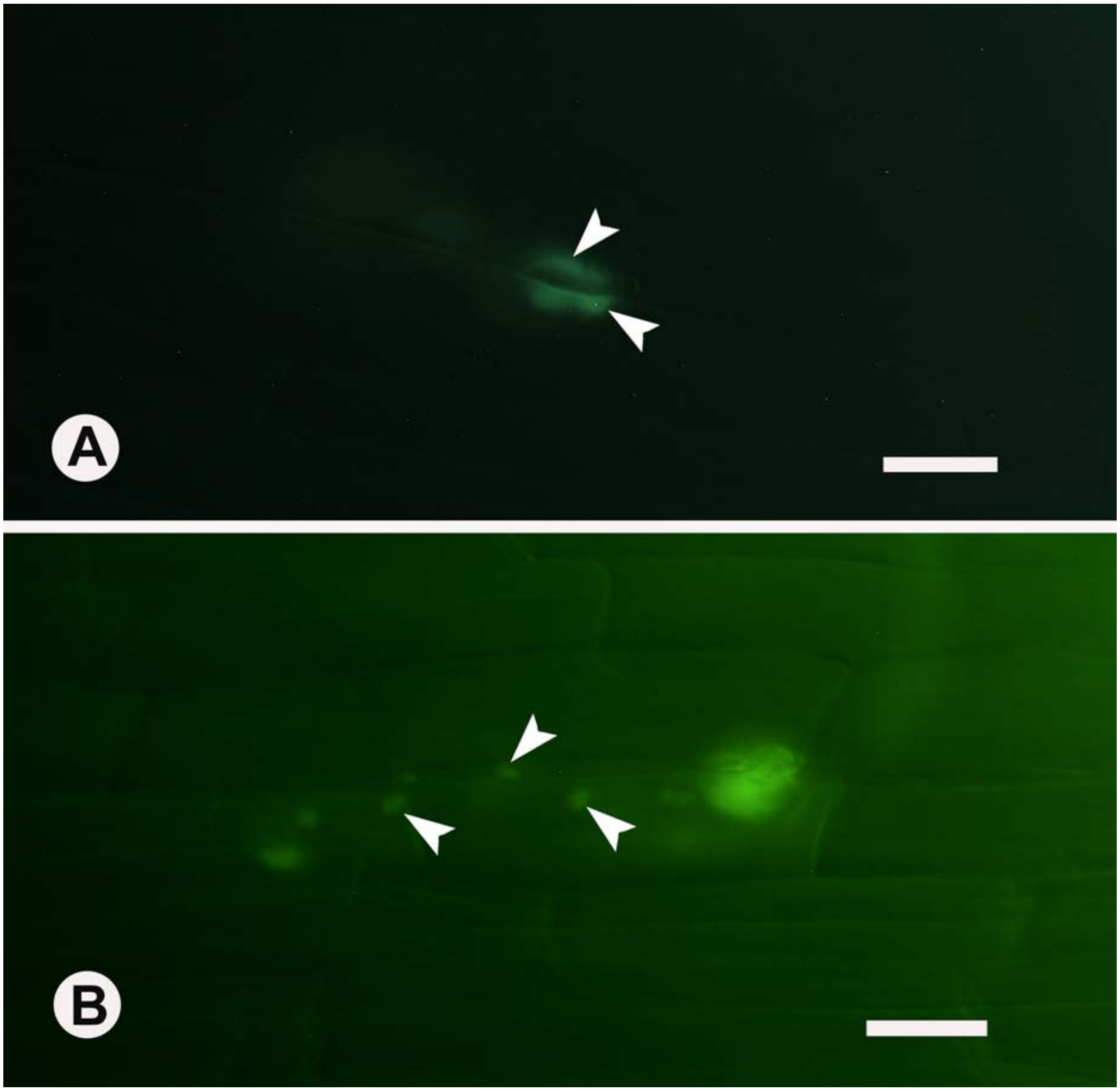
A
B

There were a few brown patches extending from epidermal cells into adjacent layers of cortical cells in the cross-sections of freshly inoculated roots of both cultivars as compared to non-incubated roots (Fig. 3.25A and C). Furthermore, this patchy browning displayed yellow fluorescence under blue light (Fig. 3.25B), whereas autofluorescence was visible only on the outer tangential epidermal cell walls of control sections (Fig. 3.25D). After staining with sudan red 7B, a positive bright red staining was visible in all brown areas (Fig. 3.25E).

Freshly incubated root segments stained with TBO displayed obvious contrasts between the resistant (Fig. 3.26A and C) and susceptible cultivars (Fig. 3.26B and D). The epidermal cells infected by the pathogen were dark brown (Fig. 3.23A), and were heavily stained with TBO in the resistant cv. Conrad (Fig. 3.26A). The infected epidermal cell in the susceptible cv. OX 760-6 was slightly stained with TBO (Fig. 3.26B). The TBO staining technique also demonstrated the limited hyphae extension in the resistant cv. Conrad (Fig. 3.26C) and extensive growth of hyphae in the susceptible cv. OX 760-6 (Fig. 3.26D).

The epidermal cells of whole, incubated roots stained with *Chelidonium majus* root extract solution fluoresced bright yellow (Fig. 3.26E and F) in both cultivars compared with control root segments. The resistant cv. Conrad (Fig. 3.26E) displayed stronger fluorescence than did the susceptible cv. OX 760-6 (Fig. 3.26F). This bright yellow fluorescence was on the cortical cell layers adjacent to the epidermis as well, and prevented visualization of more internal tissue.

3.7.3 Acid digestion

The walls of the infected cortical cells were preserved even after 5-d acid digestion in addition to the walls of the epidermis, endodermis, and xylem vessel members in inoculated soybean roots (Fig. 3.27). All walls left appeared dark brown after the treatment with concentrated sulfuric acid.

Figure 3.25 Response of soybean root to inoculation with *P. sojae*.

A Fresh, cross-section of inoculated root viewed with white light with DIC optics. Arrows denote the infected areas that turned brown. **B** Same section as A viewed with blue light. Arrows denote the infected areas displaying bright yellow autofluoresence. **C** Fresh, cross-section of non-inoculated root viewed with white light with DIC optics (a control for A). Arrow indicates the epidermis. **D**. Same section as C viewed with blue light (a control for B). Arrow indicates the autofluorescent epidermis. **E** Fresh, cross-section of inoculated root treated with sudan red 7B. Arrows indicate the positive red-stained, infected areas. Scale bars = 35 μm.

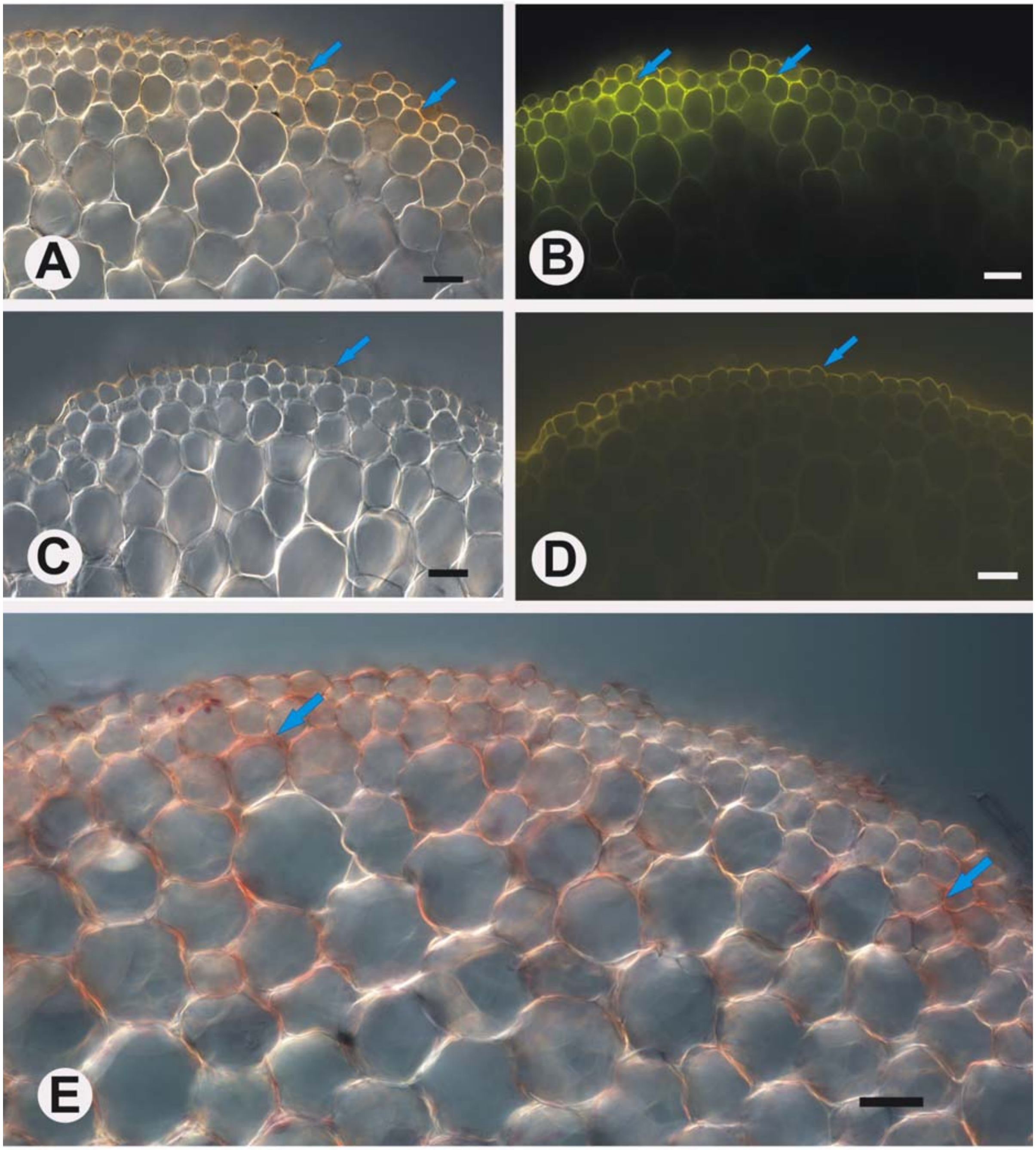
A
B
C
D
E

Figure 3.26 Penetration of *P. sojae* into soybean roots.

Fresh, whole mount, incubated soybean root segments stained with TBO and viewed with white light with DIC optics (A-D). Cleared, whole mount, incubated soybean root segments treated with *Chelidonium majus* root extract and viewed with violet light (E and F). Scale bars of A and B are 15 µm. Scale bars of C-F are 35 µm. **A** Root segment from resistant cv. Conrad. Arrow denotes an infected cell heavily stained with TBO. **B** Root segment from susceptible cv. OX 760-6. Arrow denotes an infected cell lightly stained with TBO. **C** Root segment from resistant cv. Conrad showing the heavily stained infected root, but the extension of hyphae is limited. **D** Root segment from susceptible cv. OX 760-6 displaying the lighter stained infected root as compared to resistant cv. Conrad (C) and extensive growth of hyphae. **E** Root segment from resistant cv. Conrad showing the bright yellow fluorescence in the infected area. **F** Root segment from susceptible cv. OX 760-6 showing lighter yellow fluorescence as compared to resistant cv. (E).

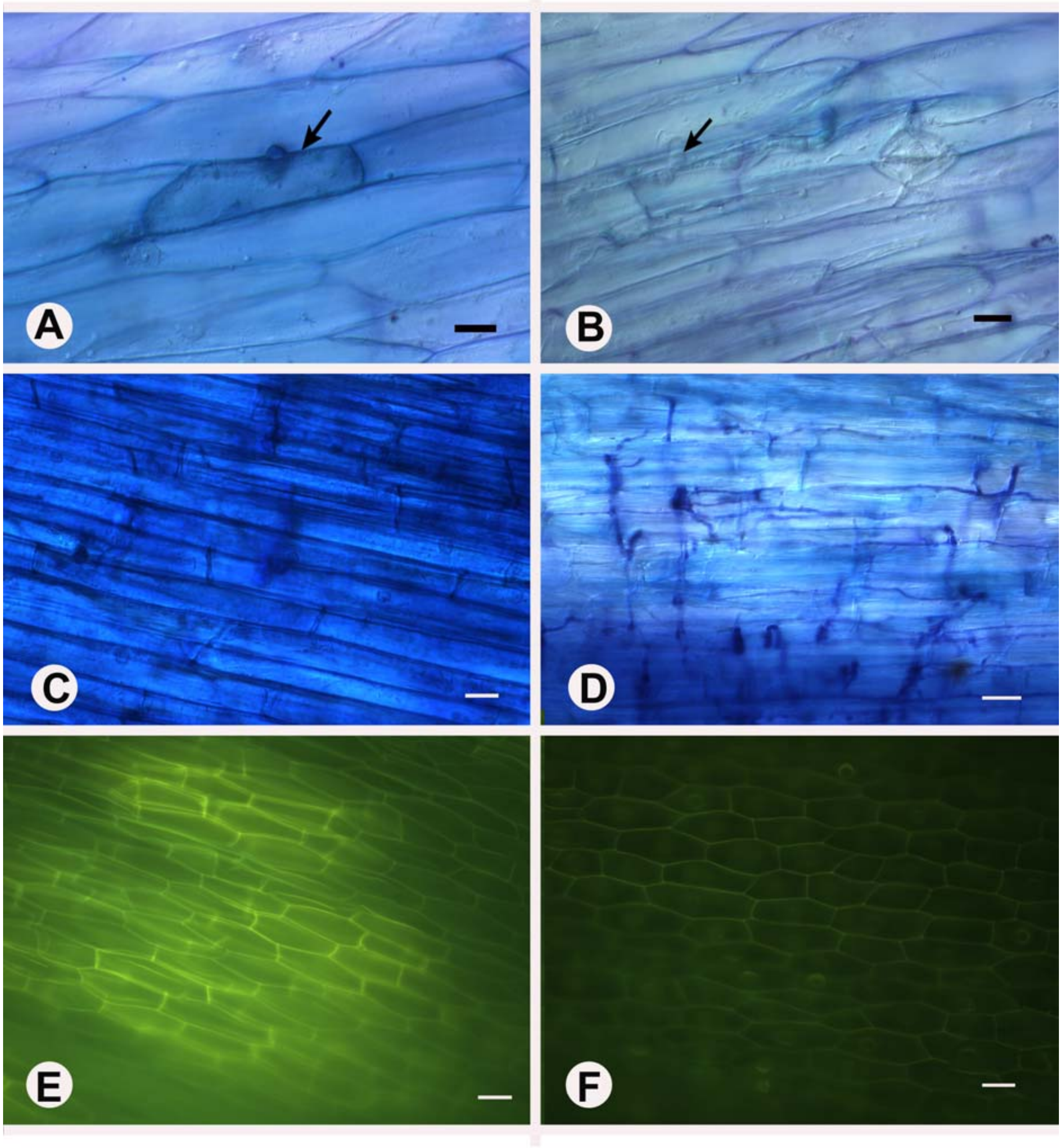
A
B
C
D
E
F

Figure 3.27 Acid digestion of inoculated soybean root.

Freehand, cross-section of inoculated soybean root taken 20 mm from the root tip and viewed under white light with DIC optics. Scale bars = 70 µm. **A** The infected cortex areas (IC) turned brown in 18-h inoculated root. **B** Same section as A treated with concentrated sulphuric acid for 30 min. Uninfected cortex started to be digested away. Endodermal Casparian bands (CB) and xylem vessels (X) appeared dark brown. **C** Same section as A and B treated with concentrated sulphuric acid for 5 d. The walls of epidermis (Ep) and infected cortex (IC), endodermal Casparian bands (CB), and a group of xylem vessels (X) were preserved and appeared dark brown.

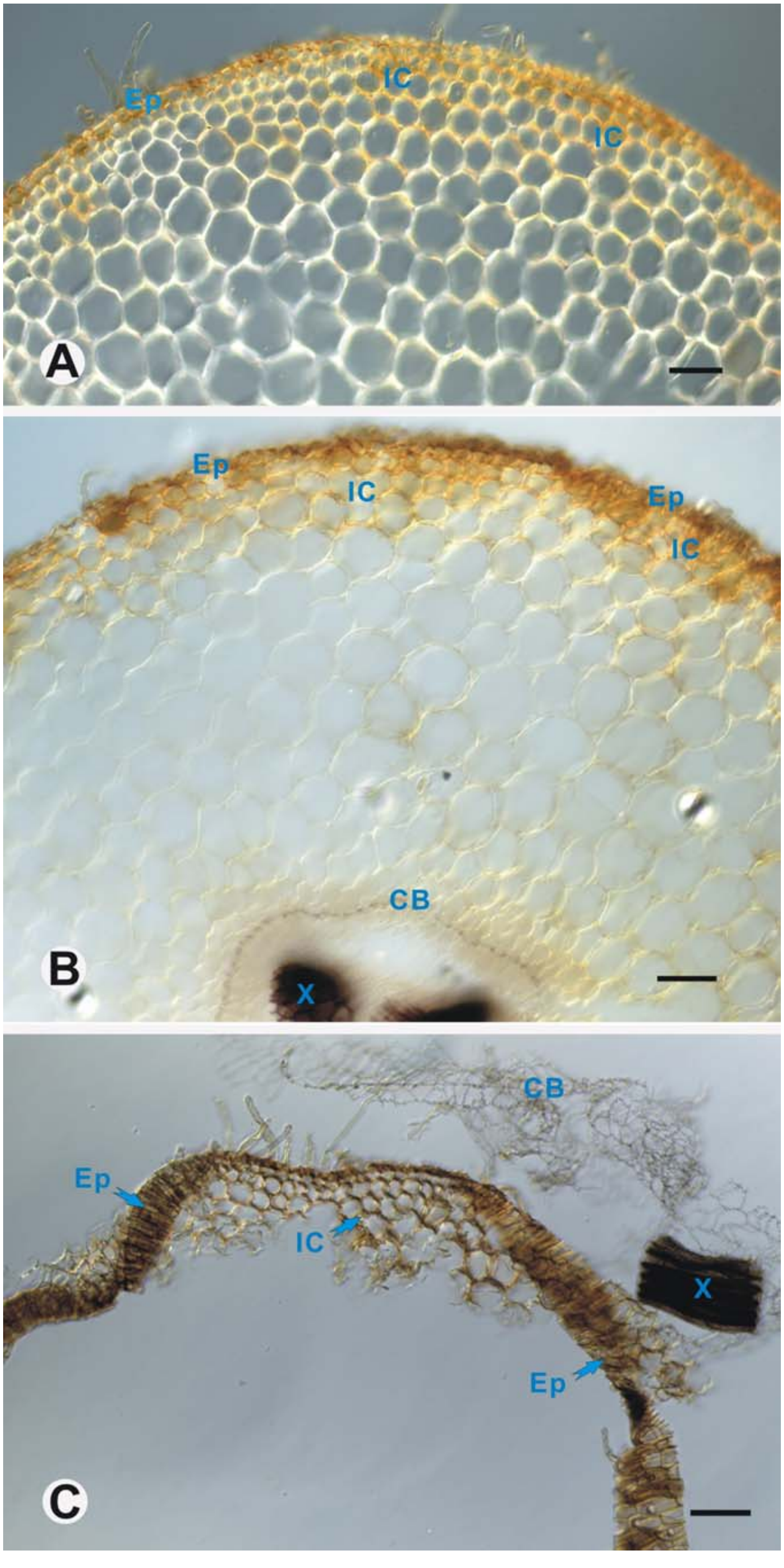
Ep
IC
IC
A
Ep
IC
Ep
IC
CB
B
X
CB
Ep
IC
X
Ep
C

4 Discussion

4.1 Chemical nature of soybean root epidermal walls as determined by histochemical tests

The results of the current study demonstrate for the first time the chemical nature of soybean epidermal cell walls, and augment the results of previous work in which suberin was identified histochemically in the epidermal cell walls of 21 of 27 tested species (Wilson and Peterson, 1983). Histochemical tests for investigating suberin were based on the widely accepted concept that this substance is a complex biopolymer containing phenols and lipids (see Kolattukudy, 1980; Kolattukudy, 1984; Bernards, 2002). Wilson and Peterson (1983) stated "suberin stains positively for polyphenols and lipids, and suberized walls resist digestion by concentrated sulphuric acid." Therefore, the staining techniques for phenols and lipids, and acid digestion were performed in the present study.

Many histochemical methods are available for staining phenolics (Johansen, 1940; Reeve, 1951; Ling-Lee et al., 1977). However, not all techniques proved to be suitable for soybean root epidermal cell walls. For example, although not reported here, the color reactions were obscured with ferric chloride that demonstrates phenols as described by Johansen (1940), Brisson et al. (1977), and Ling-Lee et al. (1977). The Hoepfner-Vorsatz (H-V) reagents described by Reeve (1951) and Ling-Lee et al. (1977) that demonstrate a positive staining of polyphenols using a nitrous acid reaction worked well for the soybean root epidermis. According to Chalker-Scott and Krahmer (1989), a range of colors from red to yellow produced by the H-V test depends on the phenolic groups present in the plant material. The H-V test used in this study imparted a brown color to the root epidermis (Fig. 3.3) except for the terminal region less than 50 mm (around three d old) from the root tip that showed an indefinite color reaction. The reason for this could be the relatively small amount or lack of phenolic compounds in this young root epidermis.

Autofluorescence is the easiest way to detect the presence of phenols. In soybean root epidermis, autofluorescent phenols were observed as close as 5 mm from the root tip and were progressively deposited centripetally extending into the cortical cell walls (Fig. 3.2).

This observation suggests that some phenolics are present in the young part of the epidermal walls, but are not sensitive to the above phenol testing. The centripetal fashion of phenolic deposition is generally found in other plant species as well, for example, in the suberized epidermal walls of onion roots (Peterson et al., 1978), and in the suberized periderm of wound potato tuber (Lulai and Corsini, 1998). The two soybean cultivars had slight differences when sections were taken the same distances from the root tips, the epidermal walls of cv. OX 760-6 (the susceptible cv.) displaying a slightly higher intensity of autofluorescence than those of cv. Conrad (the resistant cv.). This was roughly quantified by comparing the exposure times of an automatic camera. The cortical walls displayed uneven autofluorescence in the mature region of the roots in both cvs. Soybean differs from onion roots, in which the autofluorescence is absent in the central cortical walls and only limited to the epidermal, exodermal, and endodermal walls (Peterson et al., 1978). Onion possesses Casparian bands in the hypodermis (thus called an exodermis) as compared to the non-exodermal soybean root. However, Enstone and co-worker (1988, 1992) reported that both corn (an exodermal species) and broad bean (a non-exodermal species) displayed autofluorescence in their central cortical cells as well. Evidently, some of the aromatic components produced by the cells of the epidermis or the central cortex link to these epidermal or central cortical walls.

Various lipid-staining procedures were employed on the soybean root sections. According to Brundrett et al. (1991), sudan red 7B is the best nonfluorescent stain and can be used on fresh root sections. Hence, this procedure was employed in the present study. The results showed that sudan red 7B partitioned into the lipophilic matrix of the modifying substance in the mature root epidermal walls (Fig. 3.4). However, compared to the intense red staining of suberin lamellae in the exodermis or endodermis, the staining of the epidermal walls was relatively faint. Furthermore, the reaction was much more conspicuous in older sections (greater than 50 mm from the root tip), a region giving a stronger reaction to the H-V phenol test. These phenomena suggest that the deposition of lipophilic and phenolic components is quantitatively different in various plant tissues, and even at different positions along the root.

Concentrated sulphuric acid was also applied to the soybean root sections. The epidermal walls, including their root hairs, remained intact while all the central cortical cells were digested away (Fig. 3.5). This phenomenon demonstrates the polymeric characteristic of the modifying substance in the epidermal walls and agrees with the view of Esau (1965) and Wilson and Peterson (1983), in which they pointed out the walls of the epidermis, hypodermis and endodermis are generally modified but not those of the central cortex. Interestingly, the radial walls of epidermal cells were wavy, a feature that became evident when some wall areas toppled to give a paradermal view (Fig. 3.5B). These undulations are generally found in the anticlinal walls of endodermis with Casparian bands (Schreiber et al., 1994; Enstone and Peterson, 1997; Raven et al., 1999).

The fact that epidermal walls of soybean root are highly resistant to acid digestion indicates the modifying substance of the walls is a polymer, and histochemical tests indicated the presence of phenols and lipids. These results taken together indicate that this phenolic and lipidic substance in the soybean epidermal walls is suberin.

Alternating bands of light and dark electron density, seen when osmium-stained sections are viewed with a transmission electron microscope, are a diagnostic feature of typical suberized walls such as suberin lamellae and suberized periderm. It has been reported in various plant species by many investigators (Kolattukudy, 1984; Ma and Peterson, 2001; Nawrath, 2002; and Bernards, 2002). Kolattukudy (1984) proposed that the alternating dark bands were suberin phenolics and the light bands were suberin aliphatics embedded in wax. However, this hypothesis was revised by Bernards (2002). From his point of view, the suberin poly(phenolic) domain is covalently linked to primary cell wall carbohydrates, while the suberin poly(aliphatic) domain ranges as successive layers of light aliphatics and dark esterified phenolics (as well as wax) in a manner analogous to bilayers (Fig. 1.5).

Generally, Casparian bands exhibit an electron-dense region in the anticlinal walls of endodermis and exodermis at the ultrastructural level. This typical feature of Casparian bands could be due to the tightly associated suberin and lignin with other wall components.

In the present study, characteristic suberin lamellae between the cell's primary wall and plasma membrane as described in the above-suberized tissues were not observed. However, the outer tangential wall of the epidermis fixed in glutaraldehyde-OsO_4 displayed indistinct alternating electron-dense and less electron-dense regions (Fig. 3.6). This layered characteristic of epidermal walls was also reported by Peterson et al. (1978), who suggested "suberin may be present in a non-lamellar form interspersed with other wall components in the epidermis." This type of suberin was termed "diffuse suberin" by Peterson et al. (1978).

4.2 Chemical nature of soybean root epidermal walls as revealed by monomer analyses

A general indication of the chemical nature of root epidermal walls was obtained from the results of histochemical tests coupled with electron microscopy. Chemical depolymerizations in combination with chromatography (see Fig. 1.6) provided the qualitative and quantitative results necessary for a more precise understanding of the chemical characteristics of the epidermal walls.

4.2.1 Isolation and chemical compositions

Schreiber's group has isolated pure endodermal walls by enzymatic digestion from roots of some monocotyledonous species such as *Clivia miniata*, *Allium cepa*, *Iris germanica*, and *Zea mays* (Zeier and Schreiber, 1997 and 1998; Zeier et al., 1999b) and some dicotyledonous species such as *Pisum sativum*, *Cicer arietinum*, and *Ricinus communis* (Zeier et al., 1999a). The chemical composition of isolated rhizodermal/hypodermal walls was studied by Zeier et al. (1999a and 1999b) as well. These authors referred to the root epidermis as a "rhizodermis," while the hypodermis they described is an exodermis with Casparian bands. In their studies, these two layers remained together even after extensive enzymatic digestion. However, the chemical nature of epidermal walls alone from roots of a dicotyledonous species has not been investigated. In the present study, non-exodermal soybean roots were digested with cellulase and pectinase according to the technique described in Schreiber et al. (1994). Epidermal walls are able to withstand such an enzymatic digestion due to their embedded modifying substance. Scanning electron micrographs of the isolated epidermal walls demonstrated that complete epidermal walls could be separated from the entire roots; however, these epidermal walls were also attached to the outer tangential and radial edge of the first cortical layer in the more mature root region (above 40 to 50 mm from the root tip, Fig. 3.7). This phenomenon is in contrast to results of the acid digestion experiment, in which the cortical cells were all digested away (Fig. 3.5). The reasons for this discrepancy could be many. For example, the time of enzymatic digestion may not have been long enough to remove all wall carbohydrates and some of the wall components were not digested away with the use of cellulase and pectinase. Alternatively, the modifying substances of epidermal walls extended into the adjacent cortical walls and resisted to enzymatic digestion. In addition, Schreiber and his co-workers reported that yields of wall-modifying substances of endodermal walls never exceeded 10% of the extracted isolated wall samples (Zeier and Schreiber, 1997, 1998; Zeier et al., 1999a) since additional compounds such as carbohydrates and proteins were present as well. Furthermore, suberin is always tightly attached to cell walls and cannot be isolated completely (Kolattukudy, 1980). Therefore, the amount of monomers measured is expressed on per unit root surface area in the present study. This should be more informative than units per dry weight.

The epidermal walls of soybean root contained polymers of phenols and lipids, as indicated by histochemical investigations. According to Kolattukudy (1980, 1984), this is an indication of the presence of suberin, similar to that found in the underground parts and at wound surfaces of other higher plants. Therefore, the modifying substance, consisting of phenols and lipids, observed within the epidermal walls of soybean roots is likely to be suberin. With the above suggestion drawn from the histochemical studies, further chemical analyses were applied to clarify the chemical nature of the wall-modifying substance. Following the previous work of other investigators, BF_3-MeOH transesterification is a traditional depolymerization method for the analysis of aliphatic suberin (Kolattukudy and Agrawal, 1974; Karl et al., 1980; see Kolattukudy, 1984; Matzke and Riederer, 1991; Zeier and Schreiber, 1997). However, some of the aromatic suberin linked with ester bonds can be cleaved into their corresponding monomers with the use of this method as well (see Fig.1.6). Nitrobenzene oxidation was primarily designed to degrade lignin (Freudenberg, 1939), this depolymerization technique has also been used to analyze suberin in the study of Cottle and Kolattukudy (1982), due to the similarity of phenolic matrix of both suberin and lignin (Kolattukudy, 1980). In addition, the waxes associated with the suberin were fractionated and analyzed with chromatography as described in Riederer and Schönherr (1986, see Fig. 1.6).

The results of the chemical analyses conducted on the polymeric material from soybean root epidermal walls agree with those from the histochemical tests. Both lipids and phenols are components of the modifying substance in the epidermal walls. The compounds isolated by BF_3-MeOH transesterification show that four classes of monomers are present, i.e. ω-hydroxycarboxylic acid, α,ω-dicarboxylic acids, carboxylic acids and 1-alkanols (Fig. 3.8, Appendices 1 and 2). These are linked to each other with ester bonds. The most abundant monomers were ω-hydroxycarboxylic acids (77% of the total aliphatic components of both cultivars, Appendices 1 and 2). This finding is similar to those obtained from analyses of epidermal/exodermal cell walls of various monocotyledonous species by Zeier and Schreiber (1997), Zeier et al. (1999b), and Schreiber et al. (1999). By contrast, no 2-hydroxycarboxylic acids were found in soybean root epidermal walls, even though these were one of the dominant substance classes in epidermal/exodermal cell walls described by these authors. Based on the structural differences between both exodermis and epidermis, (i.e. suberized Casparian bands are present in the radial walls of exodermal but not epidermal cells), this qualitative difference of chemical components of both cell wall layers is understandable. According to Bernards (2002), all four monomers classes are common for the suberin poly(aliphatic) domain. In addition, Kolattukudy (1984) pointed out that "long-chain hydroxy- and dicarboxylic acids are typical suberin components" and Matzke and Riederer (1991) indicated that α,ω-dicarboxylic acids are diagnostic markers only found in suberized tissue. Therefore, the aliphatic components depolymerized from extracted soybean root epidermal walls are likely derived from the poly(aliphatic) domain of suberin consistent with the previous histochemical data. These aliphatic components are all even-numbered, long-chain fatty acids (ranging from C16 to C24) with a high proportion of saturated acids (around 70%, Appendices 1 and 2).

For a long time, researchers refered to the aromatic components of suberin as a lignin-like phenolic domain (Kolattukudy, 1980 and 1984). However, Bernards (1995, 1998, and 2002) pointed out that the phenolic polymers of suberin are unique and contain significant amounts of hydroxycinnamic acids. In the present study, two hydroxycinnamic acids, i.e. ferulic acid and *p*-coumaric acid were released after BF_3-MeOH transesterification (Fig. 3.10), in addition to the four classes of poly(aliphatic) components. The amount of ferulic acid is predominant and is over three orders of magnitude greater than that of *p*-coumaric acid (Fig. 3.10, Appendix 3). This result is in good agreement with those from suberized periderm analyses described by Riley and Kolattukudy (1975), Bernards and Lewis (1992), and Graça and Pereira (1997), in which the hydroxycinnamic acids (principally ferulic acid) were identified in the tested plant species. However, the authors of papers on suberin in exodermal and endodermal cell walls described *p*-coumaric acid as a dominant substance of the ester-linked aromatic components (Zeier and Schreiber, 1997; Zeier et al., 1999b). In addition, other hydroxycinnamates such as ferulates are found in the wound periderm of potato (Bernards and Lewis, 1992), but not in soybean root epidermal walls.

In all compounds released from BF_3-MeOH transesterification, the yield of hydroxycinnamic acids expressed on per unit surface area basis is much less than the amount of aliphatic substances extracted from soybean root epidermal walls (aliphatics vs esterified aromatics: 164.9 vs 7.8 ng mm^{-2} in cv. Conrad; 69.5 vs 3.8 ng mm^{-2} in cv. OX 760-6).

Vanillin and syringin were liberated from polymeric material of soybean root epidermal walls degraded by microscale alkaline nitrobenzene oxidation (Fig. 3.13, Appendix 3). However, in the suberized model tissue, potato periderm, approximately half of the amount of aromatic benzaldehydes released by nitrobenzene oxidation was *p*-hydroxybenzaldehyde (Lapierre et al., 1996). This benzaldehyde is absent in suberized soybean root epidermal walls. Similar to that of esterified aromatic components, the absolute yield of total nitrobenzene oxidation products from soybean root epidermal walls is low, as compared to aliphatics (4.7 ng mm^{-2} in cv. Conrad, 5.0 ng mm^{-2} in cv. OX 760-6). As a result, the constitution of suberin in the soybean walls is 93% poly(aliphatic) domain and only 7%

poly(aromatic) domain (Appendix 3), assuming complete depolymerisation by the techniques employed.

In addition to the all polymeric material from suberized epidermal walls, suberin-associated waxes were extracted with an organic solvent. The absolute amounts of waxes obtained from the epidermal walls were 51.3 and 28.1 ng mm^{-2} in cv. Conrad and cv. OX 760-6, respectively (Appendices 4 and 5). These values are in reasonable agreement with the reports of Espelie et al. (1980), in which the amount of wax extracted from the periderm of the seven underground storage organs ranged from 2 to 32 µg cm^{-2} (20 to 320 ng mm^{-2}). The wax components detected in the present study were a mixture of alkanes, carboxylic acids, and alcohols with the alkanes dominating (Fig. 3.11). The alkanes contained a broad distribution of homologes ranging from C23 to C32 with a high propotion of C28 and C29 alkanes (Fig. 3.11). Carboxylic acids and alcohols were generally shorter in chain-length compared to the alkanes. Furthermore, the chain length of carboxylic acids (C16 to C25, Fig. 3.11, Appendices 4 and 5) displayed a comparable distribution as the esterified poly(aliphatic) domain (C16 to C24, Fig. 3.8, Appendices 1 and 2).

4.2.2 The relationship of suberized epidermal walls to pathogen resistance

Chemical analyses of the polymeric material proves that the epidermal walls of soybean roots are suberized. It is obvious that the composition of this suberin varies compared to that of suberin from other sources, i.e. the periderm of potato tuber, exodermis, and endodermis of roots. Are there qualitative or quantitative differences in the epidermal suberin content of soybean cv. Conrad (resistant to *P. sojae*) vs. cv. OX 760-6 (susceptible to *P. sojae*)? Does this preformed suberin play a role in plant defence? The results from chemical analyses indicated that there are no differences in the identities of the suberin monomers between the two soybean cultivars; however, there are significant ($P < 0.05$) quantitative differences. In fact, the epidermal walls of cv. Conrad contain over twice the quantity of aliphatic suberin than those of cv. OX 760-6; moreover, cv. Conrad has a greater quantity of both aromatic suberin (especially ferulic acid) and suberin-associated waxes than does cv. OX 760-6. According to the physiological functions of suberin described by Kolattukudy (1980 and

1984), Schreiber et al. (1999), and Bernards (2002), suberized cell walls act as preformed and/or induced barriers to microbial attack. These authors also pointed out that the aromatic domain of suberin is important in protection against pathogen invasion. The results from the current study support the above point of view, in which the amount of esterified aromatic suberin (i.e. ferulic acid, *p*-coumaric acid) in resistant cv. Conrad (7.8 ng mm^{-2}) is twice as high as that of the susceptible cv. OX 760-6 (3.8 ng mm^{-2}, Fig. 3.10, Appendix 3). This quantitative variation between the *P. sojae* quantitative resistant and susceptible cultivars is consistent with the hypothesis that preformed suberization plays a role in plant defence.

4.3 Physical properties of soybean root epidermal walls

The histochemical and chemical studies of the current research reveal that epidermal walls of soybean roots are modified with suberin, a polymer of phenolics and lipids. The authors of early studies proposed one of the striking physical properties of the suberized walls is to be a barrier toward solute movement (Kolattukudy, 1984; Peterson, 1987; Peterson et al., 1993; Hose et al., 2001; Enstone et al., 2003; North and Peterson, 2005). These investigations mainly involved "typical" suberin deposits, i.e. Casparian bands and suberin lamellae. However, the physical properties of the suberized epidermal walls have seldom been investigated. In the present study, the viability, permeability, and intermicrofibrillar pore sizes of soybean root epidermal walls were determined.

4.3.1 Viability of the epidermal cells

The viability of soybean root epidermal cells varies little with root age; the majority of the cells remain alive for at least six days. This finding differs from the developmental sequence in onion roots, described by Barrowclough and Peterson (1994), in which the viability of the epidermal cells declined irrespective of the growing conditions. The tendency of epidermal cells to die was also discovered in the roots of *Citrus reticulata* and *C. medica* (Walker et al., 1984; Storey and Walker, 1987). One common feature of these roots is that they have an exodermis that can function as a protective layer after the epidermis dies (Stasovski and Peterson, 1993; Enstone et al., 2003). However, soybean does not possess Casparian bands and suberin lamellae in the hypodermis and is a non-exodermal species. Thus, living epidermal cells with modified walls may be especially important as a barrier toward pathogen attack.

The viability results obtained from the two tests employed was slightly different. Evan's blue indicated more living cells than did uranin. Evan's blue is excluded from the protoplasts of living cells but stains the nucleus and cytoplasm of dead cells (Gaff and Okong'O-Ogola, 1971; Fischer et al., 1985). From the present observation, this vital staining ability is obvious in the younger root region, in which the dead cells are still "fresh" and have a nucleus and cytoplasm, whereas in the older root region, few or no cells are stained. It can be assumed that cells stained with Evan's blue indicate the loss of selective permeability on death; however, the converse is not true, that is, the absence of staining does not prove the survival of cells. This is because some dead cells do not accumulate Evan's blue due to the degradation of plasma membranes, nuclei, and cytoplasms. In this regard, the uranin test is more accurate. Living cells are evident by the presence of yellowish green fluorescence in the protoplasm. Overall, 60-80% epidermal cells are alive along the root length of the six-day-old soybean root.

4.3.2 Intermicrofibrillar pore sizes of epidermal cell walls

The pore diameters of soybean root epidermal walls ranging from 2.2 to 3.5 nm, as measured by means of the plasmolysis/cytorrhysis method in the present study, are in good agreement with the pore sizes measured in other plant cell walls. For example, Carpita et al. (1979) found the maximum pore sizes of hair cells from *Raphanus sativus* (radish) roots and from *Gossypium hirsutum* (cotton) fibers to be somewhat smaller than 3.5 nm. These authors also indicated that pore sizes varied depending on cell type; for example, palisade parenchyma cells had a larger pore size than did hair cells of the roots. From the previous histochemical studies, the root epidermal walls are impregnated with suberin. Such a modifying substance generally displaces the water from the intermicrofibrillar channels of the cell walls (Peterson and Cholewa, 1998). Therefore, the smaller pore size in soybean root epidermal walls is consistant with the view that these walls are suberized but that the suberin does not completely occlude the intermicrofibrillar spaces in the walls.

4.3.3 Permeability of epidermal walls

The permeability studies of soybean root epidermal walls corroborate the earlier results of Peterson et al. (1981); Peterson and Perumalla (1984); Enstone (1988); and Enstone and Peterson (1992a and b), in which they investigated the apoplastic impermeability of the extreme root apices and the apoplastic permeability of the epidermal and cortical walls. In the present study, two fluorochromes, cellufluor and berberine, were used as apoplastic tracers but they displayed different penetration patterns. Cellufluor stained the outer walls of the epidermal cells in the young regions of the soybean roots tested, i.e. 0-40 mm from the root tip (Fig. 3.18 B and D), and then as the root aged, it penetrated into all the epidermal walls and also the outer tangential walls of the first cortical layer (80-100 mm from the root tip, Fig. 3.18 F and H). This penetration pattern occurs not only in exodermal species but also in non-exodermal species (Enstone, 1988). The reason for lack of deeper penetration in non-exodermal species could be the charge of cellufluor. This tracer bears a positive charge that would bind with the negatively charged cell walls, and then becomes immobilized. Another important reason could be due to its large size, which was evident in the present investigation. The molecular weight of cellufluor is 960 Da, and this approximately corresponds to a molecular diameter of 3.5 nm (estimated from Fig. 1 of Carpita et al., 1979). The epidermal wall pore sizes ranged from 2.2 to 3.5 nm 40-90 mm from the root tip (Table 3.2). Therefore, in the regions of 0-40 mm tested, the diameter of cellufluor was too large to enter the epidermal walls. As the root aged (80-100 mm from the root tip), the pore size increased (Table 3.2), cellufluor penetrated through the epidermal walls, bond to the outer tangential walls of the first cortical cells, and then became immobilized. Furthermore, when cellufluor binds to a cell wall, it is capable of making its pore size smaller and thus blocks further dye movement through the wall. This could be the reason that this dye did not proceed beyond the first cortical layer.

The berberine-thiocyanate tracer experiment properly displayed the different permeabilities of the epidermal and endodermal walls in soybean roots. The tracer moved freely into the epidermis and the cortex, and was stopped by the Casparian bands in the endodermis, confirming that soybean root does not possess an exodermis. Further, the modifying substances in the walls of the epidermis and endodermis are undoubtedly different in their spatial distributions. These different spatial distributions, in turn, affect the physical property of the walls, i.e. permeability to solutes or microorganisms. The molecular weight of berberine (336 Da) is similar to the molecular weight of sucrose (340 Da). According to Carpita et al. (1979), this molecular weight corresponds to a molecular diameter of 1 nm, a value that is much smaller than the pore size of soybean root epidermal walls detected in the present study. Therefore, the penetration of berberine and thiocyanate is much freer than that of cellufluor. Berberine, being positively charged, would bind to the walls. Only excess berberine would react with KSCN to form crystals.

The permeability experiment also showed that there were no crystals formed in the modified walls, i.e. epidermis and endodermis. Earlier, Enstone (1988) found the same results in roots of other species (i.e. onions, corns, broad beans, peas and sunflowers) and suggested the modifying substance in those walls prevented crystals from forming. However, the present pore size measurement experiment proved that pore sizes increased as the root regions aged even though more suberin was deposited into the epidermal walls. Nevertheless, in the oldest regions of the root tested, crystals of berberine thiocyanate did not form in the walls. According to Dr. Mark Bernards, the poly(phenolic) components of suberin would add more negative charges to the cell wall because of their additional carboxylic acid functional groups; thus, more berberine would bind to wall components, preventing crystal formation (personal communication).

In the mature root region (80-100 mm from the root tip), crystals were concentrated in the inner part of the cortex and were absent in the epidermal and outer cortical walls. From the previous development of autofluorescence, the cortical cells adjacent to the epidermis displayed uneven autofluorescence, perhaps due to the linked aromatic components. These phenolics would add to the negative charges to the cell wall. This may be the reason that no or few crystals form in the outer cortical walls in the mature root region.

The extreme root apices excluded the formation of crystals even though the penetration of berberine into them is evident when compared to control sections (Figs. 3.19A and 3.20A). The tightly associated cells and the extremely small pore spaces in epidermal walls could be reasons for the lack of crystals in this region. The root cap was completely permeable to the tracers, and the formation of numerous crystals may due to its loosely arranged peripheral cells.

The physical properties of the soybean root epidermal walls illustrate the distinctive feature of their suberin compared to the "typical" suberin in the exodermis and endodermis. The permeability of suberized epidermal walls to apoplastic tracers contrasts with the impermeability of Casparian bands in the endo- and exodermis to the same tracers. This difference may relate to the way that suberin is laid down in the cell walls. The spatial distribution of the suberin in the suberized Casparian bands is in a "condensed" form, interacting with wall components and obstructing all the intermicrofibrillar pores at least in one area of the anticlinal walls, while in epidermal walls, the suberin polymer may be interspersed among other components and not occluding the intermicrofibrillar spaces. This "diffuse" form of suberin, originally defined by Peterson et al. (1978), evidently occurs in the root epidermal walls of soybean.

4.4 Interactions between soybean roots and microorganisms

4.4.1 Wall modification vs root nodulation

The interaction of soybean root and symbiotic rhizobia can lead to the formation of root nodules that are nitrogen-fixing organs. However, plants possess preformed structural and chemical defenses against the invasion of viral, bacterial, or fungal microorganisms (Agrios, 1997; Gage, 2004). Suberin located in the walls of soybean root epidermis (found in the present study) is one of such defenses. How do rhizobia initially invade leguminous roots? According to Gage (2004), first, the rhizobia must recognize and then respond to the presence of the host-plant roots; second, the formation of Nod factor of rhizobia will initiate developmental changes of the host plant such as root hair deformation. In this process, the nearly finished growing root hairs are the most susceptible ones for rhizobia (Gage, 2004). Why are the mature root hairs unable to deform and then allow the bacteria to penetrate through the walls? One of the reasons could be the walls of the mature root hairs are modified in a manner similar to the root epidermal walls. The previous chemical analyses showed that the older epidermal regions contained significantly greater suberin than did the younger regions. Because root hairs elongate by tip growth, the end of the growing hair may possess little or no suberin and thus be easier to deform and penetrate. Rhizobia may be seeking the less modified root hairs such as the growing root hairs, and then penetrate through their tips.

4.4.2 Soybean root-*Phytophthora sojae* interactions

The previous chemical analyses of the compositions of suberized epidermal walls from two soybean cultivars revealed that the resistant cv. Conrad had a greater quantity of both the aliphatic and aromatic components of the polymer compared to the susceptible cv. OX 760-6. Do these differences play a role in root defense against *P. sojae*?

4.4.2.1 Plant material and inoculation procedure

The roots of the etiolated, three-day-old seedlings are pale and provide a nice background against which to view the microscopic differences of root-pathogen interactions. Moreover, only primary roots have developed in three-day-old seedlings. This is important because lateral roots open “windows” in the epidermal layer. Therefore, a lack of emerging laterals avoids complications from potential wounding of the epidermis, and the invasion of the pathogen is only through the intact epidermal wall surface.

Immersing etiolated seedlings directly into a zoospore suspension was a convenient and rapid mean of inoculation. A zoospore concentration of 10^4 zoospores mL^{-1} supplied sufficient zoospores to effectively adhere to the surface of roots, and observation of the development of the pathogen was accomplished satisfactorily with this inoculation procedure.

4.4.2.2 Growth condition of zoospores

Temperature and moisture are the two environmental conditions that affect the formation and germination of spores. The temperature requirement for *P. sojae* race 2 zoospores was satisfied by room temperature (ranging from 23 to 25 °C). Overnight flooding of the mycelium with water was necessary to get rid of many nutrients from the agar and promote the formation of sporangia. Since swimming, biflagellate zoospores are released from the sporangia, a liquid environment also aids the movement of the pathogen to its host.

4.4.2.3 Clearing and staining techniques

Roots of soybean were cleared successfully with lactic acid. This clearing technique was the most efficient compared to other commonly used clearing agents, such as 10% NaOH in the autoclave for 20 min. Furthermore, the lactic acid was easy to remove by rinsing, and the cleared roots were transparent and suitable for viewing the zoospores and hyphal growth on and within them.

Several techniques were tried for staining hyphae of *P. sojae*. A Chlorazol black E (CBE) staining method has been described by Brundrett et al. (1984) as the best method for walls of vesicular-arbuscular mycorrhizal hyphae. However, this technique did not stain hyphae of *P. sojae* since this pathogen is not a true fungus. The different wall compositions of vesicular-arbuscular mycorrhizal hyphae and oomycete hyphae explain the unsuccessful hyphal stainings with CBE, trypan blue, or aniline blue in lactoglycerol. Cellufluor was utilized to stain cleared, incubated roots as well. Even though cellufluor gave a strong zoospore wall staining, this dye also stained plant cell walls, obscuring visualization of hyphal development. The epidermal walls and the zoospores fluoresced bright blue and white, respectively, which indicated different wall components as well.

4.4.2.4 Disease development

The early stages of *P. sojae* root rot disease development include attraction of the zoospores to the root, zoospore adhesion, zoospore encystment, cyst germination, and hyphal invasion into the host tissue. Any differences in these five steps could theoretically influence the resistance of soybean cultivars to *P. sojae*.

In the present study, the early development of the disease was similar for both the resistant cv. Conrad and susceptible cv. OX 760-6. Zoospores were equally attracted by roots and distributed evenly over their surfaces. (Two isoflavones i.e. daidzein and genistein exuded by soybean roots have been well-characterized as specific attractants for *P. sojae* zoospores; Tyler, 2002) This means that roots of both cultivars exuded the same amounts of attractive chemicals. Thus, the differences in resistance of the cultivars to *P. sojae* cannot be ascribed to differences in exudation of such chemicals. Hickman and Ho (1966), Beagle-Ristaino and Rissler (1983), and Miller and Maxwell (1984) who studied the interaction of *Phytophthora* pathogens with plant roots also concluded that zoospore attraction is a nonspecific phenomenon.

The germ tubes from the zoospore cysts were appressed to the root epidermis, and the formation of elliptical halos was quite common on both cultivars. Similar to zoospore adhesion, the zoospore encystment and cyst germination can be stimulated by soybean isoflavones (see Tyler, 2002). The results showed that the nonspecific germination happened in both cultivars regardless of their differences in resistance to *P. sojae*. Germ tubes with swollen tips were seen occasionally. This finding is in agreement with the previous report of Beagle-Ristaino and Rissler (1983), in which only 5% of the penetrations of *Phytophthora megasperma* on soybean root surfaces occurred from swollen germ tube tips. These swollen tips from germ tubes observed in *P. sojae* were similar to appressoria that were described by Emmett and Parbery (1975). According to these authors, an appressorium is defined as a morphologically distinct entity separated from the germ tube of the hypha by a septum. In addition, the formation of appressoria by *P. sojae* was reported in the studies of Stössel et al. (1980) and Lazarovits et al. (1981). However, the majority of successful adhesions of

P. sojae zoospores to soybean root epidermis did not require the formation of swollen germ tube tips in the present study, and the germ tubes extended to invade the middle lamellae of the epidermis directly. Therefore, this study is essentially in agreement with the previous research of Enkerli et al. (1997), in which they reported germ tubes with no distinctive appressoria in the interaction of *P. sojae* race 2 with soybean roots.

The time course study of infection illustrates that there is a delay of 2-3 h in hyphal invasion through the epidermal wall of the resistant cv. Conrad (around 7-8 h) compared to the susceptible cv. OX 760-6 (around 4-6 h Fig. 3.23D and F). The invasion of hyphae is occurred through the middle lamellae of the epidermal cells. Therefore, the modifying substance in the epidermal walls would affect the penetration of hyphae. In the present study, chemical analyses have indicated a quantitative difference in suberin deposition in both soybean cultivars (Figs. 3.9 and 3.10). The significantly ($P < 0.05$) greater amount of suberin in the resistant cv. Conrad apparently acts as a preformed physical barrier toward pathogen attack, which delays the invasion of the pathogen to the host tissue. That modified epidermal walls correlated with passive host resistance was evident in the present study.

The later events of *P. sojae* pathogenesis in both soybean cultivars agreed with other reports. A pronounced higher amount of hyphae was observed in the inoculated seedlings of the susceptible cv. OX 760-6 as compared to the resistant cv. Conrad. The reason might be that pathogen infection also triggers accumulation of polymeric materials on the infected cell walls, and these polymers, in turn, prevent the spread of the invading pathogen in the host. This expression of defense resistance in cv. Conrad is stronger than in cv. OX 760-6. A delay in pathogen entry into the cortex brought about by a greater quantity of suberin in the epidermal walls would allow time for such internal defence mechanisms to be put into place.

4.4.2.5 Modifying substance relative to pathogen resistance

Most investigators use aniline blue in basic solution to identify callose, a glucose polymer induced in plant-pathogen defense systems (Kortekamp et al., 1997; Gindro et al., 2003). With this technique in the present study, deposition of callose was distinguished at the point of germ tube entry into the root, and the penetration of haustoria in both resistant and susceptible soybean cultivars. This finding is in agreement with the previous studies of Bonhoff et al. (1987) and Enkerli et al. (1997) in which soybean seedlings were infected with different races of *P. sojae*. However, a previous report of a number of hosts indicated that callose formation was not observed in response to penetration by *Phytophthora cinnamomi* in susceptible species, whereas most resistant or tolerant species produced this response to pathogen penetration (Cahill and Weste, 1983). In the present study, numerous haustoria, associated with callose deposits, were found in the interior of susceptible soybean cells in the later stages of pathogen extension, whereas only few haustoria accompanied by callose were observed in the cells of the resistant cultivar. This phenomenon suggests that formation of callose in response to pathogen attack is a primary defense reaction but could not be the only inhibition to pathogen development in the resistant root. There are other defense systems in root-pathogen interactions.

Many researchers have provided evidence that cell wall browning is associated with cell death. This wall browning is caused by host phenolases that oxidize the host phenolics, and then the plant itself sacrifices a limited number of cells to the invading pathogen in the infected areas (Friend, 1981; Keen and Yoshikawa, 1983). Ward et al. (1979) have stated that dark-brown necrosis of tissue occurred in resistant reactions of soybean hypocotyls with *P. sojae*, whereas there was little or no browning of the tissue in susceptible reactions. In the current study, the resistant cv. Conrad displayed a stronger browning reaction than the susceptible cv. OX 760-6. Even though the viability of infected cells was not investigated and the precise time for initial browning reaction was not obtained, this browning reaction might indicate a hypersensitive reaction, a type of positive resistance response. Furthermore, wall-browning reactions occur not only in infected epidermal cells but also in the subjacent cortical cells. These patchy brown areas are autofluorescent in contrast to control sections. Generally, autofluorescence is caused by phenolic compounds. Holliday et al. (1981) reported that the autofluorescence in necrotic cells of resistant soybean leaves might be due to the accumulation of the phenolic compound glyceollin (the phytoalexin of soybean). However, in the soybean root, more than just phenolics were produced. When sections of pathogen-infected soybean roots were stained with sudan red 7B, the patchy brown areas stained red indicating that a lipophilic matrix that might be suberin is also induced in response to pathogen attack. Furthermore, these infected brown areas were highly resistant to acid digestion. An extract from *Chelidonium majus* root was used to identify Casparian bands by Peirson and Dumbroff (1969), Peterson et al. (1982), and Peterson and Lefcourt (1990). The fluorochromes in this extract apparently binds with phenolic compounds and fluoresces under violet light. By using a lactic acid clearing technique in conjunction with *Chelidonium majus* root extract staining, the epidermal walls and internal cortical walls of infected roots could be seen fluorescent brightly as compared to the corresponding tissues in control roots.

The previous phenomenon suggests that host cell wall changes related to resistance responses include suberization of infected cell wall, in addition to callose deposition and accumulation of phenolics in hypersensitive response that had also been reported in earlier works of *Phytophthora* spp.-plant defense system (Holliday et al., 1981; Cahill and Weste, 1983; Bonhoff et al., 1987; Enkerli et al., 1997; Kortekamp et al., 1997; Kang et al., 2002; and Gindro et al., 2003).

4.5 Conclusions

1. Suberin is present in the walls of soybean root epidermis.
2. Epidermal suberin contains poly(aliphatic) domain and poly(aromatic) domain.
3. The suberin poly(aliphatic) domain contains four classes of monomers with the chain lengths ranging from C16 to C24.
4. Omega-hydroxycarboxylic acids are the predominant aliphatic components.
5. Hydroxycinnamic acids (especially ferulic acid) are the most abundant aromatic components.
6. Alkanes account for the dominant monomers in the suberin associated wax.
7. There is no difference in monomeric compositions between the two cultivars.
8. The resistant cv. Conrad has a greater quantity of both the aliphatic and aromatic components of the polymer than the susceptible cv. OX 760-6.
9. The resistant cv. contains more suberin-associated wax than the susceptible cv. OX 760-6.
10. Sixty percent or more epidermal cells are alive over a period of 6 days.
11. Epidermal walls are modified but permeable to an apoplastic tracer with a molecular diameter of 336 Da.
12. No exodermis is present in the soybean root.
13. Pore sizes of soybean root epidermal walls range from 2.2 to 3.5 nm.
14. The preformed suberin of soybean epidermal walls is correlated with *Phytophthora sojae* resistance and acts to delay the invasion of hyphae into roots.
15. Induced polymeric material on the infected cell walls is suberin that may slow the spread of the invading pathogen in the soybean root. Resistant cv. Conrad has stronger resistance responses than susceptible cv. OX 760-6.

5 Bibliography

Abeysekera, R. M. and McCully, M. E. 1993. The epidermal surface of the maize root tip. I. Development in normal roots. New Phytologist **125**: 413-429.

Abeysekera, R. M. and McCully, M. E. 1994. The epidermal surface of the maize root tip. III. Isolation of the surface and characterization of some of its structural and mechanical properties. New Phytologist **127** (2): 321-333.

Adjei, M. B., Ouesenberry, K. H., and Chambliss, C. G. 2002. Nitrogen fixation and inoculation of forage legumes. SS-AGR-56, Agronomy Department, Florida Cooperative Extension Service, Institute of Food and Agricultural Sciences, University of Florida, Florida.

Agrios, G. N. 1997. Plant Pathology. Fourth Edition. Academic Press. San Diego, California. ISBN 0-12-044564-6.

Albersheim, P. 1978. Concerning the structure and biosynthesis of the primary cell walls of plants. International Review of Biochemistry **16**:127-150.

Aloni, R., Aloni, E., Langhans, M., and Ullrich, C. I. 2006. Role of cytokinin and auxin in shaping root architecture: regulating vascular differentiation, lateral root initiation, root apical dominance and root gravitropism. Annals of Botany **97**: 883-893.

Aloni, R., Enstone, D. E., and Peterson, C. A. 1998. Indirect evidence for bulk water flow in root cortical cell walls of three dicotyledonous species. Planta **207**: 1-7.

Baldauf, S. L., Roger, A. J., Wenk-Siefert, I., and Doolittle, W. F. 2000. A kingdom-level phylogeny of eukaryotes based on combined protein data. Science **290**: 972-977.

Barrowclough, D. E. and Peterson, C. A. 1994. Effects of growing conditions and development of the underlying exodermis on the vitality of the onion root epidermis. Physiologia Plantarum **92**: 343-349.

Beagle-Ristaino, J. E. and Rissler, J. F. 1983. Histopathology of susceptible and resistant soybean roots inoculated with zoospores of *Phytophthora megasperma* f.sp. *glycinea*. Phytopathology **73**: 590-595.

Bernards, M. A. and Lewis, N. G. 1992. Alkyl ferulates in wound-healing potato-tubers. Phytochemistry **31**: 3409-3412.

Bernards, M. A. and Lewis, N. G. 1998. The macromolecular aromatic domain in suberized tissue: a changing paradigm. Phytochemistry **47**: 915-933.

Bernards, M. A., Lopez, M. L., Zajicek, J., Lewis, N. G. 1995. Hydroxycinnamic acid-derived polymers constitute the polyaromatic domain of suberin. Journal of Biological Chemistry **270**: 7382-7386.

Bernards, M. A. 2002. Demystifying suberin. Canadian Journal of Botany **80**: 227-240.

Bonhoff, A., Rieth, B., Golecki, J., and Grisebach, H. 1987. Race cultivar-specific differences in callose deposition in soybean roots following infection with *Phytophthora megasperma* f. sp. *glycinea*. Planta **172**: 101-105.

Brett, C. and Waldron, K. 1990. Physiology and Biochemistry of Plant Cell Walls. Unwin Hyman Ltd., London, UK. ISBN 0-04-581034-6.

Brisson, J. D., Peterson, R. L., Rauser, W. E., and Ellis, B. E. 1977. Correlated phenolic histochemistry using light, transmission, and scanning electron microscopy, with examples taken from phytopathological problems. Scanning Electron Microscopy. Vol II: 667-676.

Brundrett, M. C., Bougher, N., Dell, B., Grove, T. and Malajczuk, N. 1996. Working with Mycorrhizas in Forestry and Agriculture. ACIAR Monograph 32. Pirie Printers, Canberra, Australia. ISBN 1 86320 181 5.

Brundrett, M. C., Kendrick, B., and Peterson, C. A. 1991. Efficient lipid staining in plant material with sudan red 7B or fluorol yellow 088 in polyethylene glycol-glycerol. Biotechnic and Histochemistry **66**: 111-116.

Brundrett, M. C., Piche, Y., and Peterson, R. L. 1984. A new method for observing the morphology of vesicular-arbuscular mycorrhizae. Canadian Journal of Botany **62**: 2128-2134.

Cahill, D. and Weste, G. 1983. Formation of callose deposits as a response to infection with *Phytophthora cinnamomi*. Transactions fo The British Mycological society **80** (1): 23-29.

Campbell, N. A., Reece, J. B., and Mitchell, L. G. 1999. Biology. Fifth Edition. Addison Wesley Longman Inc., New York. pp: 524-525.

Carpita, N. C. and Gibeaut, D. M. 1993. Structural models of primary cell walls in flowering plants: consistency of molecular structure with the physical properties of the walls during growth. The Plant Journal **3**(1): 1-30.

Carpita, N. C., Sabularse, D., Montezinos, D., and Delmer, D. P. 1979. Determination of the pore size of cell walls of living plant cells. Science (Washington, D.C.) **205**: 1144-1147.

Chalker-Scott, L., and Krahmer, R. L. 1989. Microscopic studies of tannin formation and distribution in plant tissues. In Chemistry and Significance of Condensed Tannins. Ed. by R. W. Hemingway and J. J. Kerchesy, Plenum Press, New York.

Chen, C. L. 1992. Nitrobenzene and cupric oxide oxidations. In: Springer Series in Wood Science Methods in Lignin Chemistry. Ed. by S. Y. Lin and C. W. Dence. Springer-Verlag, Berlin Heidelberg, pp301-321.

Cholewa, E. and Peterson, C. A. 2004. Evidence for symplastic involvement in the radial movement of calcium in onion roots. Plant Physiology **134**: 1793-1802.

Cosgrove, D. J. 2001. Wall structure and wall loosening. A look backwards and forwards. Plant Physiology **125**: 131-134.

Cottle, W. and Kolattukudy, P. E. 1982. Biosynthesis, deposition, and partial characterization of potato suberin phenolics. Plant Physiology **69**: 393-399.

Duncan, J. 1999. *Phytophthora*-an abiding threat to our crops. Microbiology Today **26**: 114-116.

Emmett, R. W. and Parbery, D. C. 1975. Appressoria. Annual Review of Phytopathology **13**: 147-167.

Enkerli, K., Hahn, M. G., and Mims, C. W. 1997. Ultrastructure of compatible and incompatible interactions of soybean roots infected with the plant pathogenic oomycete *Phytophthora sojae*. Canadian Journal of Botany **75**: 1493-1508.

Enstone, D. E. 1988. The apoplastic permeability of plant root apices. M.Sc. thesis, University of Waterloo, Waterloo, ON.

Enstone, D. E. and Peterson, C. A. 1992a. A rapid fluorescence technique to probe the permeability of the root apoplast. Canadian Journal of Botany **70**: 1493-1501.

Enstone, D .E. and Peterson, C. A. 1992b. The apoplastic permeability of root apices. Canadian Journal of Botany **70**: 1502-1512.

Enstone, D. E. and Peterson, C. A. 1997. Suberin deposition and band plasmolysis in the corn (*Zea mays* L.) root exodermis. Canadian Journal of Botany **75**: 1188-1199.

Enstone, D. E., Peterson, C. A., and Ma, F. 2003. Root endodermis and exodermis: structure, function, and responses to the environment. Journal of Plant Growth Regulation **21**: 335-351.

Esau, K. 1965. Plant Anatomy. 2nd edition. John Wiley and Sons, New York.

Espelie, K. E., Sadek, N. Z., and Kolattukudy, P. E. 1980. Composition of suberin-associated waxes from the subterranean storage organs of seven plants: parsnip, carrot, rutabaga, turnip, red beet, sweet potato, and potato. Planta **148**: 468-476.

Evert, R. F., Botha, C. E. J., and Mierzwa, R. J. 1985. Free-space marker studies on the leaf of *Zea mays* L. Protoplasma **126**: 62-73.

Eye, L. L., Sneh, B., and Lockwood, J. L. 1978. Factors affecting zoospore production by *Phytophthora megasperma* var. *sojae*. Phytopathology **68**: 1766-1768.

Fischer, J. M. C., Peterson, C. A., and Bols, N. C. 1985. A new fluorescent test for cell vitality using calcofluor white M2R. Stain Technology **60**: 69-79.

Förster, H., Tyler, B. M., and Coffey, M. D. 1994. *Phytophthora sojae* races have arisen by clonal evolution and by rare outcrosses. Molecular Plant-Microbe Interactions **7**: 780-791.

Freudenberg, K. 1939. Lignin. Angewandte Chemie **52**: 362-363.

Frey-Wyssling. 1969. The structure and biogenesis of native cellulose. Fortschr. Chem. Org. Naturst **26**: 1-30.

Friend, J. 1981. Plant phenolics, lignification and plant disease. In: Progress in Phytochemistry. Ed by Reinhold, L., Harborne, J. B., and Swain, T. Pergamon Press, Oxford. Vol. 7, pp. 197-261.

Fry, S. C. 1989. Celluloses, hemicelluloses and auxin-stimulated growth-a possible relationship. Physiologia Plantarum **75**(4): 532-536.

Gaff, D. F. and Okong'O-Ogola, O. 1971. The use of non-permeating pigments for testing the survival of cells. Journal of Experimental Botany **22** (72): 756-758.

Gage, D. J. 2004. Infection and invasion of roots by symbiotic, nitrogen-fixing rhizobia during nodulation of temperate legumes. Microbiology and Molecular Biology Reviews **68**: 280-300.

Gijzen. M. 2004. Oomycete-plant interactions: current issues in. In: Encyclopedia of Plant and Crop Science. Edited by Goodman, R.M. University of Wisconsin, Wisconsin. pp. 843-845.

Gindro, K., Pezet, R., and Viret, O. 2003. Histological study of the responses of two *Vitis vinifera* cultivars (resistant and susceptible) to *Plasmopara viticola* infections. Plant Physiology and Biochemistry **41**: 846-853.

Graça, J. and Pereira, H. 1997. Cork suberin: a glyceryl based polyester. Holzforschung **51**: 225-234.

Grau, C. R., Dorrance, A. E., Bond, J., and Russin, J. S. 2004. Fungal diseases. In: Soybeans: Improvement, Production, and Uses. 3rd edition. Ed. by Boerma, H. R. and Specht, J. E. American Society of Agronomy, Inc. Madison, Wisconsin, USA. pp. 679-763.

Hayashi, T. 1989. Xyloglucans in the primary-cell wall. Annual Review of Plant Physiology and Plant Molecular Biology **40**: 139-168.

Hickman, C. J. and Ho, H. H. 1966. Behaviour of zoospores in plant-pathogenic Phycomycetes. Annual Review of Phytopathology **4**: 195-220.

Hofer, R. M. 1991. Root hairs. In Plant Roots The Hidden Half, ed. Y. Waisel, A. Eshel, U. Kafkafi, New York: Marcel Dekker, pp. 129–148.

Holliday, M. J., Keen, N. T., and Long, M. 1981. Cell death patterns and accumulation of fluorescent material in the hypersensitive response of soybean leaves to *Pseudomonas syringae* pv. *glycinea*. Physiological Plant Pathology **18**: 279-287.

Hose, E., Clarkson, D. T., Steudle, E., Schreiber, L., and Hartung, W. 2001. The exodermis: a variable apoplastic barrier. Journal of Experimental Botany **52**: 2245-2264

Hughes, J. and McCully, M. E. 1975. The use of an optical brightener in the study of plant structure. Stain Technology **50**: 319-329.

Johansen, D. A. 1940. Plant microtechnique. McGraw-Hill, New York.

Judelson, H. S. and Blanco, F. A. 2005. The spores of *Phytophthora*: weapons of the plant destroyer. Microbiology **3**: 47-58.

Kamoun, S. 2000. *Phytophthora*. In: Fungal Pathology. Ed by Kronstad, J. Kluwer Academic Publishers, Dordrecht. pp. 1-32.

Kamula, S. A., Peterson, C. A., and Mayfield, C. I. 1995. Impact of the exodermis on infection of roots by *Fusarium culmorum*. Plant and Soil **167**: 121-126.

Kang, Z., Huang, L., and Buchenauer, H. 2002. Ultrastructural changes and localization of lignin and callose in compatible and incompatible interactions between wheat and *Puccinia striiformis*. Journal of Plant Diseases and Protection **109** (1): 25-37.

Karl, E. E., Ronald, W. D., and Kolattukudy, P. E. 1980. Composition, ultrastructure and function of the cutin- and suberin-containing layers in the leaf, fruit peel, juice-sac and inner seed coat of grapefruit (*Citrus paradisi* Macfed.). Planta **149**: 498-511.

Kaufmann, M. J. and Gerdemann, J. W. 1958. Root and stem rot of soybean caused by *Phytophthora sojae* n. sp. Phytopathology **48**: 201-208.

Keegstra, K., Talmadge, K. W., Bauer, W. D., Albersheim, P. 1973. The structure of plant cell walls. I. The macromolecular components of the walls of suspension-cultured sycamore. Plant Physiology **51**: 158-173.

Keen, N. T. and Yoshikawa, M. 1983. Physiology of disease and the nature of resistance to *Phytophthora*. In: Phytophthora: Its Biology, Ecology and Pathology. Ed by Erwin, D. C., Bartnicki-Garcia, S., and Tsao, P. H. The American Phytopathological Society. St. Paul, Minnesota, USA, pp. 279-287.

Kolattukudy, P. E. 1978. Chemistry and biochemistry of the aliphatic components of suberin. In: Biochemistry of Wounded Plant Tissues. Ed by Kahl, G. de Gruyter, Berlin, New York, pp. 43-84. ISBN 3-11-006801-X.

Kolattukudy, P. E. 1980. Biopolyester membranes of plants: cutin and suberin. Science **208**: 990-1000.

Kolattukudy, P. E. 1984. Biochemistry and function of cutin and suberin. Canadian Journal of Botany **62**: 2918-2933.

Kolattukudy, P. E. and Agrawal, V. P. 1974. Structure and composition of aliphatic constituents of potato tuber skin (suberin). Lipids **9**: 682-691.

Kolattukudy, P. E., and Espelie, K. E. 1989. Natural products of woody plants, chemicals extraneous to the lignocellulosic cell wall (Rowe, J.,Ed), New York: Springer-Verlag, 304-367.

Kortekamp, A., Wind, R., and Zyprian, E. 1997. The role of callose deposits during infection of two downy mildew-tolerant and two-susceptible *Vitis* cultivar. Vitis **36**: 103-104.

Lamport, D. T. A. 1986. The primary cell wall: a new model. In Cellulose: Structure, Modification and Hydrolysis. Ed. Young, R.A. and Rowell, R.M., New York: John Wiley, pp.77-90.

Lapierre, C., Pollet, B., and Negrel, J. 1996. The phenolic domain of potato suberin: structural comparison with lignins. Phytochemistry **42**: 949-953.

Larkin, J. C., Brown, M. L., Schiefelbein, J. 2003. How do cells know what they want to be when they grow up? Lessons from epidermal patterning in *Arabidopsis*. Annual Review of Plant Biology **54**: 403-430.

Lazarovits, G., Stössel, R., and Ward, E. W. B. 1981. Age-related changes in specificity and glyceollin production in the hypocotyls reaction of soybeans to *Phytophthora megasperma* var. *sojae*. Phytopathology **71**: 94-97.

Lehmann, H., Stelzer, R., Holzamer, S., Kunz, U., and Gierth, M. 2000. Analytical electron microscopical investigations on the apoplastic pathways of lanthanum transport in barley roots. Planta **211**: 816-822.

Ling-Lee, M., Chilvers, G. A., and Ashford, A. E. 1977. A histochemical study of phenolic materials in mycorrhizal and uninfected roots of *Eucalyptus fastigata* Deane and Maiden. New Phytologist **78**: 313-328.

Loomis, W. E. and Schull, C. A. 1937. Methods in Plant Physiology. A Laboratory Mannul and Research Handbook. Mc-Graw-Hill, New York, NY. pp. 63.

Lulai, E. C., and Corsini, D. L. 1998. Differential deposition of suberin phenolic and aliphatic domains and their roles in resistance to infection during potato tuber (*Solanum tuberosum* L.) wound-healing. Physiological and Molecular Plant Pathology **53**: 209-222.

Ma, F. and Peterson, C. A. 2000. Plasmodesmata in onion (*Allium cepa* L.) roots: a study enabled by improved fixation and embedding techniques. Protoplasma **211**: 103-115.

Ma, F. and Peterson, C. A. 2001. Development of cell wall modifications in the endodermis and exodermis of *Allium cepa* roots. Canadian Journal of Botany **79**: 577-590.

Matern, U. and Kneusel, R. E. 1988. Phenolic compounds in plant disease resistance. Phytoparasitica **16**(2): 153-170.

Matzke, K. and Riederer, M. 1991. A comparative study into the chemical constitution of cutins and suberins from *Picea abies* (L.) Karst., *Quercus robur* L., and *Fagus sylvatica* L. Planta **185**: 233-245.

McCann, M. C., Wells, B., and Roberts, K. 1992. Complexity in the spatial localization and length distribution of plant cell-wall matrix polysaccharides. Journal of Microscopy-Oxford **166**: 123-136.

Meyer, K., Shirley, A. M., Cusumano, J. C., Bell-Lelong, D. A., and Chapple, C. 1998. Lignin monomer composition is determined by the expression of a cytochrome P450-dependent monooxygenase in Arabidopsis. Proceedings of the National Academy of Science of USA **95**: 6619-6623.

Miller, S. A. and Maxwell, D. P. 1984. Light microscope observations of susceptible, host resistant, and nonhost resistant interactions of alfalfa with *Phytophthora megasperma*. Canadian Journal of Botany **62**: 109-116.

Money, N. P. 1989. Osmotic pressure of aqueous polyethylene glycols: relationship between molecular weight and vapor pressure deficit. Plant Physiology **91**: 766-769.

Nagahashi, G. and Thomson, W. W. 1974. The Casparian strip as a barrier to the movement of lanthanum in corn roots. Science **193**: 637-648.

Nawrath, C. 2002. The biopolymers cutin and suberin. In: The Arabidopsis Book pp 1-14.

Nicholson, R. L. 1992. Phenolic compounds and their role in disease resistance. Annual Review of Phytopathology **30**: 369-389.

North, G. B. and Peterson, C. A. 2005. Water flow in roots: structural and regulatory features. In: Vascular Transport in Plants. Ed by Holbrook, N. M. and Zwieniecki, M. A. Elsevier Academic Press, London, UK. ISBN: 0-12-088457-7. pp: 131-156.

O'Brien, T. P. and McCully, M. E. 1981. The Study of Plant: Structure, Principles, and Selected Methods. Termarcarphi Pty Ltd, Australia. ISBN: 0 9594174 0 0.

O’Driscoll, D., Read, S. M., and Steer, M. W. 1993. Determination of cell-wall porosity by microscopy: walls of cultured cells and pollen tubes. Acta Botanica Neerlandica **42**(2): 237-244.

Peirson, D. R., and Dumbroff, E. B. 1969. Demonstration of a complete Casparian strip in *Avena* and *Ipomoea* by a fluorescent staining technique. Canadian Journal of Botany **47**: 1869-1871.

Perumalla, C. J., Peterson, C. A., and Enstone, D. E. 1990. A survey of angiosperm species to detect hypodermal Casparian bands. I. Roots with a uniseriate hypodermis and epidermis. Botanical Journal of Linnean Society **103**: 93-112.

Peterson, C. A. 1987. The exodermal Casparian band of onion roots blocks the apoplastic movement of sulphate ions. Journal of Experimental Botany **38**: 2068-2081.

Peterson, C. A., and Cholewa, E. 1998. Structural modifications of the apoplast and their potential impact on ion uptake. Zeitschrift Fur Pflanzenernahrung Und Bodenkunde **161**: 521-531.

Peterson, C. A., Emanuel, M. E., and Humphreys, G. B. 1981. Pathway of movement of apoplastic fluorescent tracers through the endodermis at the site of secondary root formation in corn (*Zea mays*) and broad bean (*Vicia faba*). Canadian Journal of Botany **59**: 618-625.

Peterson, C. A., Emanuel, M. E., and Wilson, C. 1982. Identification of a Casparian band in the hypodermis of onion and corn roots. Canadian Journal of Botany **60**: 1529-1535.

Peterson, C. A., Enstone, D. E., and Taylor, J. H. 1999. Pine root structure and its potential significance for root function. Plant and Soil **217**: 205-213.

Peterson, C. A. and Fletcher, R. A. 1973. Lactic acid clearing and fluorescent staining for demonstration of sieve tubes. Stain Technology **48** (1): 23-27.

Peterson, C. A. and Lefcourt, B. E. M. 1990. Development of endodermal Casparian bands and xylem in lateral roots of broad bean. Canadian Journal of Botany **68**: 2729-2735.

Peterson, C. A. and Perumalla, C. J. 1984. Development of the hypodermal Casparian band in corn and onion roots. Journal of Experimental Botany **35**: 51-57.

Peterson, C. A. and Perumalla, C. J. 1990. A survey of angiosperm species to detect hypodermal Casparian bands. II. Roots with a multiseriate hypodermis and epidermis. Botanical Journal of The Linnean Society **103**: 113-125.

Peterson, C. A., Murrmann, M., and Steudle, E. 1993. Location of the major barriers to water and ion movement in young roots of *Zea mays* L. Planta **190**: 127-136.

Peterson, C. A., Peterson, R. L., and Robards, A. W. 1978. A correlated histochemical and ultrastructural study of the epidermis and hypodermis of onion roots. Protoplasma **96**: 1-21.

Peterson, C. A., Swanson, E. S., and Hull, R. J. 1986. Use of lanthanum to trace apoplastic solute transport in intact plants. Journal of Experimental Botany **37**: 807-822.

Peterson, R. L. and Farquhar, M. L. 1996. Root hairs: specialized tubular cells extending root surfaces. Botanical Review **62**: 1-40.

Raven, P. H., Evert, R. F., and Eichhorn, S. E. 1999. Biology of Plants, 6th Ed. W.H. Freeman and Company. New York. ISBN: 1-57259-041-6.

Reeve, R. M. 1951. Histochemical tests for polyphenols in plant tissues. Stain Technology **26**: 91

Riederer, M. and Schönherr, J. 1986. Quantitative gas chromatographic analysis of methyl esters of hydroxy fatty acids derived from plant cutin. Journal of Chromatography **360**: 151-161.

Riley, R. G. and Kolattukudy, P. E. 1975. Evidence for covalently attached *p*-coumaric acid and ferulic acid in cutins and suberins. Plant Physiology **56**: 650-654.

Robards, A. W. and Robb, M. E. 1972. Uptake and binding of uranyl ions by barley roots. Science (Washington, D. C.) **178**: 980-982.

Robards, A. W. and Robb, M. E. 1974. The entry of ions and molecules into root: an investigation using electron-opaque tracers. Planta **120**: 1-12.

Robb, J., Lee, S. W., Mohan, R., and Kolattukudy, P. E. 1991. Chemical characterization of stress-induced vascular coating in tomato. Plant Physiology **97**: 528-536.

Schreiber, L. 1996. Chemical composition of Casparian strips isolated from *Clivia miniata* Reg. roots: evidence for lignin. Planta **199**: 596-601.

Schreiber, L., Breiner, H. W., Riederer, M., Düggelin, M., and Guggenheim, R. 1994. The Casparian strip of *Clivia miniata* Reg. roots: isolation, fine structure and chemical nature. Botanica Acta **107**: 353-361.

Schreiber, L., Hartmann, K., Skrabs, M., and Zeier, J. 1999. Apoplastic barriers in roots: chemical composition of endodermal and hypodermal cell walls. Journal of Experimental Botany **50**: 1267-1280.

Sinclair, T. R. 2004. Improved carbon and nitrogen assimilation for increased yield. In: Soybeans: Improvement, Production, and Uses. 3rd edition. Ed by Boerma, H. R. and Specht, J. E. American Society of Agronomy, Inc. Madison, Wisconsin, USA. pp. 537-568.

Sogin, M. L. and Silberman, J. D. 1998. Evolution of the protests and protistan parasites from the perspective of molecular systematics. International Journal for Parasitology **28**: 11-20.

Stadelmann, E. J. and Kinzel, H. 1972. Vital staining of plant cells. In: Methods in Cell Physiology. Ed by Prescott, V. D. M. Academic Press, New York. pp. 325-372.

Stasovski, E., and Peterson, C. A. 1993. Effects of drought and subsequent rehydration on the structure, vitality, and permeability of *Allium cepa* adventitious roots. Canadian Journal of Botany **71**: 700-707.

Storey, R. and Walker, R. R. 1987. Some effects of root anatomy on K, Na, and Cl loading of citrus roots and leaves. Journal of Experimental Botany **38**: 1769-1780.

Stössel, P., Lazarovits, G., and Ward, E. W. B. 1980. Penetration and growth of compatible and incompatible races of *Phytophthora megasperma* var. *sojae* in soybean hypocotyls tissue differing in age. Canadian Journal of Botany **58**: 2594-2601.

Talmadge, K. W., Keegstra, K., Bauer, W. D., and Albersheim, P. 1973. Structure of plant-cell walls. I. Macromolecular components of walls of suspension-cultured sycamore cells with a detailed analysis of pectic polysaccharides. Plant Physiology **51** (1): 158-173.

Tepfer, M. and Taylor, I. E. P. 1981. The permeability of plant cell walls as measured by gel filtration chromatography. Science **213**: 761-763.

Tyler, B. M. 2002. Molecular basis of recognition between *Phytophthora* pathogens and their hosts. Annual Review of Phytopathology **40**: 137-167.

van West, P. and Vleeshouwers, V. G. 2004. The *Phytophthora infestans*-potato interaction. In: Plant-Pathogen Interactions. Ed by Talbot, N. Blackwell Publishing Ltd. Oxford, UK. ISBN 1-4051-1433-9. pp. 219-242.

Vance, C. P., Kirk, T. K., and Sherwood, R. T. 1980. Lignification as a mechanism of disease resistance. Annual Review of Phytopathology **18**: 259-288.

Walker, R. R., Sedgley, M., Blesing, M. A., and Douglas, T. J. 1984. Anatomy, ultrastructure and assimilate concentrations in roots of *Citrus* genotypes differing in ability for salt exclusion. Journal of Experimental Botany **35**: 1481-1494.

Ward, E. W. B., Lazarovits, G., Unwin, C. H., and Buzzell, R. I. 1979. Hypocotyl reactions and glyceollin in soybeans inoculated with zoospores of *Phytophthora megasperma* var. *sojae*. Phytopathology **69**: 951-955.

Wilcox, J. R. 2004. World distribution and trade of soybean. In: Soybeans: Improvement, Production, and Uses. 3rd edition. Ed by Boerma, H. R. and Specht, J. E. American Society of Agronomy, Inc. Madison, Wisconsin, USA. pp. 1-14.

Wilson, C. A., and Peterson, C. A. 1983. Chemical composition of the epidermal, hypodermal, endodermal and intervening cortical cell walls of various plant roots. Annals of Botany **51**: 759-769.

Wrather, J. A., Anderson, T. R., Arsyad, D. M., Gai, J., Ploper, L. D., Portapuglia, A., Ram, H. A., and Yorinori, J. T. 1997. Soybean disease loss estimates for the top 10 soybean producing countries in 1994. Plant Disease **81** (1): 107-110.

Zeier, J., Goll, A., Yokiyama, M., Karahara, I., and Schreiber, L. 1999a. Structure and chemical composition of endodermal and rhizodermal/hypodermal walls of several species. Plant, Cell and Environment **22**: 271-279.

Zeier, J., Ruel, K., Ryser, U., and Schreiber, L. 1999b. Chemical analysis and immunolocalisation of lignin and suberin in the endodermis and hypodermis/rhizodermis of developing maize (*Zea mays* L.) roots. Planta **209**: 1-12.

Zeier, J. and Schreiber, L. 1997. Chemical composition of hypodermal and endodermal cell walls and xylem vessels isolated from *Clivia miniata*: identification of the biopolymers lignin and suberin. Plant Physiology **113**: 1223-1231.

Zeier, J. and Schreiber, L. 1998. Comparative investigation of primary and tertiary endodermal cell walls isolated from the roots of five monocotyledonous species: chemical composition in relation to fine structure. Planta **206**: 349-361.

http://arbl.cvmbs.colostate.edu/hbooks/pathphys/reprod/semeneval/hemacytometer.html

Appendix 1

Composition of BF_3-MeOH depolymerisates from epidermal cell wall obtained from resistant cv. Conrad roots. -, not detected.

Compound	0-70 mm from root tip			90-160 mm from root tip			160-200 mm from root tip			Total ng.mm^{-2}	% of grand total
	ng.mm^{-2}	S.E.	%	ng.mm^{-2}	S.E.	%	ng.mm^{-2}	S.E.	%		
ω-Hydroxy acids											
$C_{16:0}$	4.4	0.03	2.7	8.3	0.2	5.0	8.6	0.1	5.2	21.2	12.9
$C_{18:1}$	5.1	0.1	3.1	10.8	0.4	6.6	14.1	0.2	8.6	30.0	18.2
$C_{20:0}$	5.2	0.01	3.1	9.2	0.2	5.6	7.5	0.1	4.6	21.9	13.3
$C_{22:0}$	5.5	0.0	3.4	10.2	0.2	6.2	9.9	0.1	6.0	25.6	15.6
$C_{24:0}$	6.6	0.2	4.0	12.0	0.1	7.2	10.1	0.4	6.2	28.6	17.3
Total	26.7		16.2	50.4		30.5	50.2		30.5	127.3	77.2
Carboxylic acids											
$C_{16:1}$	0.5	0.01	0.3	2.1	0.2	1.3	0.9	0.01	0.6	3.5	2.1
$C_{16:0}$	1.4	0.01	0.9	3.8	0.4	2.3	2.0	0.1	1.2	7.3	4.4
$C_{18:1}$	1.9	0.1	1.2	7.1	0.1	4.3	4.2	0.2	2.5	13.2	8.0
$C_{18:0}$	0.5	0.03	0.3	3.2	1.1	2.0	1.3	0.2	0.8	5.0	3.1
$C_{20:0}$	0.1	0.01	0.1	0.5	0.1	0.3	0.8	0.02	0.5	1.4	0.8
$C_{22:0}$	0.3	0.01	0.2	0.9	0.2	0.5	1.5	0.04	0.9	2.7	1.6
Total	4.7		2.8	17.6		10.7	10.8		6.6	33.1	20.1
Dicarboxylic acids											
$C_{16:1}$	0.2	0.01	0.1	0.5	0.03	0.3	1.2	0.1	0.7	1.9	1.2
$C_{18:1}$	0.1	0.0	0.1	0.4	0.2	0.3	1.3	0.03	0.8	1.8	1.1
$C_{20:0}$	0.1	0.0	0.03	0.2	0.03	0.1	0.4	0.01	0.2	0.6	0.4
Total	0.4		0.2	1.1		0.7	2.9		1.8	4.3	2.6
1-Alkanols											
$C_{20:0}$	-		-	-		-	0.1	0.0	0.1	0.1	0.1
Total	-		-	-		-	0.1		0.1	0.1	0.1
Grand total	31.8		19.3	69.0		41.9	64.1		38.9	164.9	100

Appendix 2

Composition of BF_3-MeOH depolymerisates from epidermal cell wall obtained from susceptible cv. OX 760-6 roots. -, not detected.

Compound	0-70 mm from root tip			90-160 mm from root tip			160-200 mm from root tip			Total $ng.mm^{-2}$	% of grand total
	$ng.mm^{-2}$	S.E.	%	$ng.mm^{-2}$	S.E.	%	$ng.mm^{-2}$	S.E.	%		
ω-Hydroxy acids											
$C_{16:0}$	2.2	0.1	3.1	5.1	0.2	7.4	4.0	0.3	5.8	11.4	16.3
$C_{18:1}$	2.6	0.1	3.8	6.2	0.2	9.0	3.8	0.9	5.5	12.7	18.3
$C_{20:0}$	3.5	1.0	5.1	5.8	0.1	8.4	2.9	0.04	4.2	12.3	17.6
$C_{22:0}$	0.8	0.3	1.2	1.3	0.03	1.9	0.8	0.1	1.1	2.9	4.2
$C_{24:0}$	3.2	0.2	4.5	7.7	0.3	11.0	3.6	0.1	5.2	14.4	20.8
Total	12.3		17.8	26.1		37.6	15.2		21.8	53.6	77.2
Carboxylic acids											
$C_{16:1}$	0.2	0.01	0.2	0.5	0.01	0.8	0.3	0.1	0.5	1.0	1.5
$C_{16:0}$	1.0	0.1	1.4	2.5	0.1	3.6	1.4	0.2	2.0	4.8	7.0
$C_{18:1}$	0.4	0.01	0.6	1.8	0.1	2.6	1.5	0.2	2.1	3.6	5.2
$C_{18:0}$	0.1	0.03	0.2	0.4	0.1	0.6	0.4	0.2	0.6	1.0	1.4
$C_{20:0}$	0.1	0.01	0.1	0.3	0.1	0.5	1.1	0.2	1.6	1.5	2.2
$C_{22:0}$	0.1	0.01	0.2	0.4	0.04	0.5	0.6	0.1	0.9	1.1	1.6
Total	1.9		2.7	5.9		8.5	5.3		7.6	13.1	18.8
Dicarboxylic acids											
$C_{16:1}$	0.2	0.02	0.2	0.3	0.1	0.5	0.6	0.1	0.9	1.1	1.6
$C_{18:1}$	0.4	0.3	0.6	0.3	0.01	0.5	0.7	0.1	1.0	1.4	1.9
$C_{20:0}$	0.03	0.01	0.04	0.1	0.01	0.1	0.2	0.02	0.3	0.3	0.5
Total	0.6		0.8	0.7		1.0	1.5		2.1	2.8	4.0
1-Alkanols	-		-	-		-	-		-	-	-
$C_{20:0}$	-		-	-		-	-		-	-	-
Grand total	14.8		21.2	32.8		47.2	22.0		31.6	69.5	100

Appendix 3

Monomeric components released from epidermal cell walls isolated from resistant cv. Conrad and susceptible cv. OX 760-6 roots.

Variety	Compound	0-70 mm from root tip			90-160 mm from root tip			160-200 mm from root tip			Total ng.mm^{-2}	% of grand total
		ng.mm^{-2}	S.E.	%	ng.mm^{-2}	S.E.	%	ng.mm^{-2}	S.E.	%		
Conrad	Esterified aliphatics	31.8		17.9	69.0		38.9	64.1		36.1	164.9	92.9
	Esterified aromatics											
	Ferulic acid	2.0	0.1	1.1	2.1	0.02	1.2	2.1	0.0	1.2	6.2	3.5
	p-Coumaric acid	0.6	0.01	0.3	0.6	0.01	0.3	0.6	0.02	0.3	1.7	1.0
	Total	2.5		1.4	2.6		1.5	2.7		1.5	7.8	4.4
	Non-esterified aromatics											
	Vanillin	0.3		0.1	1.0		0.6	2.2		1.3	3.5	2.0
	Syringin	0.2		0.1	0.4		0.2	0.6		0.4	1.2	0.7
	Total	0.5	0.1	0.3	1.4	0.7	0.8	2.9	1.0	1.6	4.7	2.6
	Grand total	34.8		19.6	73.0		41.2	69.6		39.3	177.4	100
OX760-6	Esterified aliphatics	14.8		18.9	32.8		41.9	22		28.1	69.5	88.8
	Esterified aromatics											
	Ferulic acid	1.0	0.03	1.3	1.0	0.08	1.3	1.0	0.01	1.2	2.9	3.7
	p-Coumaric acid	0.3	0.04	0.4	0.3	0.0	0.4	0.3	0.0	0.4	0.9	1.1
	Total	1.3		1.7	1.3		1.6	1.2		1.6	3.8	4.9
	Non-esterified aromatics											
	Vanillin	1.5		2.0	0.5		0.6	1.6		2.0	3.6	4.6
	Syringin	0.7		0.9	0.3		0.4	0.4		0.6	1.4	1.8
	Total	2.2	0.02	2.8	0.8	0.2	1.0	2.0	0.01	2.5	5.0	6.4
	Grand total	18.3		23.3	34.8		44.5	25.2		32.2	78.2	100

Appendix 4

Wax monomers released from epidermal cell walls of resistant cv. Conrad roots.

Compound	0-70 mm from root tip			90-160 mm from root tip			160-200 mm from root tip			Total $ng.mm^{-2}$	% of grand total
	$ng.mm^{-2}$	S.E.	%	$ng.mm^{-2}$	S.E.	%	$ng.mm^{-2}$	S.E.	%		
Alkanes											
C_{23}	0.3	0.03	0.6	0.4	0.0	0.8	0.9	0.0	1.8	1.6	3.2
C_{24}	0.3	0.01	0.6	0.5	0.01	0.9	0.9	0.0	1.8	1.7	3.2
C_{25}	0.5	0.04	1.0	0.8	0.01	1.5	1.6	0.0	3.2	3.0	5.8
C_{26}	0.6	0.1	1.2	1.0	0.01	1.9	2.0	0.01	3.8	3.5	6.9
C_{27}	2.1	0.2	4.0	1.0	0.01	1.9	2.7	0.1	5.2	5.7	11.1
C_{28}	1.4	0.0	2.7	2.3	0.02	4.6	4.9	0.01	9.5	8.6	16.8
C_{29}	1.4	0.0	2.8	2.4	0.01	4.7	5.0	0.03	9.8	8.9	17.3
C_{31}	1.6	0.1	3.0	1.6	0.1	3.1	3.3	0.03	6.4	6.4	12.5
C_{32}	1.2	0.01	2.3	1.5	0.1	2.8	3.3	0.1	6.4	5.9	11.6
Total	9.4		18.3	11.4		22.1	24.5		47.8	45.2	88.2
Carboxylic acids											
$C_{16:0}$	0.2	0.01	0.5	0.1	0.0	0.2	0.3	0.0	0.7	0.7	1.4
$C_{17:0}$	0.1	0.0	0.1	0.1	0.0	0.2	0.3	0.0	0.5	0.4	0.9
$C_{18:0}$	0.1	0.0	0.3	0.1	0.0	0.3	0.4	0.02	0.8	0.7	1.4
$C_{20:0}$	0.1	0.0	0.2	0.1	0.0	0.3	0.3	0.0	0.6	0.5	1.0
$C_{21:0}$	0.1	0.01	0.2	0.2	0.0	0.3	0.4	0.0	0.7	0.6	1.2
$C_{22:0}$	0.1	0.0	0.2	0.1	0.0	0.2	0.3	0.0	0.6	0.5	0.9
$C_{23:0}$	0.1	0.0	0.2	0.1	0.0	0.3	0.6	0.02	0.7	0.6	1.2
$C_{24:0}$	0.1	0.0	0.2	0.1	0.0	0.3	0.3	0.0	0.5	0.5	0.9
$C_{25:0}$	0.1	0.0	0.2	0.1	0.01	0.2	0.3	0.01	0.5	0.5	0.9
Total	1.0		1.9	1.2		2.3	2.8		5.5	5.0	9.7
Alcohols											
C_{24}	0.04	0.0	0.1	0.1	0.03	0.3	0.4	0.1	0.9	0.6	1.2
C_{25}	0.1	0.02	0.1	0.1	0.01	0.2	0.2	0.01	0.3	0.3	0.6
C_{26}	0.02	0.0	0.04	0.1	0.01	0.1	0.1	0.0	0.1	0.1	0.3
Total	0.1		0.2	0.3		0.5	0.7		1.3	1.1	2.1
Grand total	10.4		20.4	12.8		25.0	28.0		54.7	51.3	100

Appendix 5

Wax monomers released from epidermal cell walls of susceptible cv. OX 760-6 roots.

Compound	0-70 mm from root tip			90-160 mm from root tip			160-200 mm from root tip			Total ng.mm^{-2}	% of grand total
	ng.mm^{-2}	S.E.	%	ng.mm^{-2}	S.E.	%	ng.mm^{-2}	S.E.	%		
Alkanes											
C23	0.3	0.1	1.0	0.2	0.0	0.9	0.4	0.1	1.4	0.9	3.2
C24	0.3	0.1	1.0	0.3	0.0	0.9	0.4	0.1	1.4	0.9	3.3
C25	0.5	0.1	1.8	0.4	0.0	1.6	0.7	0.1	2.5	1.7	5.9
C26	0.6	0.1	2.2	0.6	0.0	2.0	1.0	0.0	3.5	2.2	7.7
C27	0.6	0.1	2.2	0.6	0.01	2.0	0.9	0.1	3.2	2.1	7.4
C28	1.5	0.3	5.4	1.4	0.0	4.9	2.5	0.0	8.7	5.3	19.0
C29	1.9	0.01	6.6	0.1	0.0	0.5	2.5	0.01	8.7	4.4	15.8
C31	1.4	0.1	4.8	1.0	0.02	3.6	1.5	0.01	5.3	3.9	13.8
C32	0.9	0.2	3.3	0.8	0.04	3.0	1.3	0.2	4.5	3.0	10.7
Total	7.9		28.2	5.4		19.3	11.0		39.3	24.4	86.7
Carboxylic acids											
C16:0	0.3	0.05	0.9	0.2	0.04	0.9	0.3	0.1	1.0	0.8	2.7
C17:0	0.1	0.02	0.3	0.1	0.01	0.3	0.1	0.02	0.4	0.3	1.0
C18:0	0.1	0.01	0.4	0.2	0.04	0.5	0.2	0.02	0.6	0.4	1.5
C20:0	0.1	0.02	0.3	0.1	0.0	0.3	0.1	0.02	0.4	0.3	1.0
C21:0	0.1	0.01	0.3	0.1	0.0	0.3	0.1	0.02	0.5	0.3	1.1
C22:0	0.1	0.02	0.3	0.1	0.0	0.3	0.1	0.02	0.4	0.3	1.0
C23:0	0.1	0.02	0.3	0.1	0.0	0.3	0.2	0.01	0.6	0.4	1.2
C24:0	0.1	0.02	0.3	0.1	0.0	0.3	0.1	0.02	0.4	0.3	1.0
C25:0	0.1	0.02	0.3	0.1	0.0	0.3	0.1	0.02	0.5	0.3	1.0
Total	1.0		3.4	1.0		3.4	1.3		4.7	3.2	11.5
Alcohols											
C24	0.1	0.02	0.2	0.1	0.0	0.2	0.2	0.1	0.6	0.3	1.0
C25	0.04	0.01	0.1	0.04	0.0	0.1	0.1	0.0	0.2	0.1	0.5
C26	0.02	0	0.1	0.02	0.0	0.1	0.03	0.0	0.1	0.1	0.3
Total	0.1		0.4	0.1		0.4	0.3		0.9	0.5	1.7
Grand total	9.0		32.0	6.5		23.1	12.6		44.9	28.1	100